379
N81d
no. 3888

AUTOPHOSPHORYLATION AND AUTOACTIVATION OF AN S6/H4 KINASE ISOLATED FROM HUMAN PLACENTA

DISSERTATION

Presented to the Graduate Council of the
University of North Texas in Partial
Fulfillment of the Requirements

For the Degree of

DOCTOR OF PHILOSOPHY

BY

Patrick B. Dennis, B.S.
Denton, Texas
May, 1994

379
N81d
no. 3888

AUTOPHOSPHORYLATION AND AUTOACTIVATION OF AN S6/H4 KINASE ISOLATED FROM HUMAN PLACENTA

DISSERTATION

Presented to the Graduate Council of the
University of North Texas in Partial
Fulfillment of the Requirements

For the Degree of

DOCTOR OF PHILOSOPHY

BY

Patrick B. Dennis, B.S.
Denton, Texas
May, 1994

Dennis, Patrick B., Autophosphorylation and Autoactivation of an S6/H4 Kinase Isolated from Human Placenta. Doctor of Philosophy (Biochemistry), May, 1994, 134 pp., 5 tables, 34 illustrations, bibliography, 85 titles.

A number of protein kinases have been shown to undergo autophosphorylation, but few have demonstrated a coordinate increase or decrease in enzymatic activity as a result. Described here is a novel S6 kinase isolated from human placenta which autoactivates through autophosphorylation *in vitro*. This S6/H4 kinase, purified in an inactive state, was shown to be a protein of Mr of 60,000 as estimated by SDS-PAGE and could catalyze the phosphorylation of the synthetic peptide S6-21, the histone H4, and myelin basic protein. Mild digestion of the inactive S6/H4 kinase with trypsin was necessary, but not sufficient, to activate the kinase fully. Subsequent incubation of the trypsin-treated S6/H4 kinase with MgATP resulted in the rapid autophosphorylation of a Mr 40,000 fragment along with a coordinate increase in kinase activity. Autophosphorylation of the Mr 40,000 protein was positively correlated with MgATP incubation time and an increase in S6/H4 kinase activity. Isoelectric focusing resolved at least two phosphoprotein isoforms generated rapidly during the autophosphorylation time course, indicating the existence of multiple autophosphorylation sites. Tryptic phosphopeptide mapping supported this by resolving four phosphopeptides generated from fully autoactivated S6/H4 kinase. To determine how many and which of these sites functioned in the autoactivation mechanism, tryptic phosphopeptide peptide mapping was used to identify the sites that correlated with autoactivation. This strategy implicated two phosphopeptides in the mediation of S6/H4 kinase autoactivation at early time points one of which yielded the sequence SSMVGTPY. A third phosphopeptide containing an autophosphorylation site implicated in the

autoactivation of the S6/H4 kinase at later time points yielded the sequence SVIDPVPAPVGDSHVDGAAK. Phosphoamino acid analysis indicated that autophosphorylation of sites associated with these phosphopeptides occurred exclusively on serine residues. Taken together, these data support the hypothesis that this previously uncharacterized S6 kinase belongs to a unique family of protein kinases which utilize autophosphorylation as part of their *in vivo* activation mechanism.

TABLE OF CONTENTS

Page

LIST OF TABLES........ v

LIST OF ILLUSTRATIONS........ vi

LIST OF ABBREVIATIONS........ viii

Chapter

I. INTRODUCTION........ 1

S6 Kinase Structure and Function........ 1
Hypothesis........ 5

II. EXPERIMENTAL PROCEDURES........ 6

Materials........ 6
Purification of S6/H4 Kinase........ 6
Assay of S6/H4 Kinase Activity........ 8
8-Azido-[α-^{32}P]ATP labeling of S6/H4 Kinase........ 8
Chromatofocusing of the S6/H4 Kinase........ 9
Chromatography of trypsin-treated S6/H4 Kinase........ 9
Autoradiography of phosphorylated S6/H4 Kinase........ 10
Western blot analysis of S6/H4 Kinase........ 10
Two-dimensional SDS-PAGE........ 11
Purification of autophosphorylated pp40........ 11
Proteolytic digestions........ 12
Peptide mapping by two-dimensional TLE/TLC........ 13
Phosphoamino acid analysis........ 13
Peptide purification........ 14
Peptide sequencing........ 15

III. RESULTS........ 16

Purification of the S6/H4 Kinase from human placenta........ 16
Substrate specificity of the S6/H4 Kinase........ 17
Identification of the S6/H4 Kinase as an Mr 60,000 Protein........ 19
Role of ATP in S6/H4 Kinase activation........ 22
Isolation of the p40 S6/H4 Kinase catalytic unit........ 23
Correlation of S6/H4 Kinase activation and autophosphorylation........ 25
Phosphorylation of the inactive p60 S6/H4 Kinase by the autoactivated pp40 form of the enzyme........ 26

Mechanism of p40 S6/H4 Kinase autoactivation.................................. 27
Resolution of p40 S6/H4 Kinase phosphoprotein isoforms................... 28

Tryptic phosphopeptide mapping of autophosphorylated pp40 S6/H4 Kinase.. 29
Correlation of autophosphorylation sites with autoactivation.................. 34
Sequence determination of the S6/H4 Kinase autophosphorylation sites...... 36
Phosphoamino acid analysis of autophosphorylated pp40 S6/H4 Kinase..... 39

IV. DISCUSSION.. 113

REFERENCES.. 129

LIST OF TABLES

Table Page

I. Purification of the S6/H4 Kinase from Human Placenta................................ 40

II. Activation and Substrate Specificity of the S6/H4 Kinase.............................. 41

III. R_f Values of Tryptic Phosphopeptides Generated from Autophosphorylated pp40 S6/H4 Kinase 42

IV. Sequencing of Tryptic Phosphopeptides Generated from Autophosphorylated pp40 S6/H4 Kinase.. 43

LIST OF ILLUSTRATIONS

Figure

1. Sephacryl S200 Chromatography of S6 Kinases from Human Placenta.............45
2. Mono S Chromatography of S6/H4 Kinase...47
3. Mono Q Chromatography of S6/H4 Kinase...49
4. HPLC Analysis of S6-21 Phosphorylated by the S6/H4 Kinase..................... 51
5. HPLC Analysis of S6-21 Phosphorylated by an S6 Kinase Isolated from Human Placenta...53
6. Identification of the S6/H4 Kinase as a Protein of Mr 60,000.........................55
7. Autophosphorylation and Trypsin Activation of Two S6/H4 Kinase Isoforms Resolved by Mono S Chromatography..57
8. Resolution of S6/H4 Kinase and p70 S6 Kinase in Placenta Extracts by Chromatograph on Mono Q...59
9. Time Course for S6/H4 Kinase Activation and Autophosphorylation................ 61
10. Autophosphorylation of Native and Trypsin-treated S6/H4 Kinase...................63
11. Mono Q Chromatography of Trypsin-treated S6/H4 Kinase...........................65
12. Resolution of Two S6/H4 Kinase Isoforms by Mono Q Chromatography After Incubation with MgATP... 67
13. Resolution of Two S6/H4 Kinase Isoforms by Mono Q Chromatography After Incubation with MgATP... 69
14. Autoactivation Time Course of pp40 S6/H4 Kinase Peaks Resolved by Mono Q Chromatography..71
15. Correlation of Trypsin-treated S6/H4 Kinase Activation and Autophosphorylation of p40.. 73
16. Inhibition of p40 Autophosphorylation and Activation with the H4 Substrate...75
17. Phosphorylation of the Native p60 S6/H4 Kinase by the Autoactivated p40 Form of the Enzyme..77

18. Kinetics of p40 S6/H4 Kinase Autoactivation.. 79

19. Resolution of pp40 S6/H4 Kinase Phosphoprotein Isoforms by Two-Dimensional SDS-PAGE...81

20. Mono P Chromatofocusing Chromatography of the S6/H4 Kinase...................83

21. Purification of pp40 S6/H4 Kinase to Homogeneity by Preparative SDS-PAGE..85

22. Release of Trypsin-generated pp40 S6/H4 Kinase Phosphopeptides from Nitrocellulose..87

23. Tryptic Phosphopeptide Mapping of Autophosphorylated pp40 S6/H4 Kinase.. 89

24. HPLC Analysis of Tryptic Phosphopeptides Generated from Autophosphorylated pp40 S6/H4 Kinase..91

25. Mono S Chromatography of Tryptic Phosphopeptides Generated from pp40 S6/H4 Kinase.....................................:............................93

26. Electrophoretic Mobilities of Trypsin-generated pp40 S6/H4 Kinase Phosphopeptides as a Function of pH... 95

27. Tryptic Phosphopeptide Mapping of pp40 Autophosphorylated Over a Time Course...97

28. Tryptic Phosphopeptide Mapping of pp40 S6/H4 Kinase Autophosphorylated at Varying Dilutions Over a Time Course........................99

29. Quantitation of Total p40 S6/H4 Kinase Autophosphorylation at Varying Concentration s Over a Time Course.. 101

30. Occurrence of Tryptic Phosphopeptides Generated from Autophosphorylated pp40 S6/H4 Kinase Over the Autophosphorylation Time Course.. 103

31. Occurrence of Tryptic Phosphopeptides Generated from Autophosphorylated pp40 S6/H4 Kinase as a Function of Kinase Concentration.. 105

32. Mono S. Chromatography of Chymotryptic Phosphopeptides Generated from pp40 S6/H4 Kinase..107

33. Phosphoamino Acid Analysis of Autophosphorylated pp40 S6/H4 Kinase 109

34. Proposed Model of S6/H4 Kinase Autophosphorylation and Autoactivation.. 111

ABBREVIATIONS

APE	alanine-proline-glutamate consensus triplet found in the catalytic domain of most protein kinases
DPCC	diphenylcarbamyl chloride
EGTA	ethylenebis(oxyethylenenitrilo)tetraacetic acid
MAP kinase	mitogen-activated protein kinase
MES	2-(N-morpholino)-ethanesulfonic acid
MLC(3-13)	KRAKAKTTKKRG
Mr	relative molecular weight
p40 S6/H4 kinase	trypsin-activated p60 S6/H4 kinase
pp40 S6/H4 kinase	autophosphorylated p40 S6/H4 kinase
p60 S6/H4 kinase	the inactive protein kinase purified from human placenta
p70 S6 kinase	a growth-regulated mammalian protein kinase
PAGE	polyacrylamide gel electrophoresis
PMSF	phenyl methylsulfonyl fluoride
PVP-360	polyvinylpyrrolidone-360
rsk	ribosomal S6 kinase
S6-21	AKRRRLSSLRASTSKSESSQK
S6/H4 kinase	the inactive p60 protein kinase purified from human placenta or murine lymphosarcoma
SDS	sodium dodecyl sulfate
TCA	trichloroacetic acid
TLC	thin layer chromatography
TLE	thin layer electrophoresis

CHAPTER I

INTRODUCTION

Protein kinases play a central role in cellular signal transduction by transmitting biochemical information between activated membrane-bound receptors and consequent physiological target proteins. The phosphorylation of S6, a protein in the eukaryotic 40S ribosomal subunit, has been correlated with cellular responses to growth factors (1-5). Within minutes of stimulation with mitogens, an increase in S6 phosphorylation has been observed in a variety of cell types (6-10). Phosphorylation occurs on at least five sites and is restricted to a group of serines located in the carboxyl terminal domain of the S6 protein (11,12). Although the physiological significance of S6 phosphorylation is uncertain, a number of S6 kinases have been described. Two S6 kinases with Mr ~90,000 and 92,000 were purified from unfertilized *Xenopus laevis* eggs and designated S6KI and S6KII, respectively (13). A similar kinase has also been observed in mammalian cells (14). The best characterized mammalian S6 kinases have Mr 65,000 - 70,000 (15-18). These enzyme families have been designated the *rsk* and p70 S6 kinases, respectively (reviewed in 19). S6 kinase genes from both the *rsk* and p70 families have been cloned and their primary structures predicted from the cDNA (20-22). The amino terminal half of rat S6KII is 57% homologous to the catalytic domain of rat p70 S6 kinase (22). S6KII cDNA predicts a 30% homology between the carboxyl terminal half of the kinase and the catalytic domain of phosphorylase kinase. The amino terminal half of S6KII has 30% homology with the catalytic subunit of cyclic AMP-dependent protein kinase (21). These studies suggest a domain structure similar to other protein kinases.

Both the p70 S6 kinase and the S6KII are activated in stimulated cells through serine/threonine phosphorylation by an upstream kinase (23,24). The kinase that phosphorylates and activates the p70 S6 kinase is unknown, but phosphorylation and activation of the S6KII was found to be catalyzed by the MAP kinases (24). Two MAP kinases which are more than 77% homologous have been isolated (reviewed in 25). These MAP kinases have molecular weights of 42 kDa and 44 kDa and have been termed $p42^{mapk}$ and $p44^{mapk}$, respectively (26). The regulatory pathway leading to the activation of the MAP kinases and subsequently the activation of S6KII is an example of a protein kinase cascade (reviewed in 27). The protooncogene products Ras and Raf (28) have been implicated in one of the regulatory cascades leading to the activation of the MAP kinases. The activation of the MAP kinases is thought to occur through different pathways depending on the receptor stimulated (29).

Although a regulatory cascade which mediates the activity of the p70 S6 kinase has yet to be characterized, studies have revealed that the p70 S6 kinase and the MAP kinases lie on separate regulatory pathways (30). The p70 S6 kinase is the major mammalian S6 kinase (31) whose function has been shown to be essential for G_1 progression of mitogen-stimulated cells (32). p70 S6 kinase is activated in the liver of cycloheximide-treated rats (17), and its activity can be inhibited by treatment of cells with the immunosuppressant rapamycin (33). In addition to cycloheximide, the p70 S6 kinase is activated by a number of other agents including growth factors, phorbol esters, calcium ionophores, heat shock, and transfection with v-*src* (33). Mitogen-induced activation of the p70 S6 kinase is associated with the phosphorylation of four clustered sites in the putative autoinhibitory domain (34).

Data obtained by both physical and kinetic analysis of purified protein kinases predict that these enzymes contain two domains which confer catalytic and regulatory properties (35-38). The catalytic domain contains conserved primary sequences which are necessary for nucleotide binding and enzyme catalysis. Also present in the catalytic domain are highly variable sequences which determine the individual protein/peptide substrate specificities. The regulatory domain inhibits catalytic activity via an autoinhibitory domain which contains substrate recognition motifs that have been proposed to sterically block nucleotide and protein substrate access to the catalytic center (39). In some protein kinases the autoinhibitory domain contains a phosphorylatable residue (35), whereas in other enzymes the domain is actually a pseudosubstrate since the serine or threonine in the substrate recognition sequence is replaced by a nonphosphorylated amino acid, often alanine (35).

Protein kinase activation occurs *in vivo* by dissociation of the regulatory domain from the catalytic domain thereby permitting access of MgATP and protein substrate to the active site. This conformational change occurs in response to second messenger binding (40,41) or phosphorylation of the regulatory domain at a site distinct from the autoinhibitory site (37, 42-44). *In vitro,* autoinhibitory domains can be removed by limited proteolysis (45-48). Several protein kinases, including the cyclic AMP-dependent kinase (45), protein kinase C (46), S6 kinases (47), and myosin light chain kinase (48) contain a "hinge" region which is particularly susceptible to trypsin cleavage. Proteolysis in this domain generates a catalytic fragment, which is constitutively active, and a dissociated regulatory domain.

A role for autophosphorylation within the regulatory and catalytic domains has not been clearly established. The regulatory subunit of cyclic AMP-dependent protein kinase Type II contains a phosphorylatable serine in the autoinhibitory domain, but cyclic AMP is sufficient to promote subunit dissociation and enzyme activation in the absence of autophosphorylation (49). Possible sites of autophosphorylation in the catalytic domains of the cyclic AMP-dependent protein kinase and the mammalian homologue of S6K II (insulin-stimulated protein kinase 1) have been identified. Protein kinase catalytic domains have been divided into eleven subdomains based on regions of high sequence conservation (36). The putative autophosphorylation sites found in the catalytic domains of the cyclic AMP-dependent protein kinase and the mammalian S6K II were found in catalytic subdomain VIII (50, 51). Subdomain VIII contains the consensus sequence APE found in nearly all protein kinases (36), and these putative autophosphorylation sites occur nine and five residues amino terminal to the APE consensus triplet in the cyclic AMP-dependent protein kinase and mammalian S6K II, respectively (51). However, the significance of autophosphorylation at these sites has not been shown in either kinase. Interestingly, the MAP kinases contain threonine and tyrosine residues which are ten and eight amino acids amino terminal from the APE sequence respectively. Phosphorylation at both sites in the MAP kinases has been shown to be essential for activation of the kinases (52, 53). MAP kinases and a myelin basic protein kinase isolated from bovine kidney cortex (MBPK-2) have demonstrated coordinate increases in kinase activity as a result of autophosphorylation (54,55). However, the physiological significance of these events is in doubt, since the rates of the autophosphorylation reactions are slow, and each kinase can take hours to reach full autoactivation. Both the *rsk* and p70 classes of S6 kinases also undergo autophosphorylation, though no change in activity has been associated with these autophosphorylation events (13,56).

Examples exist where autophosphorylation seems to play a more significant role in the mediation of protein kinase activity. Tyrosine kinases such as the insulin receptor and the epidermal growth factor receptor have been shown to utilize autophosphorylation as part of their activation mechanism (57,58). Damuni and coworkers (59) have isolated a serine/threonine kinase from bovine kidney cortex which phosphorylates and inactivates phosphatase 2A (60). This kinase autophosphorylates rapidly ($t_{1/2}$~ 0.5 - 1 min), and its autophosphorylation results in approximately 10-fold activation.

Previously, Masaracchia and coworkers (61) identified a protein kinase from murine lymphosarcoma cells which catalyzed the phosphorylation of the histone H4. The H4 protein kinase was distinguished from protein kinase C and the cyclic AMP-dependent protein kinase by substrate specificity and the observation that cyclic AMP, calcium, and phospholipids had no effect on H4 kinase activity (62,63). The H4 kinase was also found to catalyze phosphorylation of the S6 protein found in the eukaryotic 40S ribosomal subunit (64) and was henceforth termed the S6/H4 kinase. The partially purified S6/H4 kinase was activated by an endogenous protease in an ATP-dependent manner (65). This ATP-dependent activation could be completely inhibited by the addition of the substrate H4 (65). This suggested the possibility that autophosphorylation was involved in the activation of the S6/H4 kinase *in vitro* (65).

Hypothesis The hypothesis to be pursued in this dissertation is that autoactivation of the S6/H4 kinase by autophosphorylation plays a role in the activation of the kinase. In order to pursue this hypothesis the S6/H4 kinase was purified to apparent homogeneity and the subunit Mr of the enzyme determined. The purified enzyme was used to correlate autophosphorylation and autoactivation kinetics. In order to determine the mechanism by which autophosphorylation is coordinated with S6/H4 kinase autoactivation, autophosphorylation sites were analyzed and, in part, sequenced. Data presented here support the hypothesis and provide valuable information which can be applied to more direct studies concerning the mechanism of S6/H4 kinase autoactivation *in vivo* and *in vitro*.

CHAPTER II

EXPERIMENTAL PROCEDURES

Materials - Human placentas were obtained from term cesarean births and transported to the lab on ice. Histone fraction VIS, bovine serum albumin fraction V, and protease inhibitors were purchased from Sigma Chemical Co. [γ-^{32}P]ATP (4500 Ci/mmol) and 8-azido-[α-^{32}P]ATP (5.7 Ci/mmol) were purchased from ICN. FPLC Mono S and Mono Q columns were obtained from Pharmacia LKB Inc. Phosphocellulose, Sephacryl S200, and CM Sephadex were obtained from Sigma Chemical Co. DEAE cellulose was purchased from Whatman. Rabbit polyclonal antisera directed against a synthetic peptide (CGGGTPEYLAPEGGK; APE peptide) derived from the catalytic subunit of cyclic AMP-dependent protein kinase and preimmune sera were a kind gift from Dr. Curt Hagedorn (Vanderbuilt University School of Medicine). Affinity-purified rabbit polyclonal antibody directed against a peptide (AMIVRNAKDTAHTKAERNILEEVKHPGGC) derived from the catalytic site of the rat p70 S6 kinase was purchased from Upstate Biologicals Inc. Alkaline phosphatase-conjugated sheep anti-rabbit IgG and sequencing grade chymotrypsin were purchased from Boehringer Mannheim. Ampholytes and two-dimensional SDS-PAGE standards were purchased from BioRad. Microcrystalline cellulose acetate thin-layer chromatography plates were obtained from Kodak. Histone H4 and the synthetic peptides S6-21 and MLC(3-13) were prepared as previously described (66,67).

Purification of S6/H4 Kinase - All procedures were conducted at 4 °C with ice cold buffers. The first steps in S6/H4 kinase purification were carried out as described previously (65,66). These included chromatography on DEAE cellulose, phosphocellulose, and CM Sephadex. After elution from CM Sephadex, the sample was dialyzed against 2 liters of 10 mM MES, pH 6.8, 2 mM EDTA, 2 mM EGTA, 1 mM dithioerythritol, 6 mM benzamidine-HCl, 2 μM leupeptin, 100 μM PMSF, 10 % glycerol (Buffer A) for 2 h. The dialyzed sample was loaded onto a 5 ml Mono S HR 5/5 column equilibrated with Buffer A. The column was washed with 2 column volumes of Buffer A and proteins were eluted with a 50 ml 0-0.6 M NaCl linear gradient in Buffer A. Kinase activity eluted as two peaks at 160 mM and 200 mM NaCl; both peaks contained S6-21 and H4 kinase activity. The S6/H4 kinase peak eluting at 160 mM was taken for subsequent purification and study. From Mono S, the S6/H4 kinase fractions were directly loaded onto a 2.5 x 90 cm Sephacryl S-200 gel filtration column equilibrated with 10 mM MES, pH 6.8, 2 mM EDTA, 2 mM EGTA, 1 mM dithioerythritol, 6 mM benzamidine-HCl, 2 μM leupeptin, 100 μM PMSF, and 0.1 M KCl (Buffer B). A single symmetrical peak of S6/H4 kinase activity eluted from the Sephacryl S200 column. S6/H4 kinase fractions containing peak activity were pooled and dialyzed against 2 liters Buffer A for 2 h. The sample was reapplied to Mono S equilibrated with Buffer A and eluted as described above. The S6/H4 kinase fractions eluted from Mono S were pooled and dialyzed against 20 mM Tris-HCl, pH 7.7, 2 mM EDTA, 2 mM EGTA, 10 mM 2-mercaptoethanol, 2 μM leupeptin, 100 μM PMSF, 10% glycerol (Buffer C) and applied to a 5 ml Mono Q HR 5/5 column equilibrated with Buffer C. Proteins were eluted with a 50 ml linear gradient of 0-0.7 M NaCl in Buffer C. Peak S6/H4 kinase fractions were then rechromatographed on Mono Q as described above. The S6/H4 kinase activity fractions with peak activity from the second Mono Q chromatography were frozen in 15% glycerol. The enzyme was stable at -80 °C for at least 1 year.

Assay of S6/H4 Kinase Activity - S6/H4 kinase activity was measured by quantitating the amount of $^{32}PO_4^{-3}$ incorporated into protein or peptide substrates. All reactions described here were carried out at 30 °C for times specified. Aliquots of inactive S6/H4 kinase were subjected to limited proteolysis with 4 µg/ml DPCC-treated trypsin for 3 min. Trypsin stock solution (14 µg/ml trypsin) was prepared in a buffer containing 40 mM Tris-HCl, pH 8, 4 mM 2-mercaptoethanol, and 4 mg/ml bovine serum albumin (Sigma, fraction V). The trypsin solution was added to the sample in a ratio of 1 part trypsin stock solution to 2 parts sample (v/v). The reaction was terminated with the addition of soybean trypsin inhibitor to a final concentration of 6 µg/ml. After proteolysis, fractions were incubated in the presence of 12 mM $MgCl_2$ and 125 µM [γ-^{32}P]ATP (100-200 dpm/pmol) for 10 min after which protein or peptide substrate was added. The activated S6/H4 kinase was incubated with substrate for an additional 10 min. The final concentrations of S6-21 and H4 in the reaction mixture were 190 µM and 1 mg/ml, respectively. Assays were terminated by transferring 35 µl of reaction mixture to P81 paper (S6-21) or ET-31 paper (H4). Papers were immediately immersed in 30 % acetic acid (S6-21) or 10 % TCA (H4) and washed as previously described (68,69). Phosphorylated product was quantitated by liquid scintillation counting.

8-Azido-[α-^{32}P]ATP Labeling of S6/H4 Kinase - A sample of S6/H4 kinase was dialyzed against 10 mM MES, pH 6.8, 15 mM $MgCl_2$, 2 µM leupeptin, 100 µM PMSF, 15 % glycerol at 4°C for 1 h in a microdialyzer (Pierce) with buffer changes every 20 min. Approximately 2.6 µCi (450 pmol) of 8-azido-[α–^{32}P]ATP was spotted on a siliconized spot plate and dried under a stream of nitrogen. Dialyzed S6/H4 kinase (~4 µg) was added to the dried spot along with 17 mM $MgCl_2$ and mixed for 1 min at 4 °C. The reaction mixture was photocrosslinked with a short wavelength UV light source (254 nm, Spectroline) positioned 4 cm from the sample for 5 min. The reaction was stopped with a 10 % trichloroacetic acid precipitation. Precipitated protein was collected by centrifugation and washed twice with methanol before being resuspended in 50 mM MES, pH 6.8. SDS-PAGE sample buffer was then added to the sample and the entire mixture was allowed to sit for 1 h at room temperature. After boiling for 5 min, the sample was analyzed by SDS-PAGE according to Laemmli (70), and the dried gel was exposed to Kodak X-OMAT x-ray film for autoradiographic analysis.

Chromatofocusing of the S6/H4 Kinase - Purified S6/H4 kinase was chromatofocused on a 5 ml Mono P HR 5/5 column (Pharmacia LKB). S6/H4 kinase was placed in 25 mM bis-Tris, pH 6.5, 100 μM PMSF, 10 mM 2-mecaptoethanol, 15 mM $MgCl_2$, 10% glycerol (Buffer D) by chromatography on a BioRad 10DG desalting column equilibrated in Buffer D. The S6/H4 kinase was then loaded on to the Mono P column equilibrated with Buffer D and eluted by running 10% polybuffer 74, pH 4, 100 μM PMSF, 15 mM $MgCl_2$, 10 mM 2-mecaptoethanol, 10% glycerol (Buffer E) over the column isocratically with a flow rate of 1 ml/min. One ml fractions were collected and assayed for S6/H4 kinase activity and the pH of each fraction was determined with a pH meter.

Chromatography of Trypsin-Treated S6/H4 Kinase - Large scale trypsinization of purified S6/H4 kinase was carried out in order to provide sufficient material for the purification and characterization of the enzyme fragment generated by this procedure. The trypsin activation procedure described above was modified to contain 8 mg/ml myoglobin in place of the bovine serum albumin in the trypsin stock buffer, since bovine serum albumin and/or its proteolytic fragments cannot be resolved from the trypsin-treated S6/H4 kinase by Mono Q chromatography. Purified S6/H4 kinase was dialyzed for 1 h against Buffer C to a conductivity of < 6 mmho. The S6/H4 kinase was then trypsin digested by the addition of the modified trypsin stock buffer in the ratio of 1 part trypsin stock buffer to

2 parts sample (v/v). The digestion was stopped after 7 min by the addition of soybean trypsin inhibitor to a final concentration of 6 μg/ml. The reaction mixture was applied to a Mono Q column equilibrated with Buffer C, washed, and eluted as described above. Both trypsin and myoglobin were eluted in the unbound protein fraction. Trypsin inhibitor was eluted at higher salt concentrations than the S6/H4 kinase activity peak. Eluted fractions were assayed by incubating aliquots for 10 min with MgATP and then adding substrate for an additional 10 min. Bovine serum albumin (1 mg/ml) was used in the assay to stabilize the enzyme. Trypsin-treated S6/H4 kinase fractions, designated p40 S6/H4 kinase, were stored in 15 % glycerol at -80°C.

Autoradiography of Phosphorylated S6/H4 Kinase - S6/H4 kinase samples were incubated with Mg[γ-^{32}P]ATP (1-10 x 10^3 dpm/pmol) at 30°C for the designated times. The autophosphorylation reactions were stopped with SDS-PAGE sample buffer, boiled for 5 min, and analyzed by SDS-PAGE (12% acrylamide). Proteins were electrophoretically transferred to nitrocellulose and stained with India ink. Autoradiography was conducted with Kodak X-OMAT film. In some cases, autoradiographic bands were quantitated by densitometry using a Sierra Scientific high resolution camera and a microcomputer imaging device with M1 software (Imaging Research Inc.).

Western Blot Analysis of S6/H4 Kinase - Purified S6/H4 kinase was analyzed by SDS-PAGE (12 % acrylamide) and electrophoretically transferred to a nitrocellulose membrane. All steps subsequent to blotting were performed at room temperature. Blocking was done with 3 % skim milk dissolved in 7.5 mM KPO_4, pH 7.5, 137 mM NaCl, 3 mM KCl (PBS) for 2 h. The membrane was incubated with primary antibody (anti-rat S6 kinase, rabbit polyclonal IgG) diluted in 3 % skim milk / PBS (1 μg/ml) for 2 h and then washed with PBS. Secondary antibody incubation was done for 1 h with alkaline phosphatase-conjugated sheep anti-rabbit antibody (1:2500, in 3 % skim milk / PBS). After washing the membrane with PBS - 0.05% TWEEN 20, the immunoreactive bands were detected using the substrate 3 % nitro blue tetrazolium / 1.5 % bromochloroindoyl phosphate as per manufacturers instructions (Upstate Biologics Inc.). When probing with anti-sera raised against the cyclic AMP-dependent protein kinase APE peptide, blocking, antibody incubation, and washing steps were done with 3 % bovine serum albumin dissolved in 10 mM Tris-HCl, pH 7.5, 137 mM NaCl, 3 mM KCl.

Two-dimensional SDS-PAGE - The trypsin-treated S6/H4 kinase was autophosphorylated in the presence of Mg[γ-^{32}P]ATP (1000 dpm/pmole). Approximately 1 μg of the pp40 S6/H4 kinase was loaded onto an isoelectric focusing gel of 4% acrylamide cast with 2.0% Triton X-100, 2.4% Bio-Lyte 5/7 ampholyte, 0.6% Bio-Lyte, 3/10 ampholyte, and 9.5 M urea. First dimension gels were compatible with the Mini Protean II Dual Slab Cell apparatus (BioRad) used for electrophoresis in the second dimension. The samples were focused between 100 mM NaOH and 10 mM H_3PO_4 for 6 h at 750 V with no pre-electrophoresis. After focusing, the polyacrylamide gels were extruded from their casting tubes and placed over 12% polyacrylamide gels for the second dimension SDS-PAGE performed according to Laemmli (70). Phosphorylated proteins were visualized by autoradiography. Isoelectric points were calculated from a calibration curve generated by cutting 1 cm sections of a focused tube gel with an established pH gradient from 5 to 7. Each section of gel was incubated in 0.5 ml of water for 10 min. The pH of the solution was then determined and plotted against the distance each gel section was cut from the end.

Purification of Autophosphorylated pp40 - To generate enough pp40 S6/H4 kinase for peptide sequencing of proteolytic fragments, preparative SDS-PAGE was performed using a BioRad Model 491 Prep Cell. The p40 S6/H4 kinase generated from mild trypsin digestion was autophosphorylated in the presence of Mg[γ-^{32}P]ATP (~2,000 dpm/pmol) as described earlier. The reaction was stopped by the addition of SDS-PAGE sample buffer and boiled for 10 min. A discontinuous polyacrylamide gel system was used with an 8% resolving gel (12 cm) and a 4% stacking gel (3 cm). Electrophoresis was carried out at 40 mA constant current for 5 h until the tracking dye had reached the bottom of the gel. Fractions were then collected for an additional 5 h at a flow rate of 60 ml/h. Aliquots of eluted [^{32}P]pp40 S6/H4 kinase were analyzed by SDS-PAGE on a 12% polyacrylamide gel and visualized by autoradiography. Fractions containing [^{32}P]pp40 S6/H4 kinase were then pooled and dialyzed overnight to remove the bulk of the SDS. To facilitate movement of SDS through the dialysis membrane, the fractions were diluted so that the concentration of SDS was below its critical micelle concentration (~1 mM). After dialysis, the sample was lyophilized to dryness and loaded onto a Sephadex G-25 superfine column (0.7 x 10 cm) equilibrated with propionic acid/formic acid/water (2:1:2, v/v) to separate residual SDS from the protein as described by Amons *et al.* (71). The flow rate used was 3 ml/h with 0.1 ml fractions being collected. [^{32}P]pp40 S6/H4 kinase was located by spotting a small aliquot from eluted fractions onto ET-31 filter paper and quantitation by liquid scintillation counting. Radiolabelled protein was found to elute in the void volume. The sample was then dried on a SpeedVac (Jouan) and neutralized with freshly prepared 0.1 M ammonium bicarbonate, pH 7.8. The purified [^{32}P]pp40 S6/H4 kinase was then ready for digestion with proteases or for phosphoamino acid analysis.

Proteolytic Digestions - The amount of [^{32}P]pp40 S6/H4 kinase to be digested was determined by the Bradford protein assay using a calibration curve determined from known concentrations of BSA. All digestions were done with a substrate to protease ratio of 20:1 by weight and a final substrate concentration of 1 mg/ml. Digestion with trypsin (DPCC-treated, Sigma) was carried out in 0.1 M ammonium bicarbonate, pH 7.8 at 37°C for 24 h with half the trypsin being added in the first 12 h and the other half being added by quarters in 6 hour intervals. Chymotrypsin digestion was carried out in a digestion buffer of 0.1 M Tris-HCl, pH 7.8, and 0.1 M $CaCl_2$ for 10 h at 25°C with the entire amount of chymotrypsin (sequencing grade, Boehringer Mannheim) being added at the beginning of the reaction. Reactions were stopped by freezing at - 20°C. Thermolysin digestion of the phosphoS6-21 peptide was carried out as described by Brandon and Masaracchia (66).

Peptide Mapping by Two-dimensional TLE/TLC - Peptide mapping was carried out following the guidelines of Boyle *et al.* (72). Briefly, proteolytically digested samples were spotted in 0.5 μl aliquots onto 160 μm microcrystalline cellulose plates with acetate backing (Kodak). In preparation for first-dimensional thin-layer electrophoresis, the plates were pre-sprayed with the running buffer (2% formic acid, 8% acetic acid, pH 1.9) then electrophoresed for 1h at 1000 V on a 4°C cooling tray (DeSaga Brinkman). After electrophoresis, the plate was thoroughly dried under a cool fan and placed in a thin-layer chromatography chamber pre-equilibrated with the mobile phase (37.5% n-butanol, 25% pyridine, and 7.5% acetic acid) for running in the second dimension. When the mobile phase had migrated 1 cm from the top of the plate, the plate was removed from the chamber and dried under a fan. $^{32}PO_4^{-3}$ labelled phosphopeptides were then visualized by autoradiography.

Phosphoamino acid analysis - Purified [^{32}P]pp40 S6/H4 kinase was suspended in 6 N HCl and placed into a hydrolysis tube and air was evacuated with a vacuum pump. The tube was heated to 110°C, and partial amino acid hydrolysis was allowed to occur for 1 h. After hydrolysis, the sample was removed from the tube and dried on a SpeedVac. The reconstituted hydrolysate was then spotted onto a 160 μm microcrystalline cellulose plate along with 7 μg each of phosphoserine, phosphothreonine, and phosphotyrosine standards. The spotted samples were electrophoresed in two dimensions, the first dimension with a running buffer of 2% formic acid and 8% acetic acid for 2 h at 800 V and the second dimension with a running buffer of 1% pyridine and 10% acetic acid for 1 h at 800 V. Phosphoamino acids were visualized by pre-spraying the plates with 10% triethylamine in dichloromethane and then spraying the plates with 0.6 mg/ml fluorescamine dissolved in acetone. Fluorescent spots were observed by viewing the plates under UV light (254 nm). Radiolabelled phosphoamino acids were observed by autoradiography.

Peptide Purification - Tryptic and chymotryptic peptides generated from [^{32}P]pp40 S6/H4 kinase were first loaded onto a Mono S HR 5/5 column equilibrated with 10 mM H_3PO_4, pH 2, and eluted with a 0 - 0.6 M NaCl gradient in 10 mM H_3PO_4, pH 2 (50 ml). Radioactive peaks were detected by spotting aliquots of the eluted fractions onto ET-31 filter paper and quantitating by liquid scintillation counting. Peaks of radioactivity were then pooled and dried down on a SpeedVac. Individual peaks were loaded on a Synchrompak reversed phase C_{18} column (0.46 x 25 cm) equilibrated with either 2.5% acetonitrile/0.1% trifluoroacetic acid or 100% water/0.1% TFA. Phosphopeptides were eluted with a 2.5-40% acetonitrile/0.1% TFA linear gradient (100 ml) at a flow rate of 1 ml/min or an acetonitrile gradient described by Juhl and Soderling (73) of 0-5% (10 min), 5-38% (100 min), and 38-50% (5 min). Eluted phosphopeptide peaks were quantitated by scintillation counting as described before, and peptide purity was assessed by monitoring the absorbance of the eluent at 220 nm. Phosphopeptides which could not be purified by HPLC chromatography were purified by gel filtration on a BioGel P4 superfine column

(BioRad; 0.9 x 13 cm) equilibrated with 0.1 M ammonium bicarbonate, pH 7.8 and 0.1 M NaCl . Fractions were collected (0.1 ml) with a flow rate of 1.6 ml/h. Phosphopeptides eluted from the BioGel P4 column were diluted 3-fold with water and directly loaded onto a Mono Q HR 5/5 column equilibrated with 10 mM ammonium bicarbonate, pH 7.8 and eluted with a 0-0.65 M NaCl linear gradient (50 ml) at a flow rate of 0.5 ml/min. Phosphopeptide peaks eluted from both columns were located by scintillation counting.

Peptide Sequencing. - Purified peptides were sequenced at the Baylor College of Medicine Core Facility on an Applied Biosystems Model 473A sequencer using amino terminal Edman degradation chemistry . Amounts of eluted PTH-amino acid derivatives were calculated from pre-run standards.

CHAPTER III

RESULTS

Purification of the S6/H4 kinase from Human Placenta - In previous studies a protein kinase that catalyzes the phosphorylation of the 40S ribosomal protein S6 and the histone H4 was purified from murine lymphosarcoma cells and human placenta (65,66). This protein kinase was termed S6/H4 kinase based on its substrate specificity. Based on the purification procedures outlined by de la Houssaye *et al.* (65) and Masaracchia *et al.* (74) the purification of the human placenta S6/H4 kinase was carried out further. The S6/H4 kinase was purified 5700-fold by successive chromatography on DEAE cellulose, phosphocellulose, CM sephadex, Mono S, Sephacryl S200, and Mono Q (Table I). The enzyme was obtained in an inactive form in all steps subsequent to the phosphocellulose chromatography. In order to assay the inactive enzyme, samples were subjected to limited proteolysis with trypsin prior to incubation with MgATP and substrate. All steps from DEAE cellulose through Mono Q chromatography gave percent yields greater than 100% with total activity increasing from the crude cell extract through phosphocellulose. This could be explained by the removal of a protein that inhibits the activation or activity of the kinase throughout these steps. Also, some proteins may interfere with the trypsin digestion of the S6/H4 kinase. Removal of these proteins throughout purification would result in higher H4 kinase activities. Chromatography on CM Sephadex resulted in a large loss in total activity and percent yield with only a modest increase in purification. No loss of S6/H4 kinase seemed to occur from Sephacryl S200 to Mono S. Chromatography by gel filtration on a Sephacryl S200 column resolved two peaks of trypsin-activated S6-21 kinase activity (Figure 1). The earlier eluting peak also demonstrated trypsin-activated H4 kinase activity which identified it as the S6/H4 kinase, whereas the later eluting peak showed no activity towards H4 with or without trypsin treatment. Two peaks of trypsin-activated S6/H4 kinase activity were detected in the Mono S eluate (Figure 2). The first peak (peak I) eluted at a mean NaCl concentration of 160 mM. The S6/H4 kinase eluting at the higher salt concentration (200 mM) was selected for further study and was termed peak II. After Sephacryl S200 and Mono S chromatography, the S6/H4 kinase was loaded onto a Mono Q column as the final purification step (Figure 3). A single peak of S6/H4 kinase activity was eluted. The peak of S6/H4 kinase activity eluted from Mono Q was symmetrical and occurred at a mean salt concentration of approximately 170 mM (Figure 3). The specific activity of the purified enzyme was 120 nmol phosphate transferred to S6-21/min-mg (Table II). The apparent Km of the kinase for the S6-21 peptide was previously determined to be 22 μM (66).

Substrate Specificity of the S6/H4 Kinase - In addition to S6-21 and H4, the activated enzyme catalyzed phosphorylation of myelin basic protein; however, the rates of phosphorylation of these substrates were not equivalent (Table II). Casein, phosvitin, protamine, or MLC (3-13), a synthetic peptide which is an excellent substrate for protein kinase C (67), did not appear to be substrates for the enzyme (Table II).

Full activation of the S6/H4 kinase required both limited proteolysis and incubation with MgATP in the absence of protein substrate (Table II). Maximum activity with each substrate was determined by subjecting the enzyme to limited proteolysis and incubation with MgATP prior to addition of protein substrate. When the proteolytic step was carried out for 5 min, the specific activity of the activated enzyme was 120 nmol/min/mg with S6-

21, 79 nmol/min/mg with H4, and 100 nmol/min/mg with myelin basic protein (Table II). When proteolysis was omitted, but the enzyme was incubated with MgATP prior to initiation of the kinase assay, the phosphotransferase activity observed with S6-21, H4 or myelin basic protein was less than 1 nmol/min/mg. These data demonstrate that incubation with MgATP in the absence of limited proteolysis does not activate the enzyme. When the enzyme was subjected to proteolysis, but no incubation with MgATP prior to assay, about 5-20% of the maximum activity was observed. The data suggest a two-step activation mechanism which first requires a conformational change at the active site and a MgATP-dependent reaction which is inhibited in the presence of substrate.

The substrate specificities of the two S6 kinases resolved with Sephacryl S200 chromatography were analyzed using the S6-21 peptide (AKRRRLSSLRASTSK-SESSQK). This peptide contains the mitogen-inducible phosphorylation sites found at the carboxyl terminus of the S6 protein. Phosphorylation of the S6-21 peptide by the S6/H4 kinase generated three phosphorylated products, as shown by HPLC analysis (Figure 4A), with a major product representing 45% of the total radioactivity. Previous analysis of this major product by thin-layer electrophoresis indicated that it was the most highly phosphorylated form of the three phosphopeptide products (66). Phosphorylation of the S6-21 peptide by the second S6 kinase also generated three phosphoproducts (Figure 5A), but the major phosphoproduct, which represented 80% of the total radioactivity, eluted at the same position as a minor product generated by S6/H4 kinase phosphorylation of the peptide. Thermolysin digestion was used to investigate which phosphorylation sites in the S6-21 peptide were preferred by each S6 kinase. The substrate specificity of thermolysin predicts that the S6-21 peptide would be cleaved into three fragments with the sequences AKRRR, LSS, and LRASTSKSESSQK. Only the last two fragments contain phosphorylation sites and represent the amino and carboxyl terminal domains of the peptide respectively. HPLC analysis of thermolysin digested S6-21, which had been phosphorylated with the S6/H4 kinase, revealed four peaks of radioactivity (Figure 4B). Thin-layer chromatography and autoradiography revealed that peptide I was acidic and peptides II, III, and IV were basic (66). Since the thermolysin-derived fragment LSS would be the only fragment to become acidic after phosphorylation, it was concluded that peptide I was the phosphorylated form of LSS. Sequencing of peptides II, III, and IV showed that these peptides were phosphorylated forms of the fragment LRASTSKSESSQK, and thin-layer electrophoresis indicated that peptide II was the most highly phosphorylated form of this fragment (66). Therefore, the S6/H4 kinase phosphorylated sites in both the amino and carboxyl terminal domains of the S6-21 peptide. In contrast, S6-21 phosphorylated by the second S6 kinase yielded the same phosphopeptide fragments after thermolysin digestion but in significantly different proportions (Figure 5B). Approximately 70% of the radioactivity incorporated onto the peptide by this kinase was at the site(s) contained in peptide I, revealing that this S6 kinase has a preference for the site(s) at the amino terminal domain of the peptide. These results show that these two kinases can be differentiated by the types of phosphorylation sites they modify in addition to their chromatographic properties.

Identification of the S6/H4 Kinase as an Mr 60,000 Protein - Once the S6/H4 kinase was prepared in a purified form, the molecular weight of the kinase was estimated. Using 12% SDS-PAGE and Coomassie Blue staining, the apparent molecular weight of the major protein in the purified S6/H4 kinase fraction was 60,000 (Figure 6A), although the protein was eluted from gel filtration chromatography with a Mr of 120,000 (Figure 1).

Incubation of the purified S6/H4 kinase with Mg[γ-^{32}P]ATP resulted in the phosphorylation of the Mr 60,000 protein as determined by SDS PAGE and autoradiography (Figure 6B). The phosphorylation of the Mr 60,000 protein was slow. After 10 min less than 0.038 pmol of phosphate were transferred into approximately 5 pmol of Mr 60,000 protein. This is consistent with the low activity of the S6/H4 kinase observed under these conditions, i.e. in the absence of proteolytic activation. No other protein in the purified preparation was significantly labeled under these conditions.

To investigate if the Mr 60,000 protein phosphorylation was autocatalytic, the purified S6/H4 kinase was incubated with $MgCl_2$ and 8-azido-[α-^{32}P]ATP, and the ligand was crosslinked by exposure to ultraviolet light. A protein migrating at Mr 60,000 was the only protein in the purified S6/H4 kinase preparation which was labeled by this reagent (Figure 6C). The addition of 2 mM ATP blocked labeling of the Mr 60,000 protein by approximately 80% as determined by densitometric analysis of the resulting autoradiograph. No labeling was observed when ultraviolet light exposure was omitted (data not shown), demonstrating that the Mr 60,000 protein is labeled at an ATP binding site by 8-azido-[α-^{32}P]ATP in a light-dependent manner.

To confirm that the Mr 60,000 protein was likely the protein kinase, a Western blot analysis of the S6/H4 kinase was conducted using a rabbit polyclonal antibody to the cyclic AMP-dependent protein kinase sequence CGGGTPEYLAPEGGK (75). Only the Mr 60,000 protein was recognized by the antibody (Figure 6D). Similarly, when crude extracts of human placenta were fractionated by Mono Q chromatography, the only protein detected by the antibody in fractions containing S6/H4 kinase activity was the Mr 60,000 protein. The data taken together establish that the Mr 60,000 protein is likely the S6/H4 kinase.

At the Mono S step in the purification scheme of S6/H4 kinase, the enzyme elutes as two peaks (Figure 2). To investigate how these two S6/H4 kinase peaks might differ, each peak was purified separately over Mono Q. The peaks were then incubated with Mg[γ-

^{32}P]ATP individually to observe the autophosphorylated products and analyzed by SDS-PAGE and autoradiography (Figure 7, *left panel*). The S6/H4 kinase which eluted at the lower salt concentration from Mono S (peak I) demonstrated autophosphorylation of a protein with a Mr of 60,000. A protein of Mr 55,000 was observed to be autophosphorylated when the S6/H4 kinase peak II was incubated with MgATP. Both forms of the kinase were isolated in an inactive form and could be significantly activated with mild trypsin digestion and incubation with MgATP (Figure 7, *right panel*). It is unknown at this time what causes the difference in electrophoretic mobility between the two S6/H4 kinase isoforms.

Identification of the S6/H4 kinase as a protein with of Mr 60,000 indicated the possibility that this kinase was the p70 S6 kinase or was related to it. Although SDS-PAGE analysis of the p70 S6 kinase indicates an apparent molecular weight of ~70,000, a molecular weight of 56,160 Da was predicted from the cDNA sequence (20). The p70 S6 kinase is thought to undergo proteolysis (18). To test if the S6/H4 kinase was a proteolytic product or a dephosphorylated form of the p70 S6 kinase, a polyclonal antibody to the p70 kinase was used to test if the p60 protein would cross-react. Human placenta (50 g) was homogenized, centrifuged and the supernatant chromatographed on Mono Q as described by Grove *et al.* (76) for COS cells transfected with the p70 cDNA. Fractions were assayed for trypsin-activated S6/H4 kinase activity with the substrates S6-21 and H4 (Figure 8, *middle and lower panels*). In addition, Western blot analysis of the fractions was conducted using a rabbit antibody directed to amino acid residues 105-130 in the catalytic domain of rat p70 S6 kinase (Upstate Biological Research) (Figure 8, *upper panel*). The major portion of protein kinase activity eluted as a sharp peak at approximately 170 mM NaCl. The S6-21 and H4 kinase activities associated with this peak were expressed only after trypsin treatment. A second peak of S6-21 activity was eluted as a broad peak at approximately 280 mM NaCl. With S6-21 as substrate, this activity was approximately 10% that observed in major peak. This protein kinase activity was not enhanced by trypsin treatment and no H4 phosphorylation was detected in these fractions. The anti-p70 S6 kinase antibody reacted with a protein coeluting with this minor S6 kinase activity, but not the major peak of trypsin-dependent S6/H4 kinase activity (Figure 8). The apparent molecular weight of the protein which reacted with the antibody (Figure 8, *upper panel*) was approximately 60,000. However, it is unlikely that this is the S6/H4 kinase, since the fractions which contain the S6-21 and H4 activity do not coincide with the immunoreactive fractions. This is in agreement with Western blot analysis of the purified S6/H4 kinase which demonstrated no crossreactivity with the anti-p70 S6 kinase antibody (data not shown). In addition, the S6/H4 kinase activity in this crude preparation eluted at a salt concentration comparable to that at which the enzyme elutes in the final purification step (Figures 3 and 8), suggesting that the S6/H4 kinase is not generated by proteolysis during the enzyme purification. Finally, since the anti-p70 S6 kinase antibody recognizes a sequence in the catalytic domain which would likely be retained in a proteolytic product with catalytic activity, it is unlikely that the S6/H4 kinase is derived from the p70 S6 kinase since the catalytic domain of the S6/H4 kinase is clearly intact but no antibody reactivity is observed.

Role of ATP in S6/H4 Kinase Activation - Many protein kinases appear to be regulated by autoinhibitory domains within the enzyme which interact with the active site and block substrate access (35,37). *In vitro* these autoinhibitory domains can often be removed by limited proteolysis which generates a fully active catalytic product (44-47). The inactive S6/H4 kinase could be activated by limited trypsin digestion. Under the experimental conditions selected, the S6/H4 kinase was 86% activated after trypsin treatment for 1 min and maximum activation was observed after 7 min treatment (Figure 9). A comparable time course for activation was observed when either S6-21 or H4 was used as the enzyme substrate. Trypsin activation of the S6/H4 kinase rapidly generated a new protein which migrated with a Mr 40,000 as determined by SDS-PAGE analysis on 12% polyacrylamide gels (Figure 9A). When the reaction mixture was incubated with Mg[γ-^{32}P]ATP after the trypsin treatment, the pp40 protein was observed to be a prominent phosphoprotein (Figure 10, *lane* 2). As the time of trypsin incubation was varied through the interval previously shown to be appropriate for activation, a loss of the p60 autophosphorylation was observed (Figure 9B) and a marked increase in the occurrence of the phosphorylated p40 was observed (Figure 9A). The rate of phosphate incorporation into the p40 fragment was approximately 6 times faster than the p60 phosphorylation. At trypsin incubation times longer than 5 min, the enzyme appeared to be fully activated (Figure 9) and essentially no phosphorylated p60 could be observed (Figure 10, *lane* 2). Since the trypsin-dependent activation step was carried to completion before the Mg[γ-^{32}P]ATP was added to some of these samples, it is unlikely that p60 catalyzed phosphorylation of p40. Instead, the data suggest that p40 undergoes autophosphorylation. The amount of $^{32}PO_4^{-3}$ incorporated into p40 directly correlated with the increasing activity of the processed S6/H4 kinase (Figure 9A). This correlation between p40 phosphorylation and enzyme activation was observed with H4 (Figures 9A), S6-21 or myelin basic protein as substrates (data not shown).

Isolation of the p40 S6/H4 Kinase Catalytic Unit - To further investigate the correlation between activation and autophosphorylation, the p40 S6/H4 kinase catalytic unit was chromatographed on Mono Q. Purified S6/H4 kinase was trypsin-digested under conditions which predicted maximum activation of the enzyme (Figure 9). A preliminary assay confirmed that the enzyme still required MgATP incubation prior to assay to express activity. The reaction products were applied to a Mono Q column and eluted as described in Figure 3. The trypsin-treated S6/H4 kinase activity eluted at a slightly higher salt concentration due to the exclusion of 10 mM $MgCl_2$ in the buffer (Figure 11). The peak protein kinase activity coeluted with the $A_{280\ nm}$ peak (Figure 11). The S6/H4 kinase activity was dependent on prior incubation with MgATP (Figure 11), and a constant specific activity of 350 nmol/min/mg with the S6-21 was observed across the peak of eluted enzyme. SDS-PAGE analysis of the eluted fractions followed by staining with Coomassie Blue (Figure 12, *upper panel*) revealed that a protein of Mr 40,000 coeluted with the activity peak. Additionally, an autophosphorylated protein of Mr 40,000 correlated with the elution of S6/H4 kinase activity when the fractions were incubated with Mg[γ-^{32}P]ATP prior to SDS-PAGE analysis and autoradiography (Figure 12, *middle and lower panels*).

Stronger binding of a protein to an anion exchange column could suggest phosphorylation since added phosphates would increase the negative charge density on the surface of the protein thereby requiring a higher salt concentration for elution. To determine if incubation of trypsin-treated S6/H4 kinase with MgATP would produce a form of the S6/H4 kinase which would bind tighter to an anion exchange column (Mono Q), trypsin-treated S6/H4 kinase was incubated with MgATP for 10 min at 30°C and chromatographed on a Mono Q column as in Figure 11. When incubation of the trypsin-treated S6/H4 kinase with MgATP preceded Mono Q chromatography, S6/H4 kinase activity eluted in two peaks (Figure 13). Each peak was then assayed for the ability to activate in the presence of MgATP (Figure 14). The S6/H4 kinase peak eluting from Mono Q at the lower salt concentration (peak I) demonstrated 10-fold activation in the presence of MgATP. The S6/H4 kinase peak eluting at the higher salt concentration (peak II) was constitutively active and gained no additional activity in the presence of MgATP. These data support the idea that incubation of the trypsin-treated S6/H4 kinase in the presence of MgATP generates a phosphorylated, active form of the kinase which will bind more tightly to an anion exchange column than the nonphosphorylated, inactive form.

Correlation of S6/H4 Kinase Activation and Autophosphorylation - p40 S6/H4 kinase obtained from Figure 11 was incubated for various time intervals with Mg[γ-^{32}P]ATP and the products were analyzed by SDS-PAGE and autoradiography (Figure 15, *upper panel*). Only the p40 protein was significantly phosphorylated. The distribution of the autophosphorylated p40 precisely correlated with the S6/H4 kinase activity. When the phosphate incorporation into p40 was quantitated, a positive correlation between activation of the S6/H4 kinase and phosphorylation of the p40 protein was observed (Figure 15). These results demonstrate that autophosphorylation of the p40 fragment is necessary for activation of the S6/H4 kinase. However, these data do not conclusively establish that p40 contains the catalytic site. The low rate of autoinhibitory domain phosphorylation (Figure 10, *lane 1*) and the inhibition of MgATP-dependent activation by high substrate concentrations (Table II) suggest that the autoinhibitory (pseudosubstrate) domain and the exogenous protein substrate block access of MgATP to the catalytic site in the nonphosphorylated enzyme. To test this hypothesis, p40 S6/H4 kinase obtained from Figure 11 was either incubated with MgATP alone or with MgATP in the presence of histone substrate (H4). Both activity and autophosphorylation of the p40 protein were determined. As noted previously, when the p40 S6/H4 kinase fraction was incubated with MgATP, autophosphorylation and activation were observed (Figure 16, *left and middle panels*). However, when substrate was included in the MgATP incubation, autophosphorylation of the p40 protein was decreased by ~80%. The extent of autophosphorylation correlated with the amount of enzyme activity observed in the presence and absence of competing substrate in the activation reaction. The data are consistent with the interpretation that binding of substrate to the inactive enzyme blocks MgATP access to the catalytic site thereby preventing autophosphorylation and autoactivation..

Phosphorylation of the Inactive p60 S6/H4 Kinase by the Autoactivated pp40 Form of the Enzyme - p60 S6/H4 kinase is the inactive form of the kinase which autophosphorylates slowly and does not autoactivate. Subsequent to mild trypsin proteolysis, autophosphorylation of the p40 S6/H4 kinase increases approximately 6-fold along with a concomitant increase in S6/H4 kinase activity (Figure 15). Since autophosphorylation of the p40 S6/H4 kinase resulted in its activation, it was tested whether the autoactivated p40 S6/H4 kinase could phosphorylate and activate the native p60 S6/H4 kinase. A high concentration of p60 S6/H4 kinase was incubated with Mg[γ–^{32}P]ATP for 5, 10 and 20 min alone (Figure 17, *lanes 1, 2, and 3*) and with catalytic concentrations of p40 S6/H4 kinase (Figure 17, *lanes 7, 8, and 9*). Phosphorylated proteins were resolved on a 12% polyacrylamide gel using SDS-PAGE and visualized with autoradiography. Quantitation of autoradiographic bands was performed by densitometric analysis. Autophosphorylation of the p60 S6/H4 kinase was detected at each of the time points and showed no increase from 5 min to 20 min. When the p60 S6/H4 kinase was incubated with the p40 S6/H4 kinase, phosphate incorporation increased with both forms of the kinase at all three time points. The addition of p40 S6/H4 kinase increased phosphate incorporation into the p60 S6/H4 kinase 8%, 27% and 100% at the 5, 10 and 20 min time points, respectively. However, phosphate incorporation also increased on the p40 S6/H4 kinase indicating an increase in protein kinase activity (Figure 17, *lanes 7, 8, and 9*). To test if this apparent increase was due to an increase in activity associated with the p60 S6/H4 kinase, activity assays were done by incubating inactive p60 S6/H4 kinase with the fully autoactivated pp40 S6/H4 kinase in the presence of MgATP for various time intervals and measuring subsequent kinase activity with the synthetic peptide S6-21. Since the p40 S6/H4 kinase was fully active, no additional activity would be generated from this form of the kinase, and any increase in activity could be attributed to the p60 S6/H4 kinase. Incubation of the p60 S6/H4 kinase with MgATP alone demonstrated constant S6-21 kinase activity over time which was approximately 10% of the activity of the kinase when fully activated with trypsin treatment. Incubation of the autoactivated pp40 S6/H4 kinase alone with MgATP also showed constant S6-21 kinase activity over time which was twice that of the p60 S6/H4 kinase. When the pp40 S6/H4 kinase was incubated with the p60 S6/H4 kinase and MgATP for the same time interval, the S6-21 kinase activity increased to an amount that was additive of the individual activities of each S6/H4 kinase form. No further increase in S6-21 kinase activity was observed over time. When the pp40 S6/H4 kinase activity was subtracted from the combined activities, the difference was still approximately 10% of the activity of the fully activated p60 S6/H4 kinase. These data indicate that autophosphorylation site(s) exist on the p60 S6/H4 kinase which are accessible to bimolecular autophosphorylation. However, phosphorylation of the autophosphorylation site(s) does not activate the kinase when it is in its native form.

Mechanism of p40 S6/H4 Kinase Autoactivation - Three possible mechanisms for the autoactivation of the p40 S6/H4 kinase by autophosphorylation were considered. First, an intramolecular autophosphorylation mechanism which could include phosphorylation at a pseudosubstrate domain would be characterized by a rate of autoactivation which is independent of kinase concentration. Second, intermolecular autophosphorylation which would be bimolecular and would be characterized by an autoactivation rate dependent on kinase concentration. Third, a combined mechanism where both intramolecular and intermolecular autophosphorylation occurs and one or both events promote autoactivation.

To determine which mechanism of autoactivation applied to this kinase, an activation time course was conducted at varying p40 S6/H4 kinase concentrations (Figure 18, *left panel*). At each of the p40 S6/H4 kinase concentrations, slow activation was observed at the early time points followed by a more rapid rate of activation which decreased as the kinase reached full activity. The rate at which the specific activity of the kinase changed in the linear region of the time course was plotted against kinase concentration (Figure 18, *right panel*) to indicate if the rate of activation was dependent on kinase concentration. When plotting the change in specific activity against the kinase concentration, a positive correlation of activation rate with kinase concentration was observed. Since intramolecular kinetics would have shown an activation rate which was independent of kinase concentration, these results indicate that an intermolecular event is involved in the autoactivation of the p40 S6/H4 kinase in the linear region of the activation time course.

Resolution of p40 S6/H4 Kinase Phosphoprotein Isoforms - To further elucidate the mechanism by which autophosphorylation promotes activation, the number of autophosphorylation sites was investigated by two-dimensional SDS-PAGE. Purified S6/H4 kinase was incubated with trypsin for 7 min followed by incubation in the presence Mg[γ-^{32}P]ATP for 3 or 15 min (Figure 19). The enzyme was 54% activated after the 3 min incubation and 100% activated after and 15 min incubation. The phosphorylated isoforms were then separated by isoelectric focusing in a pH 5-7 gradient followed by SDS-PAGE in a 10 % polyacrylamide gel. The pI of unphosphorylated p40 S6/H4 kinase was determined to be 6.3 based on silver staining of the two-dimensional gel.

Isoelectric focusing of pp40 S6/H4 kinase incubated for 3 min with Mg[γ-^{32}P]ATP resolved three phosphorylated proteins of Mr 40,000. The two major phosphoproteins migrated with isoelectric points of 5.8 and 5.9 compared to the minor phosphoprotein which demonstrated a pI of 6.2. At the 15 min time point, the phosphoprotein isoform with the pI of 5.8 became the major phosphoprotein. This was the most acidic pI of the three phosphoproteins, suggesting that this isoform represented the most highly phosphorylated protein. The most acidic, and presumably the most highly phosphorylated form of the enzyme, represented less than 10% of the total phosphorylated pool at the 3 min time point. However, at the 15 min time point, the relative percentage of this phosphoprotein increased to 53%. As p40 S6/H4 kinase incubation time in the presence of Mg[γ-^{32}P]ATP increased, the amount of $^{32}PO_4^{-3}$ incorporated into the most acidic isoforms of the kinase increased. This observation was consistent with the additive autophosphorylation of the p40 S6/H4 kinase at multiple sites over the time course.

Since two-dimensional SDS-PAGE analysis was not performed on the p60 S6/H4 kinase, chromatofocusing was used to obtain an estimate of the p60 S6/H4 kinase isoelectric point. Chromatofocusing works by exploiting the overall charge of a protein at a given pH. When the pH of the running buffer is greater than the pI of a protein being analyzed by chromatofocusing, the protein will have an overall negative charge and bind to the positively charged column matrix. When the pH of the running buffer reaches the isoelectric point of the protein, the protein becomes electrically neutral and is eluted from the column. The p60 S6/H4 kinase was chromatofocused on a Mono P column using a linear pH gradient from 6-4 (Figure 20). The p60 S6/H4 kinase eluted from the column at a mean pH of 5. This suggested that the p60 S6/H4 kinase has an isoelectric point lower than that of the p40 S6/H4 kinase.

Tryptic Phosphopeptide Mapping of Autophosphorylated pp40 S6/H4 Kinase - Two-dimensional SDS-PAGE analysis indicated that autophosphorylation of the S6/H4 kinase may occur on multiple sites (Figure 19). To further support this observation and to facilitate the study of each site separately, phosphopeptide mapping was used to characterize the individual autophosphorylation sites. To assure that only phosphorylation sites on the pp40 protein were being observed, the protein was further purified subsequent to autophosphorylation. For large scale production of the pp40 protein, an SDS-PAGE continuous flow preparatory cell was used. Autophosphorylated pp40 was completely resolved from proteins with only a 10% difference in molecular weight (Figure 21, *left panel*). This permitted the purification of the pp40 fragment to homogeneity (Figure 21, *right panel*). For small scale production of pp40, a method described by Luo *et al.* (77) was used. Briefly, autophosphorylated pp40 S6/H4 kinase was resolved by SDS-PAGE, and proteins were electrophoretically transferred to nitrocellulose. The pp40 band was located by autoradiography and excised. The immobilized pp40 was digested with proteases without interference from contaminating radioactivity from other phosphoproteins. To facilitate the release of peptides from the nitrocellulose membrane, the membrane was treated in a 100 mM acetic acid, 0.5% polyvinylpyrrolidone solution for 30 min at 37°C. After thoroughly washing the membrane with water, digestion of the membrane bound proteins was carried out at 37°C for 4 h in the presence of 0.2 mg/ml trypsin (300 µl) dissolved in 50 mM ammonium bicarbonate, pH 7.8. Trypsin digestion of pp40 immobilized on nitrocellulose released 97% of the bound radioactivity with phosphopeptides being digested and released in the same proportions as those observed when the pp40 protein was digested in suspension (Figure 22).

Substrate determinant studies involving the substitution of residues amino terminal to the phosphorylation site indicated that dibasic residues, one residue removed from the phosphorylated serine, were necessary for optimum phosphorylation kinetics (62). Tryptic phosphopeptide mapping was used on the assumption that the autophosphorylation sites, like other S6/H4 kinase substrates, would contain basic residues proximal to the phosphorylated residue and therefore could be isolated with trypsin digestion.

p40 S6/H4 kinase was autoactivated to 100 % activity in the presence of Mg[γ-^{32}P]ATP. The [^{32}P]pp40 S6/H4 kinase was digested 24 h with trypsin (5% mass of substrate) and spotted onto a microcrystalline cellulose plate for subsequent two-dimensional TLE/TLC analysis (Figure 23). TLE with a running buffer pH of 1.9 (2% formic acid and 8% acetic acid) resolved four phosphopeptides on the basis of their charge to mass ratios. At this pH, all of the phosphopeptides generated from the tryptic digest had net positive charges and were numbered according to increasing R_f values (Table III). TLC, which separates peptides on the basis of their relative hydrophilicities, was used to resolve the phosphopeptides in the second dimension. The buffer system recommended for the resolution of phosphopeptides (37.5% n-butanol, 25% pyridine and 7.5% acetic acid) resolved phosphopeptides 1 and 3 from 2 and 4 with no other phosphopeptides being detected (Figure 23). This was considered further evidence that four phosphopeptides were generated by exhaustive trypsin proteolysis. The individual phosphopeptides were quantitated by scraping the cellulose region containing the phosphopeptide from the plate and suspending it in an aqueous scintillation fluor (Universol Cocktail). Liquid scintillation counting of this mixture showed that phosphopeptides 1, 3 and 4 contained 22%, 19% and 16% of the total radioactivity, respectively. Phosphopeptide 2 was found to have 43% total radioactivity which represented approximately twice the level of incorporated $^{32}PO_4^{-3}$ compared to the other three phosphopeptides (Figure 22).

As with peptide mapping by TLE/TLC, reversed-phase chromatography on an HPLC C_{18} column resolved four tryptic phosphopeptides (Figure 24). Phosphopeptides were generated from tryptic digestion of [^{32}P]pp40 S6/H4 kinase immobilized on nitrocellulose as described earlier. The digest was then loaded onto a reversed-phase HPLC C_{18} column

(0.46 x 25 cm) equilibrated with 98% water, 2% acetonitrile, and 0.1% TFA. The peptides were eluted with a linear gradient to 40% acetonitrile and 0.1% TFA in 100 min at a flow rate of 1 ml/min. Phosphopeptide peaks eluted from the C_{18} column were analyzed by TLE at pH 1.9, and R_f values were used to determine the identity of each peak on the TLE/TLC phosphopeptide map (Figure 23, and Table III). Phosphopeptides 1, 2, 3, and 4 eluted from the column at 14%, 19%, 10% and 3.6% acetonitrile, respectively. This information was used in the subsequent purification of selected peptides to be sequenced.

Since the tryptic phosphopeptides were shown to have net positive charges at pH 1.9, cation exchange chromatography on a Mono S column was used to resolve the tryptic phosphopeptides (Figure 25). The Mono S column was equilibrated with 10 mM H_3PO_4, pH 2, and elution of the tryptic phosphopeptides was carried out with a 0-0.65 M NaCl linear salt gradient (50 ml) in 10 mM H_3PO_4, pH 2. Mono S chromatography of the tryptic digest resolved three phosphopeptide peaks. The first peak to elute (peak I) was not retained by the column. The second peak to elute (peak II) was retained by the column, but eluted before the gradient started. The final peak (peak III) eluted in the gradient at a NaCl concentration of 60 mM. To identify which phosphopeptides were in each peak, the peaks were pooled individually and chromatographed on the reversed-phase HPLC C_{18} column. The resulting chromatograph revealed two phosphopeptides in the unretained phosphopeptide peak eluting from Mono S (peak I). The major phosphopeptide peak eluted from the HPLC column at 10% acetonitrile and contained 66% of the total radioactivity eluted from the column. The minor peak contained 34% of the total radioactivity and eluted from the column at 13% acetonitrile. These results establish that the major phosphopeptide peak eluting at 10% acetonitrile was phosphopeptide 3 and the minor phosphopeptide peak eluting at 13% acetonitrile was phosphopeptide 1 (Table III).

When the phosphopeptide peak II, which was retained by the Mono S column, but eluted before the gradient, was chromatographed on the HPLC column, a single phosphopeptide peak eluted at 17% acetonitrile. The elution profile of this peak corresponded to phosphopeptide 2 (Table III). Finally, peak III which eluted from Mono S in the salt gradient was shown to elute from the HPLC column at 1.5% acetonitrile which corresponded to the elution of phosphopeptide 4 (Table III).

In order to characterize the phosphopeptides with respect to their isoelectric points, the tryptic phosphopeptides were subjected to two-dimensional TLE at a variety of pH's. The phosphopeptides eluted from HPLC were electrophoresed in the first dimension was at pH 1.9 as described earlier so that each phosphopeptide could be identified. The second dimension was carried out with electrophoresis buffers at two different pH's (Figure 26). At pH 3.5, phosphopeptides 2, 3, and 4 still had net positive charges (Figure 26, *upper panel*), though their migration to the cathode was slower. Phosphopeptide 1 was essentially neutral at this pH with no migration from the origin detected. At this pH, the carboxyl terminus of the peptides would become more negative, but the charge at other side groups would not be predicted to change. When the electrophoresis buffer was changed to pH 6.5 (Figure 26, *lower panel*), phosphopeptides 1, 2, and 4 exhibited net negative charges and migrated toward the anode. Phosphopeptide 3 retained a net positive charge and migrated slowly towards the cathode. At pH 6.5, negative charge increases would be expected to come from the phosphates and the amino acids glutamate and aspartate. Therefore, phosphopeptides 1, 2, and 4 are acidic near a neutral pH, whereas phosphopeptide 3 seems to contain more basic residues. The electrophoretic behavior of phosphopeptide 3 suggests that basic residues were preserved in the sequence during the trypsin digestion and/or few acidic residues occur in this phosphopeptide.

Correlation of Autophosphorylation Sites with Autoactivation -Since multiple sites could be modified by autophosphorylation during the autoactivation of the p40 S6/H4 kinase, the number and identity of the autophosphorylation sites which correlated with activation were investigated. An experimental strategy was developed based on the assumption that autophosphorylation of sites responsible for activation would occur before the modification of other sites. p40 S6/H4 kinase was autophosphorylated in the presence of Mg[γ-^{32}P]ATP at differing kinase concentrations for time intervals less than those required for full autoactivation of the kinase. p40 S6/H4 kinase autophosphorylated at each time point was resolved by SDS-PAGE on a 10% polyacrylamide gel. [^{32}P]pp40 S6/H4 kinase was then electrophoretically transferred to a nitrocellulose membrane and prepared for tryptic digestion of phosphoproteins from the membrane as described previously. After digestion of the phosphoproteins with trypsin, each digestion mixture was spotted onto a TLE plate to be resolved by electrophoresis in one dimension at pH 1.9 and visualized by autoradiography (Figure 27). In addition to autoradiographic analysis, radioactivity in the phosphopeptides on the TLE plates was quantitated using a Bioscan System 200 Imaging Scanner (Figure 28). Radioactivity in the phosphopeptide, expressed as area in the peaks, was analyzed with respect to the time of MgATP incubation and the amount of S6/H4 kinase in the incubation.

When the total amount of radioactivity in the recovered phosphopeptides was summed and analyzed with respect to the time course of total phosphorylation for each enzyme concentration (Figure 29), the pattern of phosphorylation was comparable to that observed in previous autophosphorylation/autoactivation correlation studies (Figure 18). At high enzyme concentrations (2.4 μg protein) the initial rates of autophosphorylation were nearly linear at the early time points. However, at more dilute enzyme concentrations, more than one autophosphorylation rate was observed throughout the time course. At rate of autophosphorylation markedly increased in the time interval between 3 and 5 min. By 10 min the enzyme appeared to be approaching maximum phosphorylation at both he high (2.4 μg) and intermediate (1.8 μg) S6/H4 kinase concentrations.

Quantitation of individual phosphopeptides demonstrated that two phosphopeptides predominated at the early time points for all enzyme concentrations tested (Figure 30 and 31). The calculated R_f values for these peptides were 0.32 and 0.85. These values correlate with values determined for phosphopeptides 1 and 3, respectively, in previous studies (Table III). At the lowest p40 S6/H4 kinase concentration (12.2 μg) autophosphorylation of both peptides 1 and 3 was at least twice as fast as rates of phosphorylation for the other peptides detected. At higher enzyme concentrations this rate difference decreased.

As shown by the lines with filled symbols in Figures 30 and 31, the autophosphorylation rates of phosphopeptides 1 and 3 were comparable throughout the time course at all enzyme dilutions tested. In addition, the maximum phosphorylation of phosphopeptides 1 and 3 occurred by 5 min, a time at which near maximal enzyme activation is observed (data not shown) and prior to the time required for maximum phosphorylation of the third major phosphopeptide generated in the trypsin digestion. The comparable phosphorylation rates of phosphopeptides 1 and 3, the co-elution of the peptides from Mono S, and the similar elution behavior in reversed phase HPLC analysis suggests that these two peptides may contain a common phosphorylation sequence. The TLE data shown in Figure 23 suggests the peptides may differ by an acidic or basic residue.

A third major phosphopeptide was observed in the trypsin digest of pp40 S6/H4 kinase (Figures 27, 28, 29, 30, and 31). After TLE analysis at pH 1.9 this phosphopeptide migrated comparable to phosphopeptide 2 (Table III). The rate of peptide 3 autophosphorylation was nearly linear at all enzyme concentrations tested. This is in contrast to the behavior of phosphopeptides 1 and 3 which appeared to reach a plateau level phosphorylation at early time points. At the longest time point investigated (10 min), phosphopeptide 2 was the major phosphorylated sequence at all enzyme concentrations. At this time between 34% and 59% of the total phosphate transferred occurred in phosphopeptide 2. By contrast after 3 min incubation with MgATP, the phosphate in phosphopeptide 2 account for only 17% to 20% of the total phosphate transferred. When the data for phosphopeptide 2 accumulation with time are extrapolated (Figure 30), there appears to an approximate lag time of two minutes before phosphorylation of peptide 2 begins to accumulate. The fourth phosphopeptide observed migrated in TLE at pH 1.9 with an R_f comparable to phosphopeptide 4 (Table III). This phosphopeptide is a minor component of the total pool and appears to represent a minor modification site at short MgATP incubation times.

Sequence Determination of the S6/H4 Kinase Autophosphorylation Sites - Time course and dilution studies of p40 S6/H4 kinase autophosphorylation implicated the autophosphorylation sites contained in phosphopeptides 1 and 3 in the mediation of the autoactivation event. Since the elution profiles of these phosphopeptides from reversed-phase C_{18} chromatography were known (Table III), the peptides were further purified for direct sequencing. Prior to reversed-phase HPLC chromatography, phosphopeptides from trypsin-digested [^{32}P]pp40 S6/H4 kinase were applied to a Mono S HR 5/5 column equilibrated with 10 mM H_3PO_4, pH 2, and eluted as described earlier (Figure 25). Phosphopeptide peak I from the Mono S column was then applied to a reversed-phase C_{18} HPLC column and eluted with a gradient described by Juhl and Soderling (73) as described in "Experimental Procedures." Phosphopeptides 1 and 3 eluted at 10% and 13% acetonitrile, but only phosphopeptide 3 yielded enough material to sequence. Phosphopeptide peak II, obtained from Mono S chromatography was also purified to homogeneity by chromatography on the reversed-phase column using the same elution conditions as with peak I. Phosphopeptides 2 and 3 were subjected to N-terminal sequence analysis utilizing Edman degradation chemistry (Table IV).

Sequence analysis of phosphopeptide 3 yielded SSMVGTPY. The first sequencing cycles from phosphopeptide 3 produced adjacent serines with subsequent cycles producing threonine and tyrosine before the signal was lost. The phosphoserine breakdown product dehydroalanine was detected in the first two cycles indicating that one or both of the serines may have been phosphorylated. The possibility that one or both of the serines were phosphorylated was strengthened by the location of the trypsin cleavage site relative to the serines. This would place a basic residue close to the N-terminal side of the serines which would fit the substrate determinant motif necessary for phosphorylation by the S6/H4 kinase (62). An S6/H4 kinase substrate determinant motif at this site would be consistent with the early phosphorylation kinetics observed during the autophosphorylation event.

Sequencing of phosphopeptide 2 also gave a serine and dehydroalanine breakdown product in the first cycle producing the sequence SVIDPVPAPVGDSHVDGAAK. This phosphopeptide which was characterized by a stretch of prolines separated by hydrophobic amino acids. Three aspartates were also present in this sequence which was consistent with its acidic nature at neutral pH. As with the sequence of phosphopeptide 3, the amino terminal cleavage site was adjacent to a serine indicating a possible substrate consensus sequence for the S6/H4 kinase before this residue.

In an attempt to determine additional sequence N-terminal to the serine residues, chymotrypsin digestion of the homogeneous [^{32}P]pp40 fragment was performed. For the autophosphorylation reaction, a Mg[γ-^{32}P]ATP incubation time which represented a time point before complete autoactivation was chosen. This strategy was chosen in order to minimize the contribution of phosphopeptides 2 and 4 and favor the generation of phosphosequences associated with sites 1 and 3. The autophosphorylation reaction was allowed to proceed for 8 min at 30°C before being stopped by the addition of SDS-PAGE sample buffer and boiling for 10 min. The 8 min incubation period represented a point where 90% autoactivation occurred. Homogeneous [^{32}P]pp40 was digested with chymotrypsin for 10 h at 25°C as described in "Experimental Procedures." Mono S chromatography of the chymotrypsin-generated phosphopeptides was carried out in 10 mM H_3PO_4, pH 2 as described for the tryptic phosphopeptides. The resulting chromatograph (Figure 32) contained two major peaks of radioactivity eluting before the gradient. Interestingly, these two peaks eluted in the same positions that trypsin-generated phosphopeptides 1, 2, and 3 eluted.

Both chymotryptic phosphopeptides from Mono S chromatography (Figure 32) were purified for sequencing. Chymotryptic peak II was purified to homogeneity by further chromatography on a reversed-phase C_{18} HPLC column with the same elution conditions used for the purification of the tryptic phosphopeptides for sequencing. Chymotryptic peak I from Mono S (Figure 32) did not elute from the HPLC C_{18} column and was purified to homogeneity by chromatography on a Biogel P4 superfine gel filtration column (BioRad) and subsequent chromatography on a Mono Q column in a buffer of 10 mM ammonium bicarbonate, pH 7.8 as described under "Experimental Procedures." Sequencing was then performed on both of the purified chymotrypsin-generated phosphopeptides (Table V). The sequencing of chymotryptic-peak I gave the same sequence obtained from tryptic phosphopeptide 3 which was ?SMVGTPY. Furthermore, this sequence confirmed the existence of a phosphorylation site within the sequence obtained from the tryptic phosphopeptide, since the total chymotryptic peptide was sequenced. Sequencing of chymotryptic peak II gave a similar sequence to the one obtained from tryptic phosphopeptide 2 which was ??VIDPVPA?VGD. The generation of similar phosphopeptides with trypsin and chymotrypsin digestion explains the chromatographic similarities of phosphopeptides generated by the two digests on the Mono S column. Neither trypsin nor chymotrypsin were successful in generating sequence information N-terminal to the serines.

Phosphoamino Acid Analysis of Autophosphorylated pp40 S6/H4 Kinase - Peptide sequencing of a tryptic phosphopeptide which contained an autophosphorylation site implicated in mediating the early points of autoactivation revealed the sequence SSMVGTPY. Since sequencing data could not firmly establish which residues were phosphorylated, the threonine, tyrosine and two serines were possible candidates for modification by autophosphorylation. Phosphoamino acid analysis was used to determine which of these residues was phosphorylated. p40 S6/H4 kinase was fully autoactivated in the presence of Mg[γ-^{32}P]ATP and submitted to partial acid hydrolysis in the presence of 6N HCl for 1h at 110°C. Two-dimensional TLE was then used to resolve the phosphoamino acids (Figure 33) which were visualized by autoradiography. Phosphoamino acid standards were used in the identification of radiolabelled spots and were visualized with fluorescamine. Results showed that only serine was modified during autophosphorylation of p40 S6/H4 kinase. Since the complete [^{32}P]pp40 S6/H4 kinase fragment was used in the hydrolysis, this information could be applied to all of the autophosphorylation sites, indicating that serine was modified in phosphopeptide 3 and not threonine or tyrosine. However, it was not clear if one or both of the serines at the site of autoactivation were phosphorylated.

TABLE I

Purification of the S6/H4 kinase from human placenta

Human placenta (442g) was homogenized and centrifuged as described under "Experimental Procedures." Aliquots of the S6/H4 kinase fraction were taken after each purification step and assayed for H4 kinase activity after activation by 5 min trypsin incubation and 10 min incubation with Mg[γ-^{32}P]ATP (160 dpm/pmol) at 30°C as described under "Experimental Procedures." Assays were linear throughout the substrate incubation period. Protein determinations were performed using a Bradford reagent (78).

	Volume	Conc.	Total Units	Specific Activity	% Yield	Fold Purification
	ml	*mg/ml*	*nmol/min*	*nmol/min/mg*		
Crude cell extract	1000	19	120	0.0063	100	1
DEAE cellulose	700	6.7	510	0.11	420	17
60% ammonium sulfate	125	14	650	0.37	540	59
Phosphocellulose	175	2.4	770	1.8	640	290
CM Sephadex	9.35	14	260	2.0	220	320
Sephacryl S200	45	1.2	410	7.4	340	1200
Mono S	24	1.4	400	12	340	1900
Mono Q	10	0.42	150	36	130	5700

TABLE II

Activation and substrate specificity of the S6/H4 kinase

Aliquots of purified S6/H4 kinase were incubated for 3 min at 30°C in the presence or absence of trypsin. The trypsin reaction was stopped with trypsin inhibitor and the reaction mix was further incubated for 10 min in the presence or absence of $\mathrm{Mg}[\gamma\text{-}^{32}\mathrm{P}]\mathrm{ATP}$. Substrates were added at the indicated concentrations and the assay in the presence of substrate was carried out for 5 min at 30°C. Reactions were stopped with acid precipitation of reaction mixture aliquots on filter paper.

Substrate	Substrate concentration	Protein kinase activity			
		+Trypsin		-Trypsin	
		MgATP incubation			
		0'	10'	0'	10'
	mg/ml	*nmol/min/mg*			
S6-21 (200 μM)	0.47	6	120	<1	<1
Myelin Basic Protein	1	8	100	<1	<1
H4	1	15	79	<1	<1
Protamine Sulfate	1	2	5	ND[a]	<1
MLC (3-13) (100 μM)	0.28	<1	2	ND	<1
Casein	1	1	3	ND	<1
Phosvitin	1	<1	2	ND	<1

[a] Not determined

TABLE III

R_f values of tryptic phosphopeptides from autophosphorylated pp40 S6/H4 kinase

p40 S6/H4 kinase was autophosphorylated for 1 h at 30°C in the presence of Mg[γ-^{32}P]ATP and electrophoretically transferred onto nitrocellulose. Digestion of the pp40 band from nitrocellulose with trypsin was carried out as described under "Experimental Procedures." The digestion mixture was spotted on to a microcrystalline cellulose plate for TLE in one dimension at pH 1.9. The remainder of the digest was loaded onto a reversed-phase C_{18} column and eluted as described in Figure 4. Each phosphopeptide peak eluted from HPLC was concentrated separately and analyzed by TLE at pH 1.9. Phosphopeptide spots were visualized by autoradiography, and R_f values were calculated by dividing the distance from the origin by the distance to the fastest migrating spot. R_f values for the pre-HPLC chromatographs were an average from three separate experiments. Post-HPLC R_f values were an average from two separate experiments.

Phosphopeptide Number	Pre-HPLC R_f	Post-HPLC R_f	% Acetonitrile Eluted
1	0.24	0.16	14
2	0.61	0.64	19
3	0.79	0.75	10
4	1	1	2.5

TABLE IV

Sequencing of tryptic phosphopeptides from autophosphorylated pp40 S6/H4 kinase

p40 S6/H4 kinase was autophosphorylated in the presence of $Mg[\gamma\text{-}^{32}P]ATP$ (1000-5000 dpm/pmol) for 1 hour at 30°C. Approximately 100 μg of homogeneous pp40 was digested with DPCC-treated trypsin for 24 h at 37°C and the resulting phosphopeptides were purified using a Mono S HR 5/5 column and a reversed-phase C_{18} HPLC column. Sequencing was carried out with an Applied Biosystems Model 473A sequencer.

Trypsin-generated Phosphopeptides								
1			2					
Cycle	Residue	Amount	Cycle	Residue	Amount	Cycle	Residue	Amount
		pmoles			*pmoles*			*pmoles*
1	Ser	13	1	Ser	11	10	Val	16
	DTT-S[a]	24		DTT-S	28	11	Gly	15
2	Ser	3	2	Val	54	12	Asp	8
	DDT-S	4	3	Ile	45	13	Ser	0.75
3	Met	13	4	Asp	17		DTT-S	3
4	Val	15	5	Pro	23	14	His	4
5	Gly	16	6	Val	28	15	Val	9
6	Thr	4	7	Pro	25	16	Asp	8
7	Pro	6	8	Ala	24	17	Gly	9
8	Tyr	4	9	Pro	19	18	Ala	5
						19	Ala	5
						20	Lys	1

---

[a] Dithiothreitol adduct of dehydroalanine

TABLE V

Sequencing of chymotryptic phosphopeptides from autophosphorylated pp40 S6/H4 kinase

p40 S6/H4 kinase was autophosphorylated in the presence of Mg[γ-^{32}P]ATP (1000-5000 dpm/pmol) for 8 min at 30°C. Approximately 100 μg of homogeneous pp40 was digested with sequencing grade chymotrypsin for 10 h at 25°C. The resulting phosphopeptides were purified by Mono S HR 5/5 chromatography. Peak fractions were purified by HPLC or BioGel P4 superfine column chromatography and Mono Q HR 5/5 column chromatography. Sequencing was carried out on an Applied Biosystems Model 473A sequencer as described under "Experimental Procedures."

Chymotrypsin-generated Phosphopeptides								
1			2					
Cycle	Residue	Amount	Cycle	Residue	Amount	Cycle	Residue	Amount
		pmoles			*pmoles*			*pmoles*
1	?		1	?		9	Ala	2
2	Ser	2	2	?		10	?	
	DTT-S[a]	2	3	Val	4	11	Val	1
3	Met	9	4	Ile	5	12	Gly	1
4	Val	9	5	Asp	2	13	Asp	1
5	Gly	10	6	Pro	2			
6	Thr	2	7	Val	2			
7	Pro	2	8	Pro	3			
8	Tyr	2						

[a] Dithiothreitol adduct of dehydroalanine

Figure 1. Sephacryl S200 chromatography of S6 kinases from human placenta. Proteins from 270 g of human placenta were purified through CM Sephadex chromatography as described under "Experimental Procedures." The CM Sephadex eluate was applied onto an S200 column (2.5 x 90 cm) equilibrated with Buffer B and run through the column with a flow rate of 30 ml/h. Fractions were collected (4 ml) and assayed directly (*open circles, open squares*) or after trypsin activation (*closed circles, closed squares*) with either H4 (*closed squares, open squares*) or S6-21 (*closed circles, open circles*) as the substrate. Molecular weight markers are indicated by *arrows.*

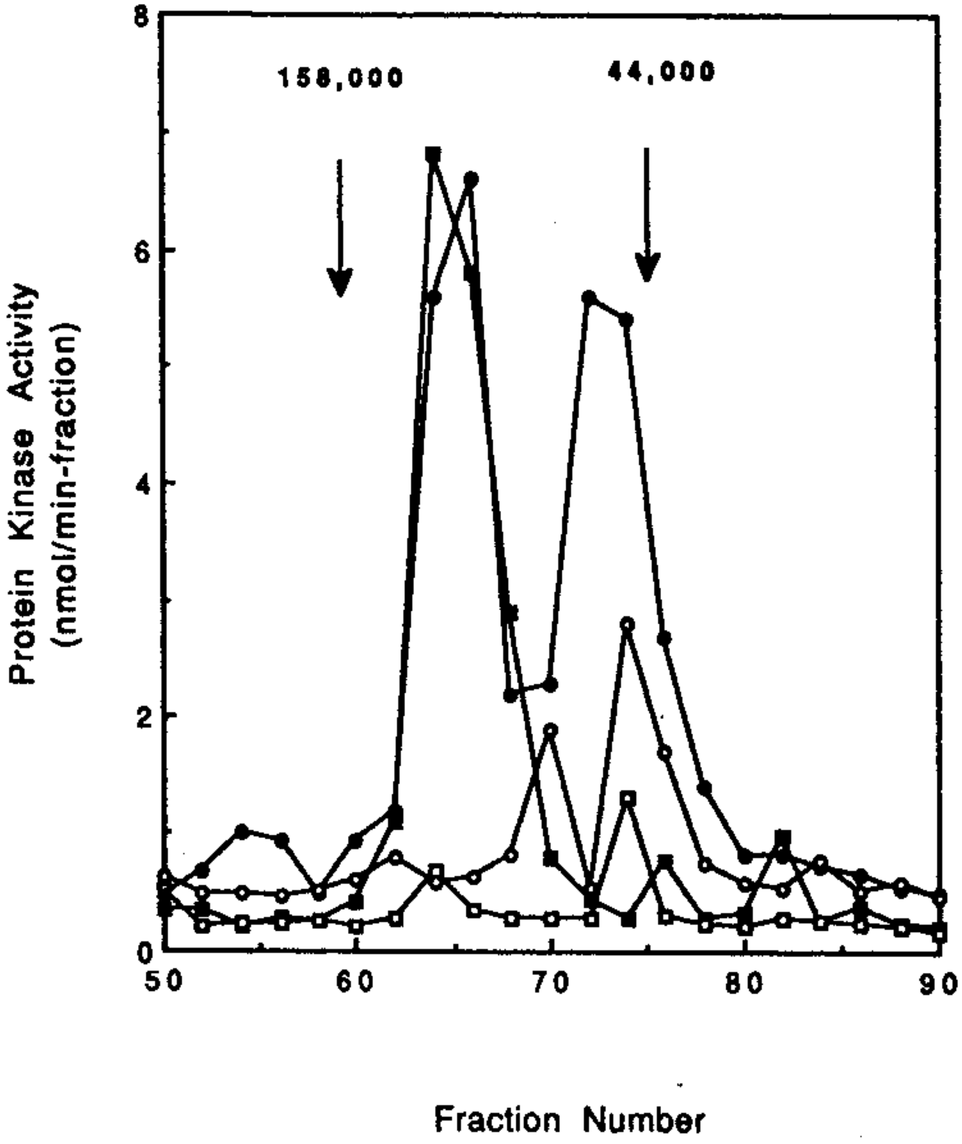
158,000
44,000
Protein Kinase Activity
(nmol/min-fraction)
Fraction Number
0
2
4
6
8
50
60
70
80
90

Figure 2. Mono S chromatography of S6/H4 kinase. S6/H4 kinase fractions (#61-68) from S200 chromatography in Fig.1 were pooled, dialyzed, and applied to a Mono S HR 5/5 column equilibrated with Buffer A. The column was washed with Buffer A and the S6/H4 kinase was eluted with a 0-0.7 M NaCl linear gradient (50 ml) in Buffer A. Fraction volumes of 1 ml were collected at a flow rate of 1 ml/min and assayed with H4 for kinase activity after activation with trypsin treatment and incubation with MgATP as described under "Experimental Procedures."

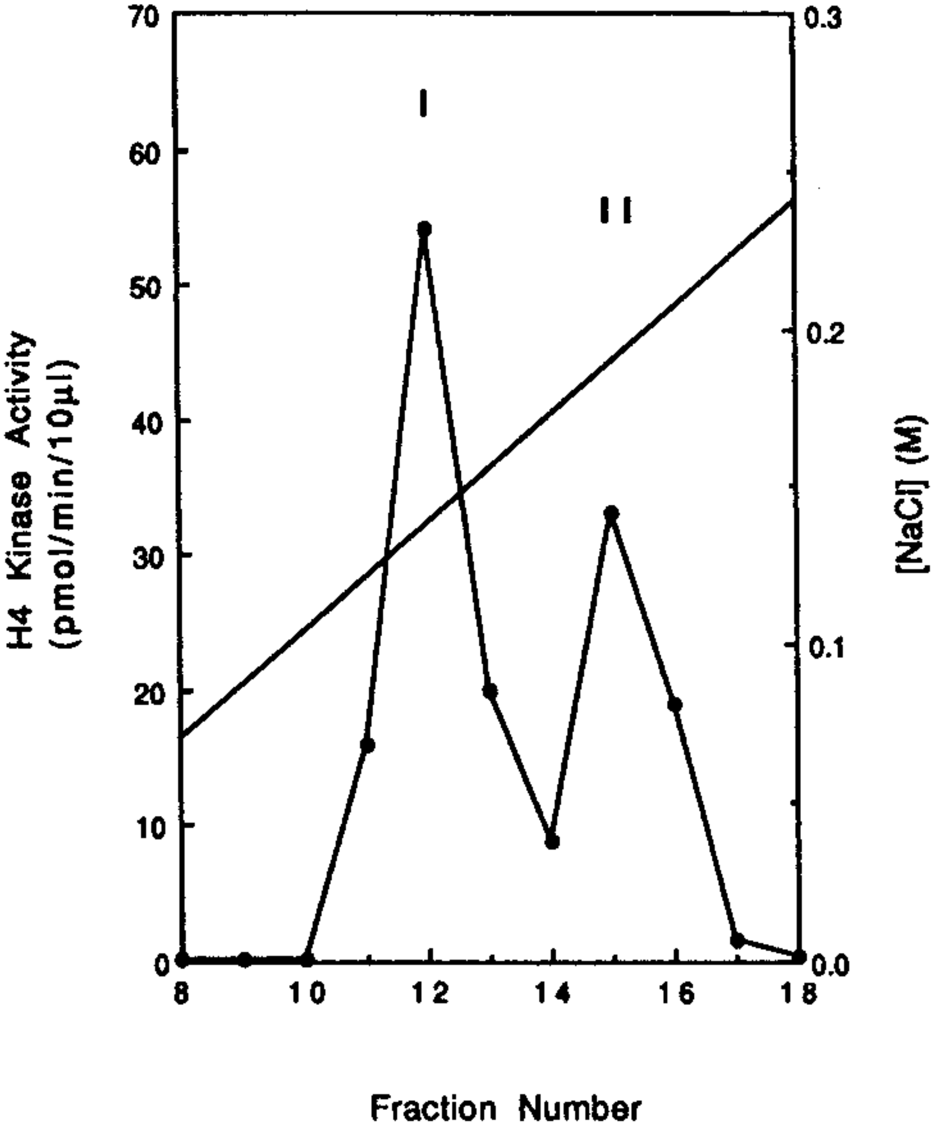
70
60
50
40
30
20
10
0
0.3
0.2
0.1
0.0
I
II
8
10
12
14
16
18
H4 Kinase Activity (pmol/min/10μl)
[NaCl] (M)
Fraction Number

Figure 3. Mono Q chromatography of S6/H4 kinase. S6/H4 kinase from 260 g human placenta was purified through the Mono S chromatography as described in "Experimental Procedures." Peak I of S6/H4 kinase activity eluted from Mono S (Fig.2) was pooled, dialyzed, and applied to a Mono Q HR 5/5 column equilibrated with Buffer C. The column was washed with Buffer C and the S6/H4 kinase was eluted with a 0-0.7 M NaCl linear gradient (50 ml) in Buffer C. Fraction volumes of 1 ml were collected at a flow rate of 1 ml/min and assayed with S6-21 for kinase activity after activation with trypsin treatment and incubation with MgATP.

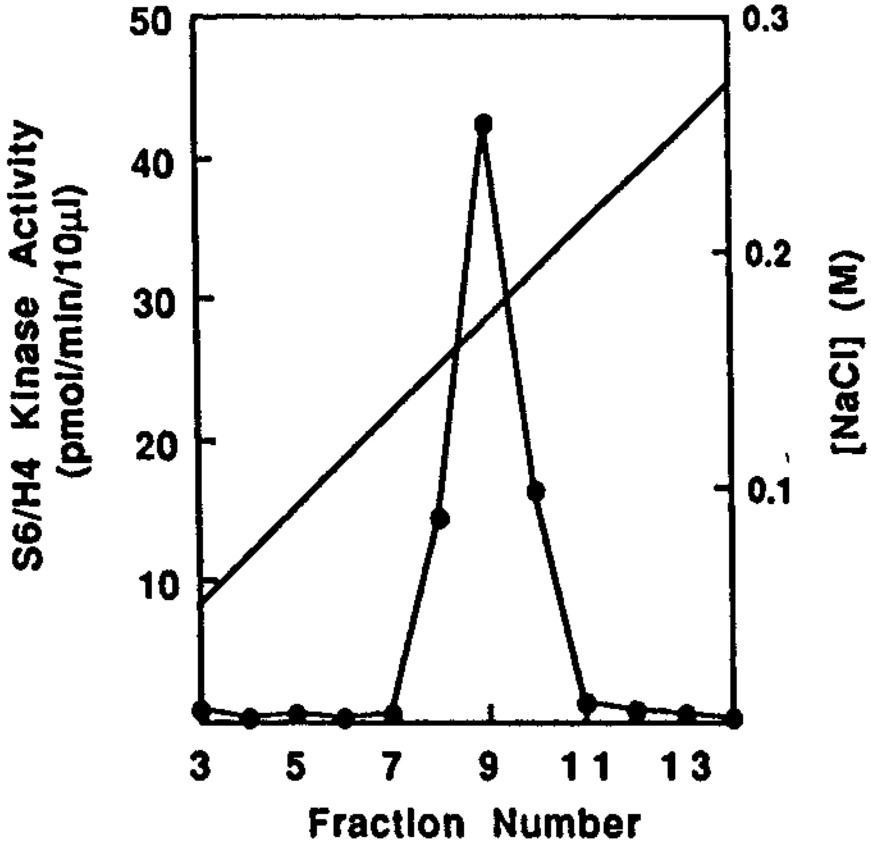
S6/H4 Kinase Activity (pmol/min/10µl)
50
40
30
20
10
0.3
0.2
0.1
[NaCl] (M)
3
5
7
9
11
13
Fraction Number

Figure 4. HPLC analysis of S6-21 phosphorylated by the S6/H4 kinase. S6-21 was incubated for 30 min at 30°C with Mg[γ-^{32}P]ATP and the trypsin-activated S6/H4 kinase obtained from Fig.1 (#61-68). Phosphorylated S6-21 was purified from residual Mg[γ-^{32}P]ATP on an AG 1-X8 column as described under "Experimental Procedures." Reversed-phase HPLC analysis was performed on the phosphorylated S6-21 peptide (*panel A*) and on the phosphorylated S6-21 peptide after digestion with thermolysin (*panel B*).

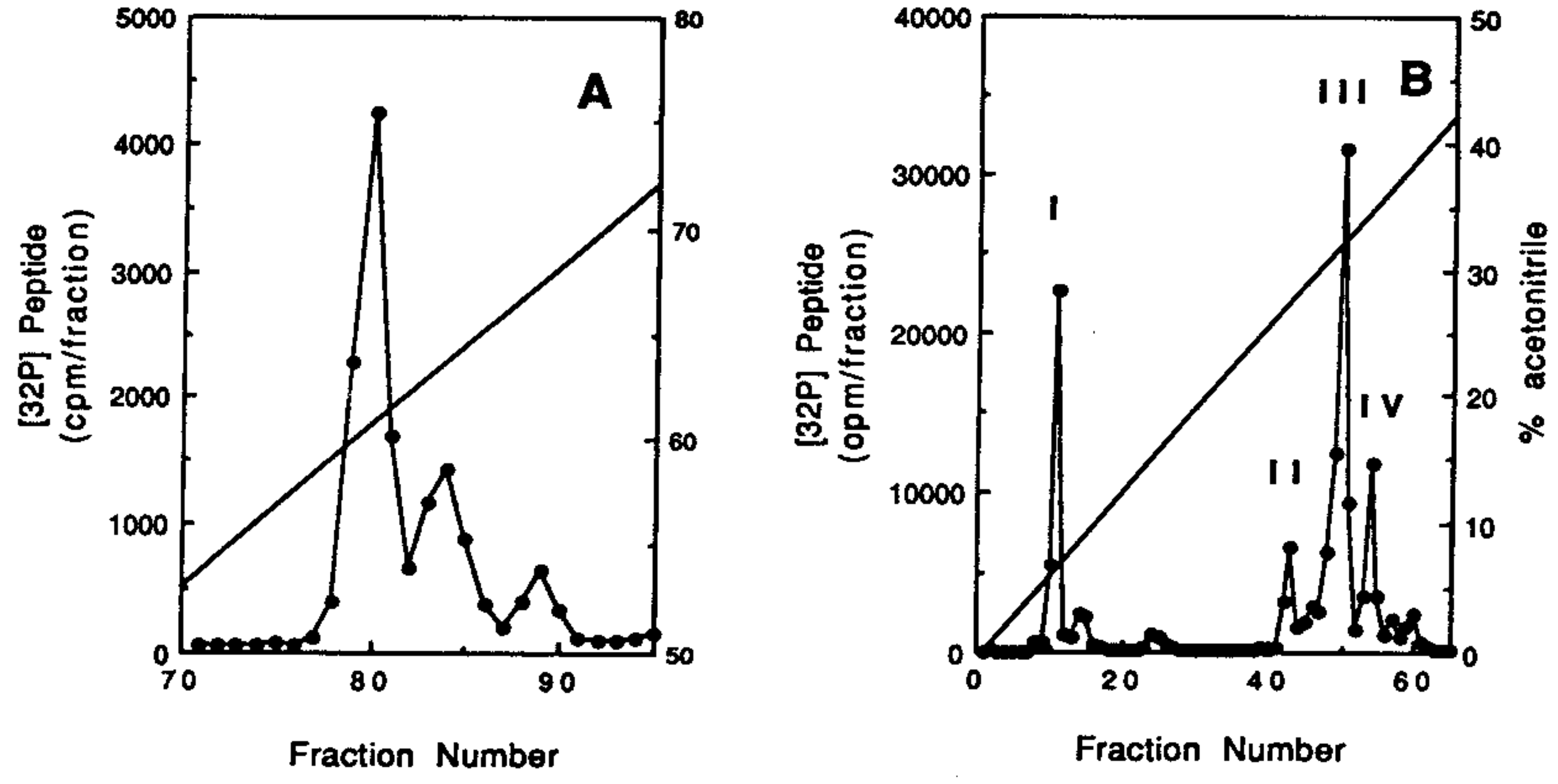
A
[32P] Peptide (cpm/fraction)
0
1000
2000
3000
4000
5000
50
60
70
80
70
80
90
Fraction Number
B
I
II
III
IV
[32P] Peptide (opm/fraction)
0
10000
20000
30000
40000
% acetonitrile
0
10
20
30
40
50
0
20
40
60
Fraction Number

Figure 5. HPLC analysis of S6-21 phosphorylated by an S6 kinase isolated from human placenta. S6-21 was incubated for 30 min at 30°C with Mg[γ-^{32}P]ATP and the trypsin-activated S6 kinase which eluted in fractions #71-76 after the S6/H4 kinase in Fig.1. Analysis of the phosphoS6-21 was performed as described in Fig.4 with reversed-phase HPLC analysis of the phosphoS6-21 (*panel A*) and the thermolysin digested phosphopeptide (*panel B*).

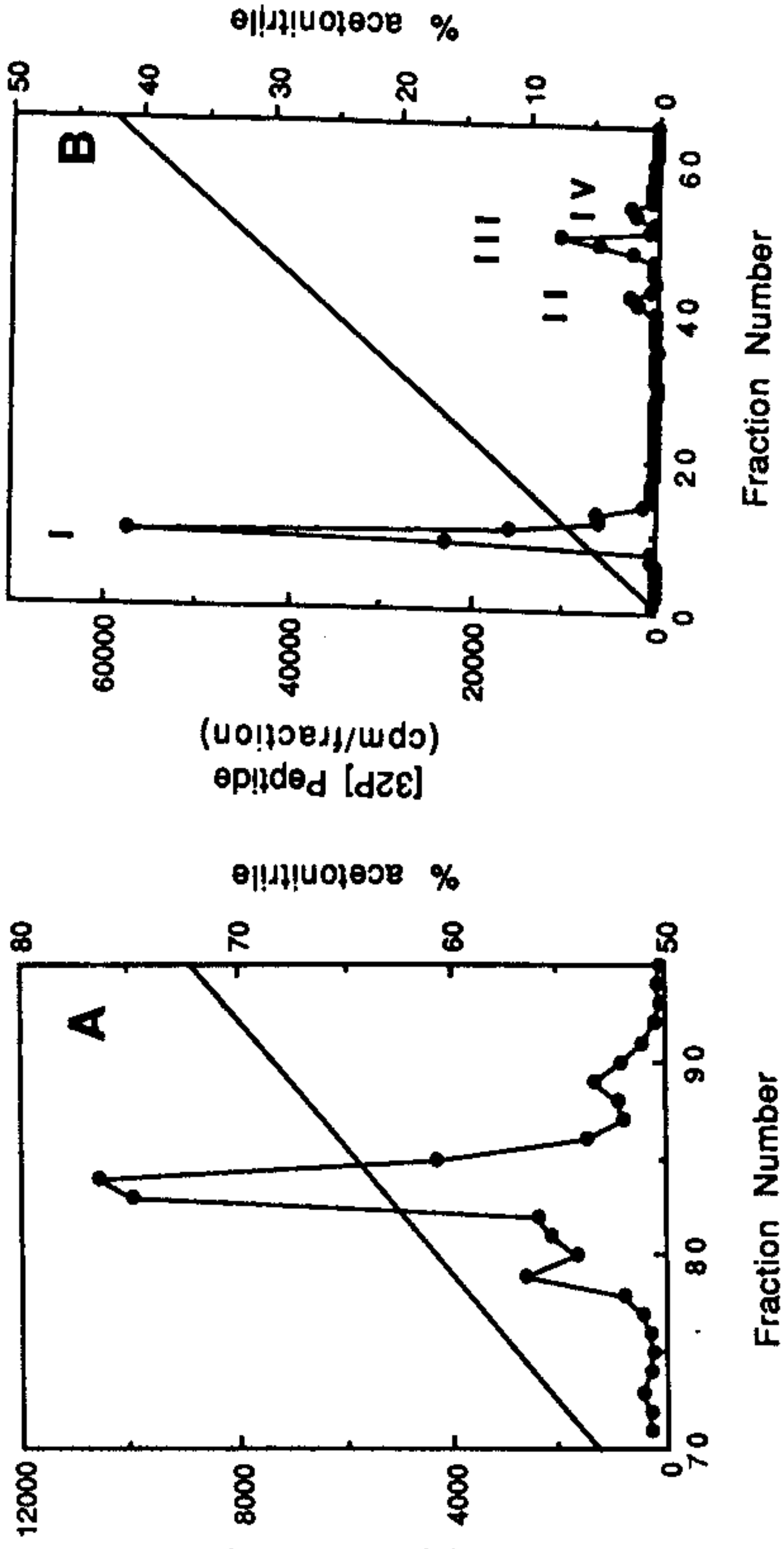
A
[32P] Peptide (cpm/fraction)
12000
8000
4000
0
70
80
90
Fraction Number
% acetonitrile
80
70
60
50
B
[32P] Peptide (cpm/fraction)
60000
40000
20000
0
0
20
40
60
Fraction Number
% acetonitrile
50
40
30
20
10
0
I
II
III
IV

Figure 6. Identification of the S6/H4 kinase as a protein of Mr 60,000. Purified S6/H4 kinase from Mono Q chromatography shown in Fig. 3 was subjected to SDS-PAGE with Coomassie Blue staining (*lane A*), autophosphorylation with Mg[γ-^{32}P]ATP followed by autoradiography (*lane B*), photoaffinity-labeling with 8-azido-[α-^{32}P]ATP and autoradiography (*lane C*), and Western blot analysis using polyclonal antisera raised against a peptide sequence derived from the catalytic domain of the cyclic AMP-dependent protein kinase (*lane D*). Protocols used in these experiments are detailed in "Experimental Procedures."

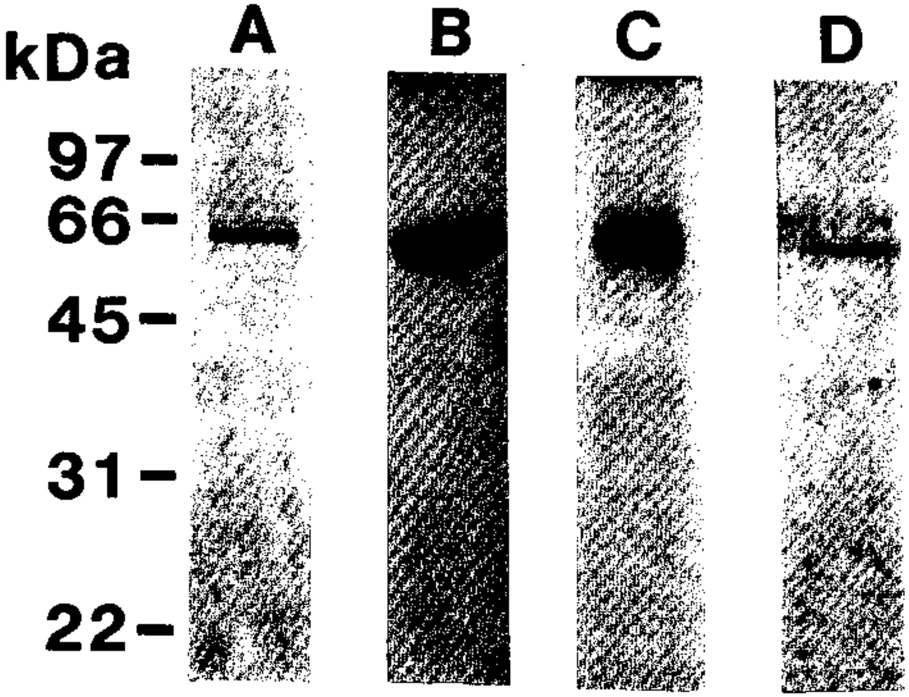
kDa
A
B
C
D
97
66
45
31
22

Figure 7. Autophosphorylation and trypsin activation of two S6/H4 kinase isoforms resolved by Mono S chromatography. The two S6/H4 kinase peaks resolved in Fig. 2 were pooled separately, dialyzed, and applied to a Mono Q column equilibrated with Buffer C. Elution of each S6/H4 kinase isoform from Mono Q was performed as described in Fig. 3. Assays for S6/H4 kinase activity were conducted after activation with trypsin treatment and incubation with MgATP. *Left Panel :* Approximately 1 μg of Mono Q purified Mono S peak I (*lane 1*) and Mono S peak II (*lane 2*) were incubated for 5 min at 30°C in the presence of Mg[γ-^{32}P]ATP. Reactions were stopped by the addition of SDS-PAGE sample buffer and boiling. The samples were then subjected to SDS-PAGE on a 7.5% acrylamide gel. Phosphorylated bands were visualized by autoradiography as described under "Experimental Procedures." *Right Panel :* Mono S S6/H4 kinase peak I (*lanes 1 and 2*) and peak II (*lanes 3 and 4*) purified from Mono Q were assayed for H4 kinase activity with (*lanes 1 and 3*) and without (*lanes 2 and 4*) trypsin treatment before a 10 min incubation with MgATP.

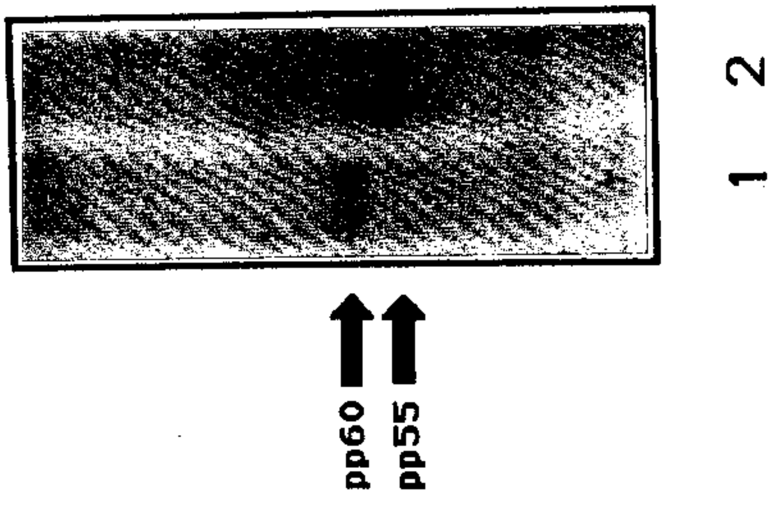
pp60
pp55
1
2

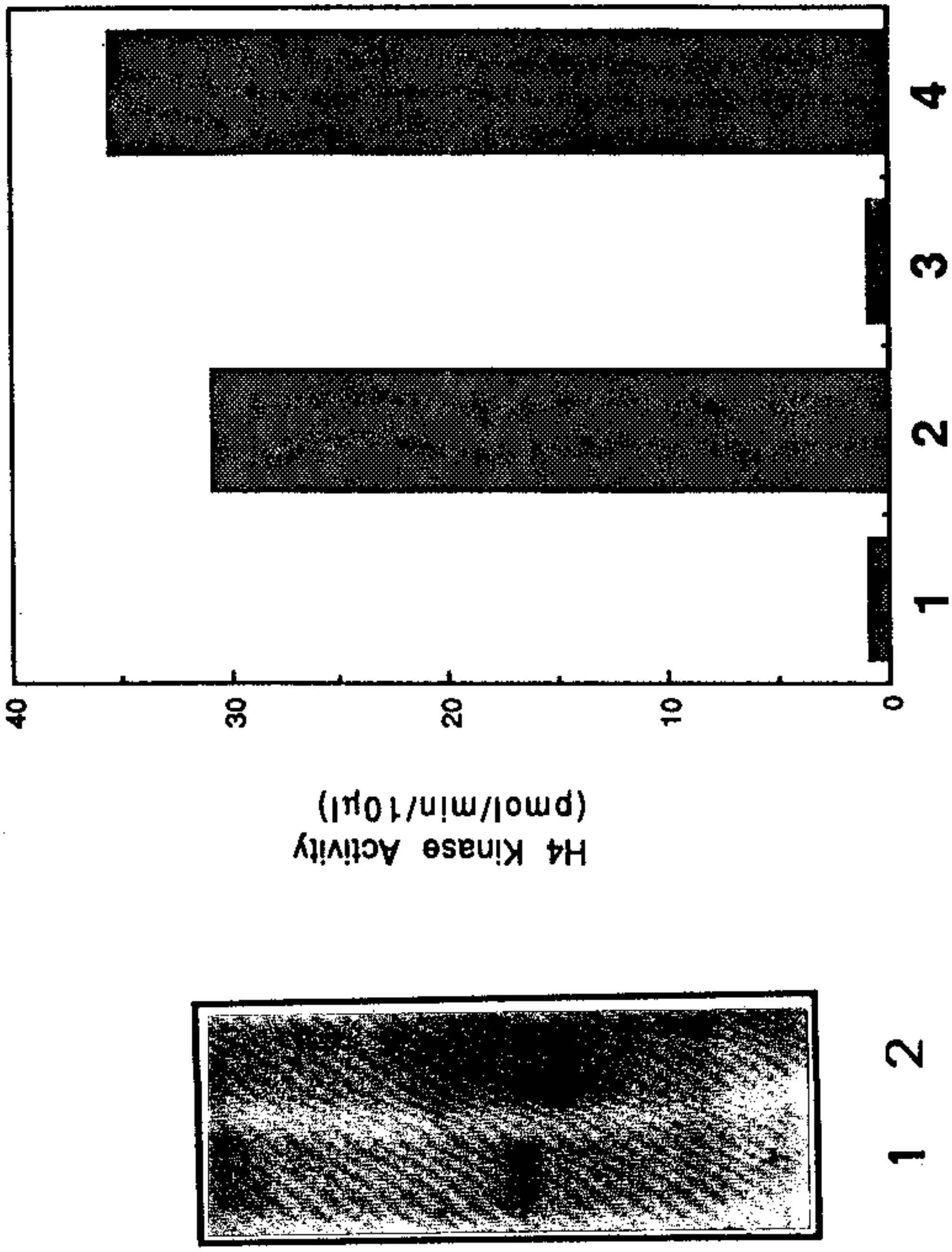
H4 Kinase Activity
(pmol/min/10µl)
0
10
20
30
40
1
2
3
4

Figure 8. Resolution of S6/H4 kinase and p70 S6 kinase in placenta extracts by chromatography on Mono Q. Human placenta (50 g) was homogenized in Buffer A and the extract was centrifuged for 20 min at 12,000 *g* and 60 min at 118,000 *g*. The supernatant fraction was applied to a Mono Q HR 5/5 column equilibrated with Buffer C. Proteins were eluted as described in Fig. 3 and aliquots from each fraction were assayed for kinase activity or subjected to Western blot analysis. Kinase assays were conducted in the presence (*shaded bars*) or absence (*open bars*) of trypsin and MgATP activation as described in "Experimental Procedures." Activity was determined with S6-21 (*middle panel*) or H4 (*lower panel*). Proteins resolved by SDS-PAGE on a 10% polyacrylamide gel and blotted to nitrocellulose were probed with affinity-purified polyclonal antibodies raised against a peptide in the catalytic domain of the p70 S6 kinase (*upper panel*). Only the portion of the gel containing protein is shown.

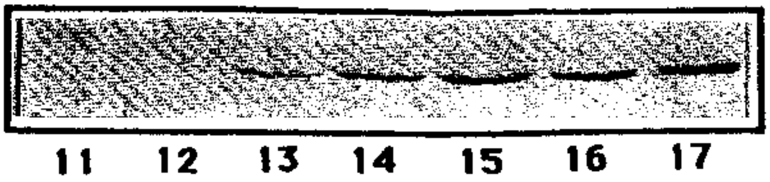
11
12
13
14
15
16
17

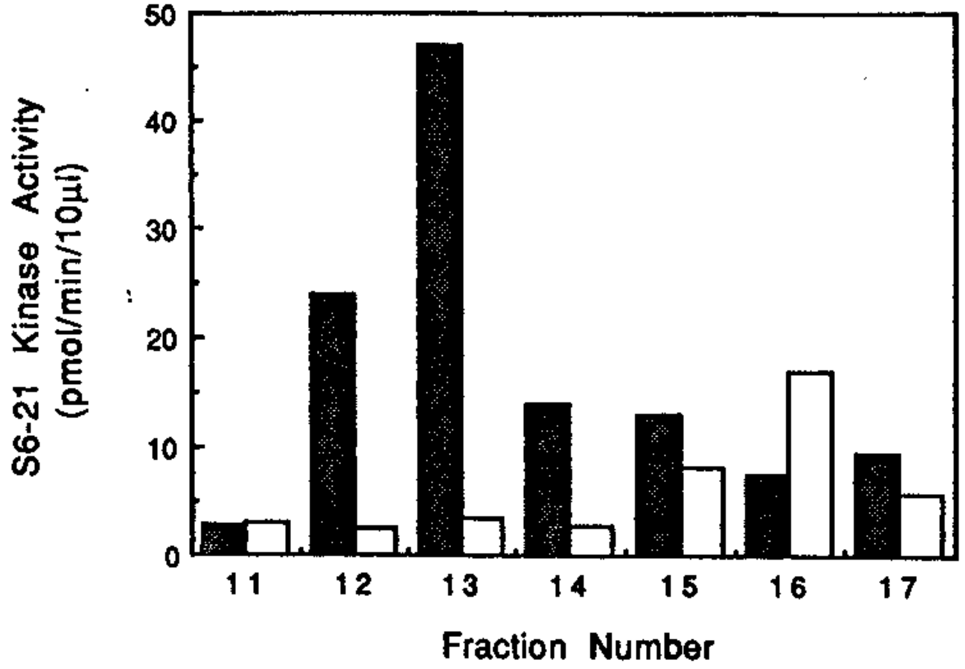
S6-21 Kinase Activity (pmol/min/10µl)
0
10
20
30
40
50
11
12
13
14
15
16
17
Fraction Number

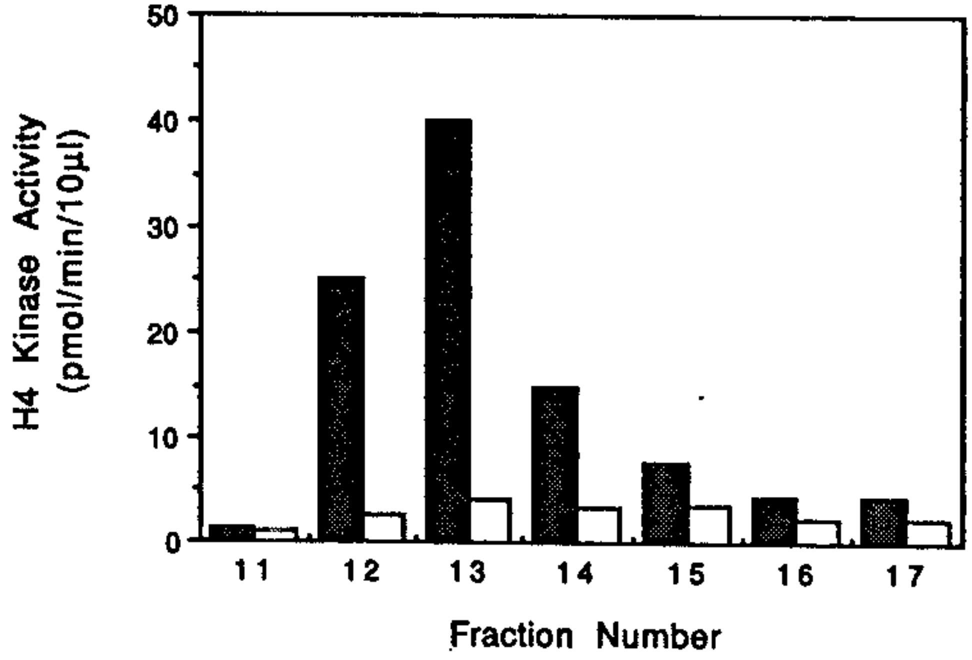
H4 Kinase Activity (pmol/min/10µl)
0
10
20
30
40
50
11
12
13
14
15
16
17
Fraction Number

Figure 9. Time course for S6/H4 kinase activation and autophosphorylation. Aliquots of purified S6/H4 kinase were trypsin digested for the time intervals indicated. Following this digestion period, reactions were stopped with addition of soybean trypsin inhibitor and incubated for 10 min in the presence of Mg[γ-^{32}P]ATP at 30°C. Protein kinase activity was determined by the addition of H4 (1 mg/ml) for 5 min (*closed circles*). Separate reaction mixtures were incubated with trypsin and Mg[γ-^{32}P]ATP for the same time intervals and the reaction was stopped with SDS sample buffer. The phosphorylated proteins were analyzed by SDS-PAGE and autoradiography. Phosphorylated bands at Mr 40,000 (*open circles*) and 60,000 (*closed squares*) were excised and radioactivity was quantitated by liquid scintillation counting of the dried gel. Details of techniques used here are provided in "Experimental Procedures."

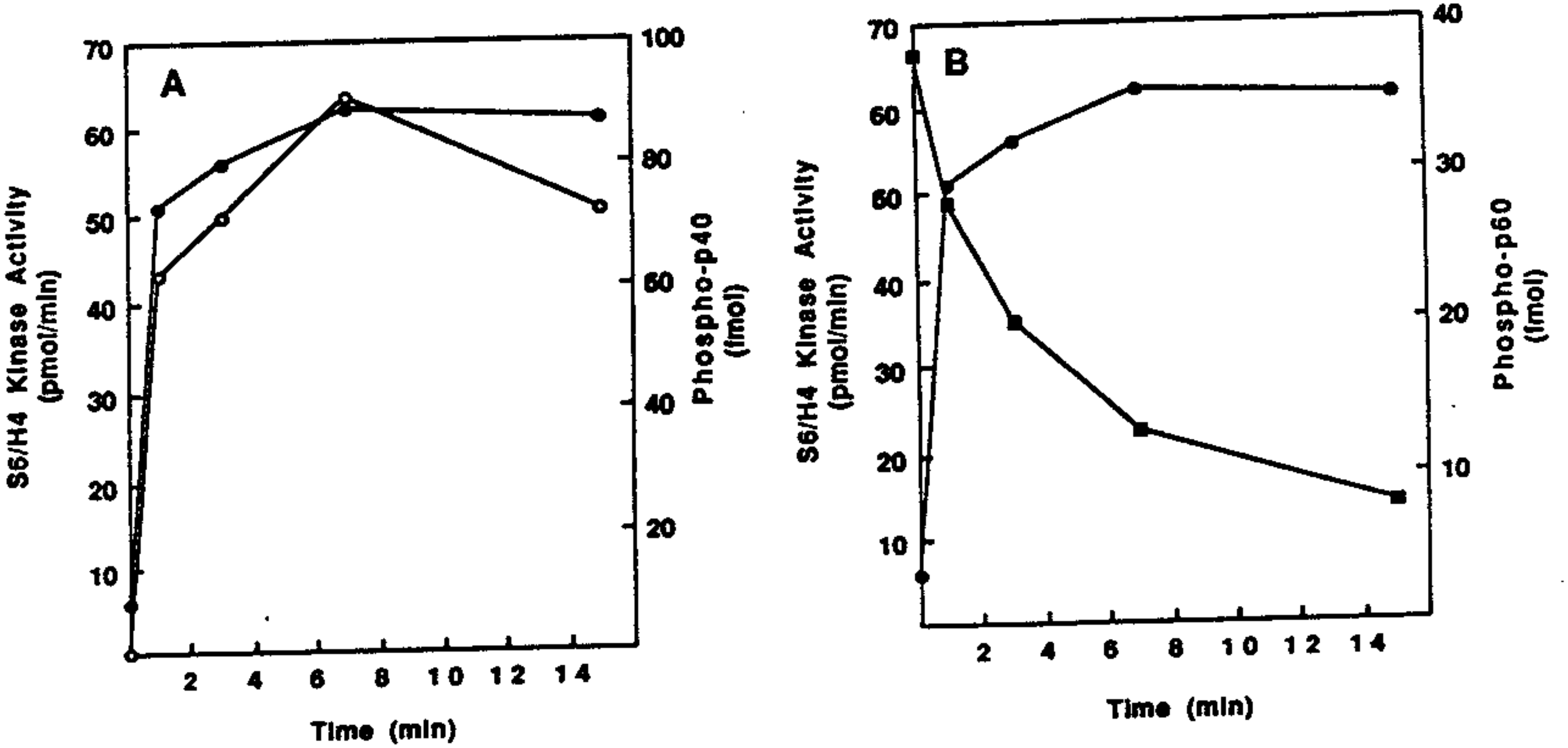
A
S6/H4 Kinase Activity
(pmol/min)
10
20
30
40
50
60
70
Phospho-p40
(fmol)
20
40
60
80
100
2
4
6
8
10
12
14
Time (min)
B
S6/H4 Kinase Activity
(pmol/min)
10
20
30
40
50
60
70
Phospho-p60
(fmol)
10
20
30
40
2
4
6
8
10
12
14
Time (min)

Figure 10. Autophosphorylation of native and trypsin-treated S6/H4 kinase. Purified S6/H4 kinase (0.27 μg) was incubated for 15 min at 30°C in the absence (*lane 1*) or presence (*lane 2*) of trypsin. The trypsin reaction was stopped with soybean trypsin inhibitor and the reaction mixtures were incubated with Mg[γ-^{32}P] ATP for 10 min at 30°C. The autophosphorylation reactions were stopped with SDS sample buffer and the samples were analyzed by SDS-PAGE on a 10% polyacrylamide gel and autoradiography as described in "Experimental Procedures." Molecular weights were calculated using an SDS standard protein mix obtained from BioRad.

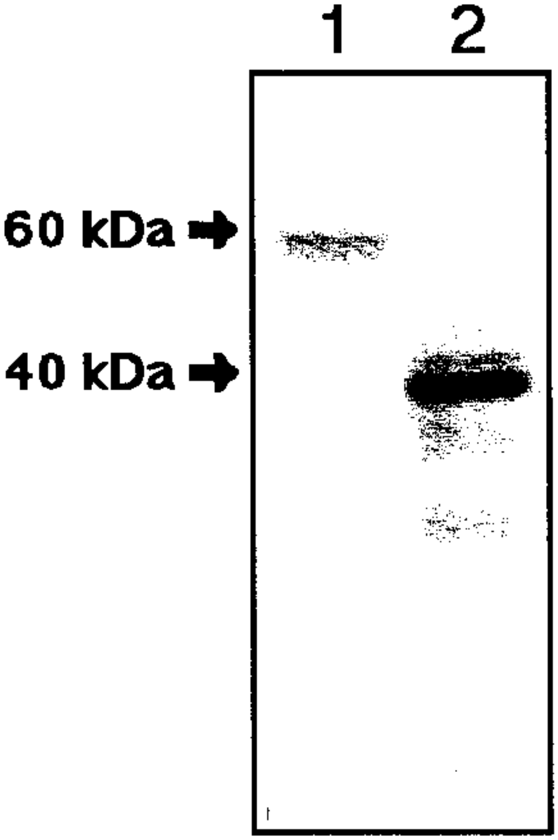
1
2
60 kDa
40 kDa

Figure 11. Mono Q chromatography of trypsin-treated S6/H4 kinase. Purified S6/H4 kinase from Mono Q chromatography was digested with trypsin for 7 min at 30°C. After termination of the proteolytic reaction with soybean trypsin inhibitor, the reaction mixture was applied to a Mono Q column equilibrated in Buffer C. Column washing and elution were carried out as in Fig. 3, and the A280 nm (*dotted line*) and S6/H4 kinase activity (*closed circles*) were determined in each fraction. Protein kinase assays were conducted in the presence of MgATP activation using S6-21 as substrate.

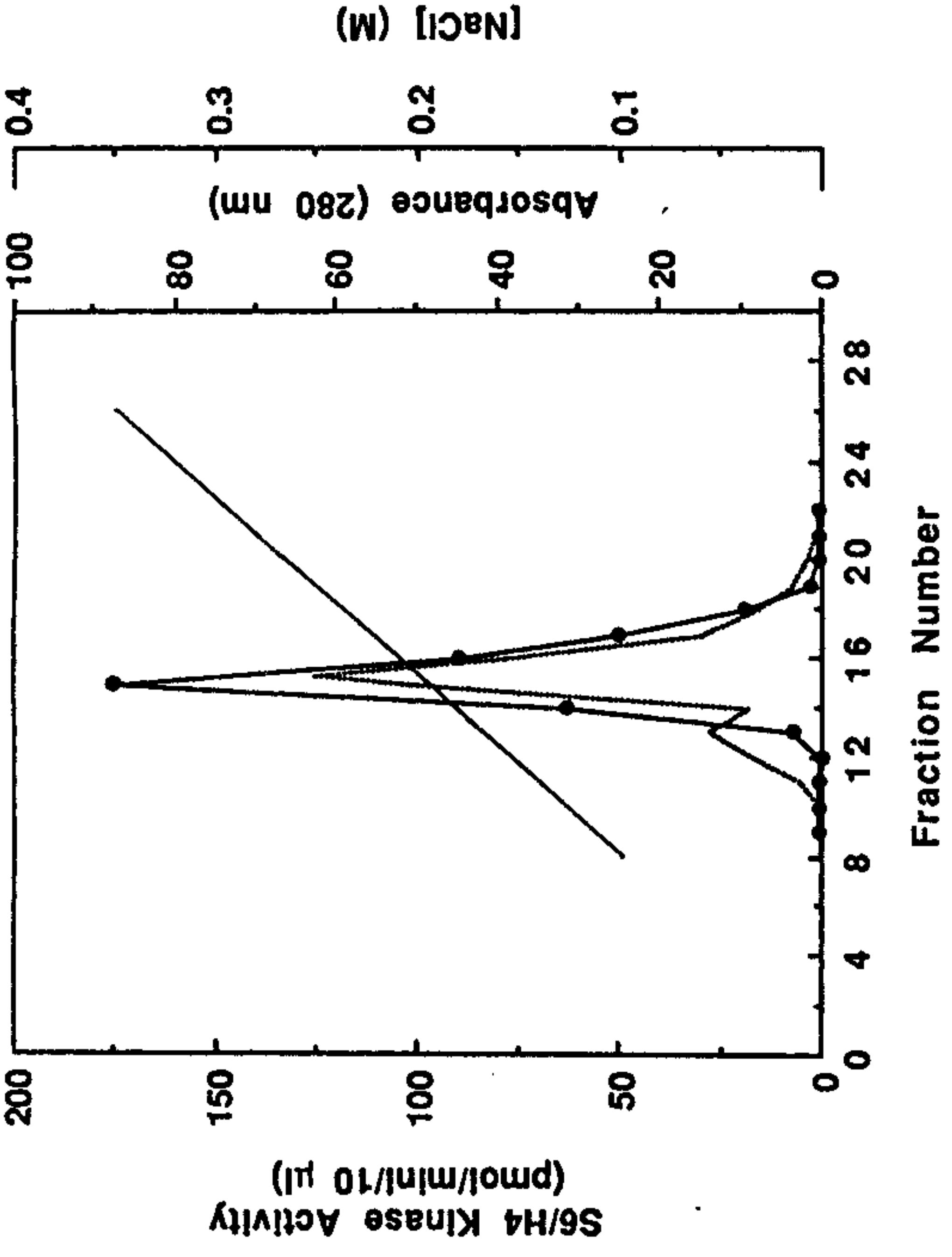
S6/H4 Kinase Activity
(pmol/min/10 µl)
0
50
100
150
200
Fraction Number
0
4
8
12
16
20
24
28
Absorbance (280 nm)
0
20
40
60
80
100
[NaCl] (M)
0.1
0.2
0.3
0.4

Figure 12. Correlation of MgATP-dependent S6/H4 kinase activation with a protein of Mr 40,000. Aliquots of trypsin-treated S6/H4 kinase eluted from Mono Q chromatography (shown in Fig.11) were analyzed by SDS-PAGE and stained with Coomassie Blue (*upper panel*). The same fractions were incubated in the presence of Mg[γ-^{32}P]ATP for 45 min at 30°C and analyzed by SDS-PAGE on a 10% polyacrylamide gel and autoradiography (*middle panel*). S6-21 kinase activity from each of the fractions was also determined after activation with MgATP (*lower panel*) as described under "Experimental Procedures."

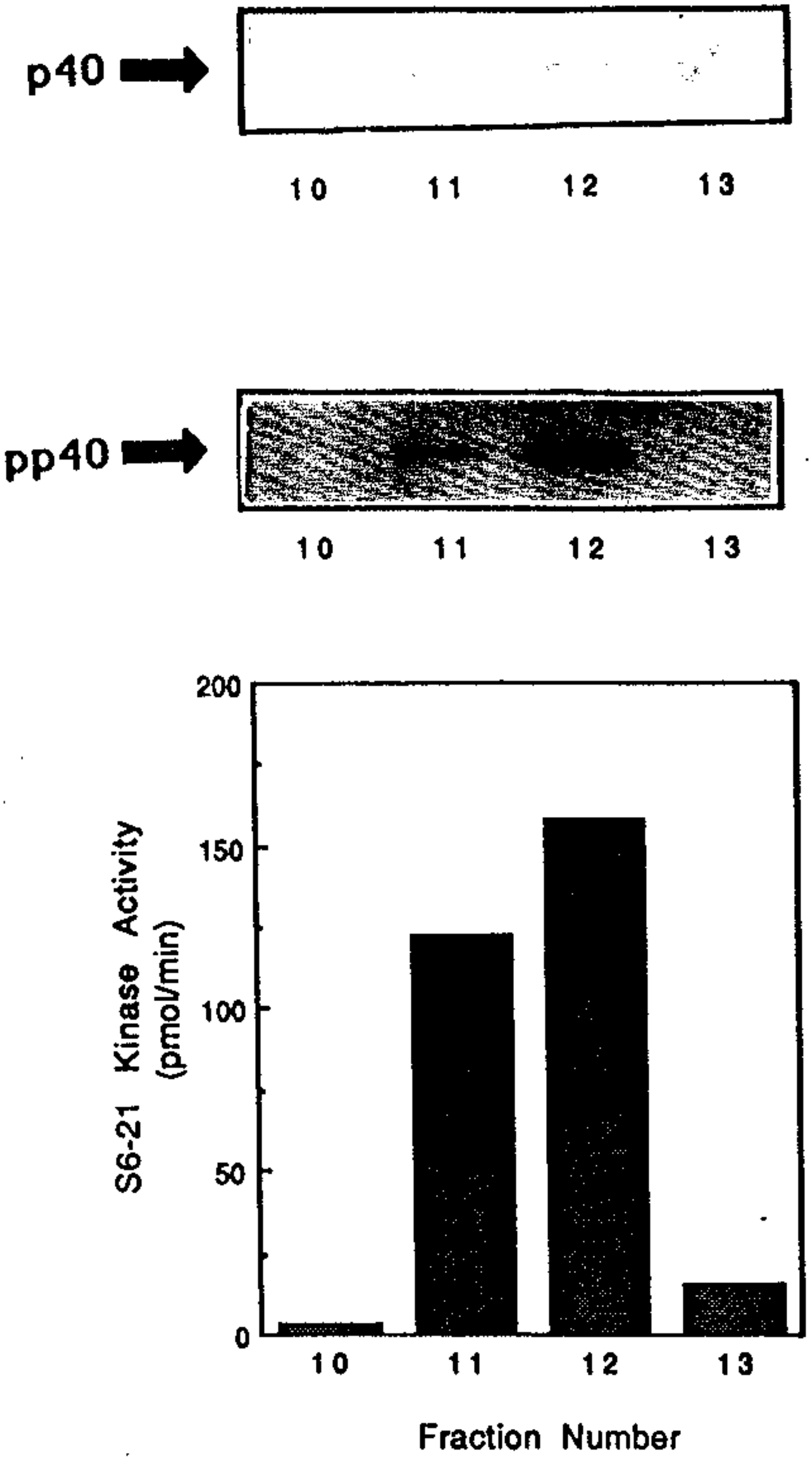
p40
10
11
12
13
pp40
10
11
12
13
S6-21 Kinase Activity (pmol/min)
200
150
100
50
0
10
11
12
13
Fraction Number

Figure 13. Resolution of two S6/H4 kinase isoforms by Mono Q chromatography after incubation with MgATP. Trypsin digestion and Mono Q chromatography were carried out as described in Fig.11 except that, subsequent to digestion with trypsin, the S6/H4 kinase was incubated for 10 min at 30°C in the presence of MgATP before loading onto Mono Q. Eluted fractions were assayed for H4 kinase activity with a further 10 min Mg[γ-^{32}P]ATP incubation at 30°C before incubation with H4 (1 mg/ml) for an additional 10 min at 30°C.

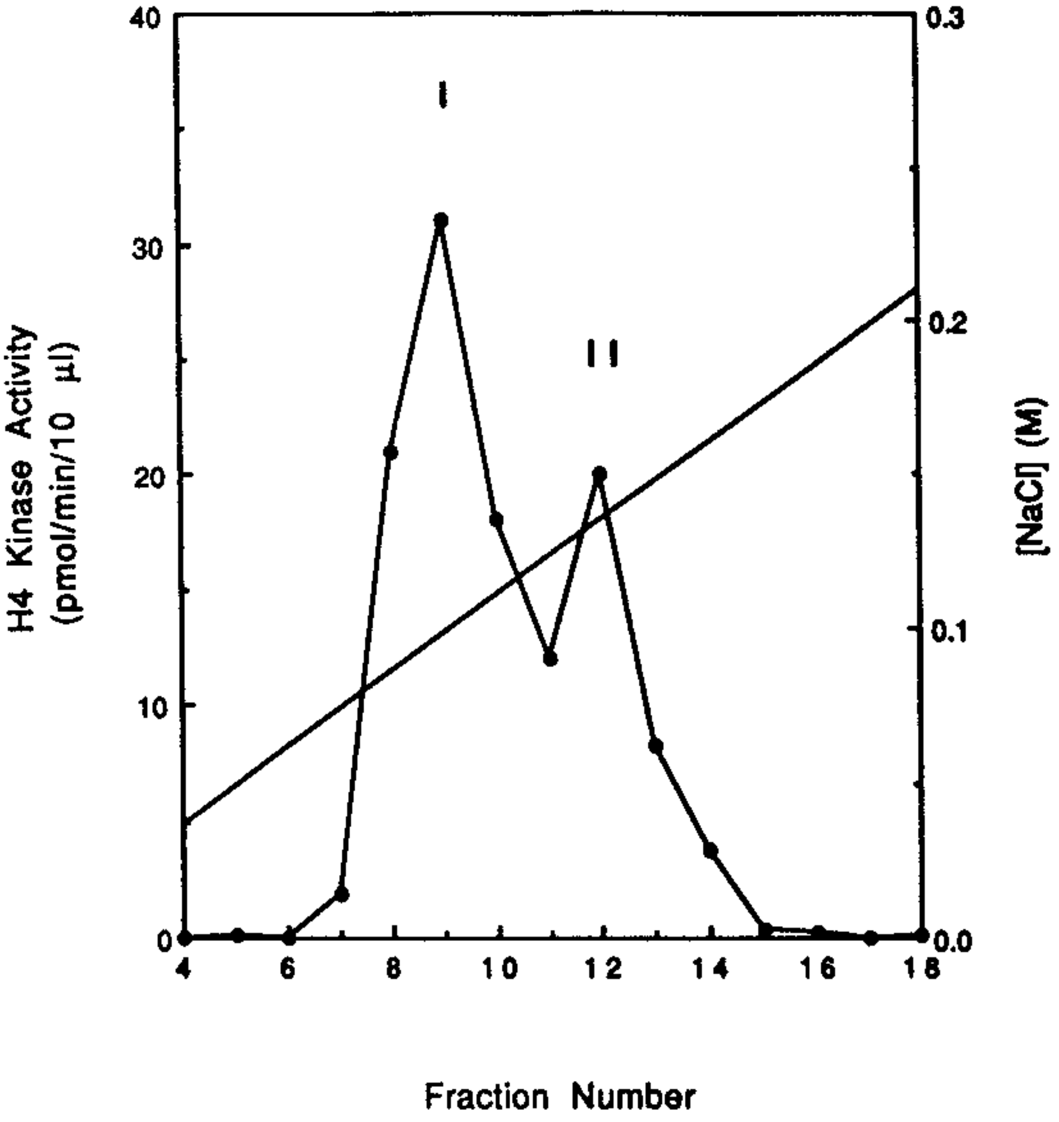
I
II
40
30
20
10
0
0.3
0.2
0.1
0.0
4
6
8
10
12
14
16
18
H4 Kinase Activity (pmol/min/10 µl)
[NaCl] (M)
Fraction Number

Figure 14. Autoactivation time course of pp40 S6/H4 kinase peaks resolved by Mono Q chromatography. Aliquots of the trypsin and MgATP-activated S6/H4 kinase peak I (*closed circles*) or peak II (*open circles*) from Mono Q chromatography in Fig.13 were incubated with Mg[γ-^{32}P]ATP for designated time intervals before the addition of S6-21 (190 μM). S6-21 kinase activity was assessed as described under "Experimental Procedures."

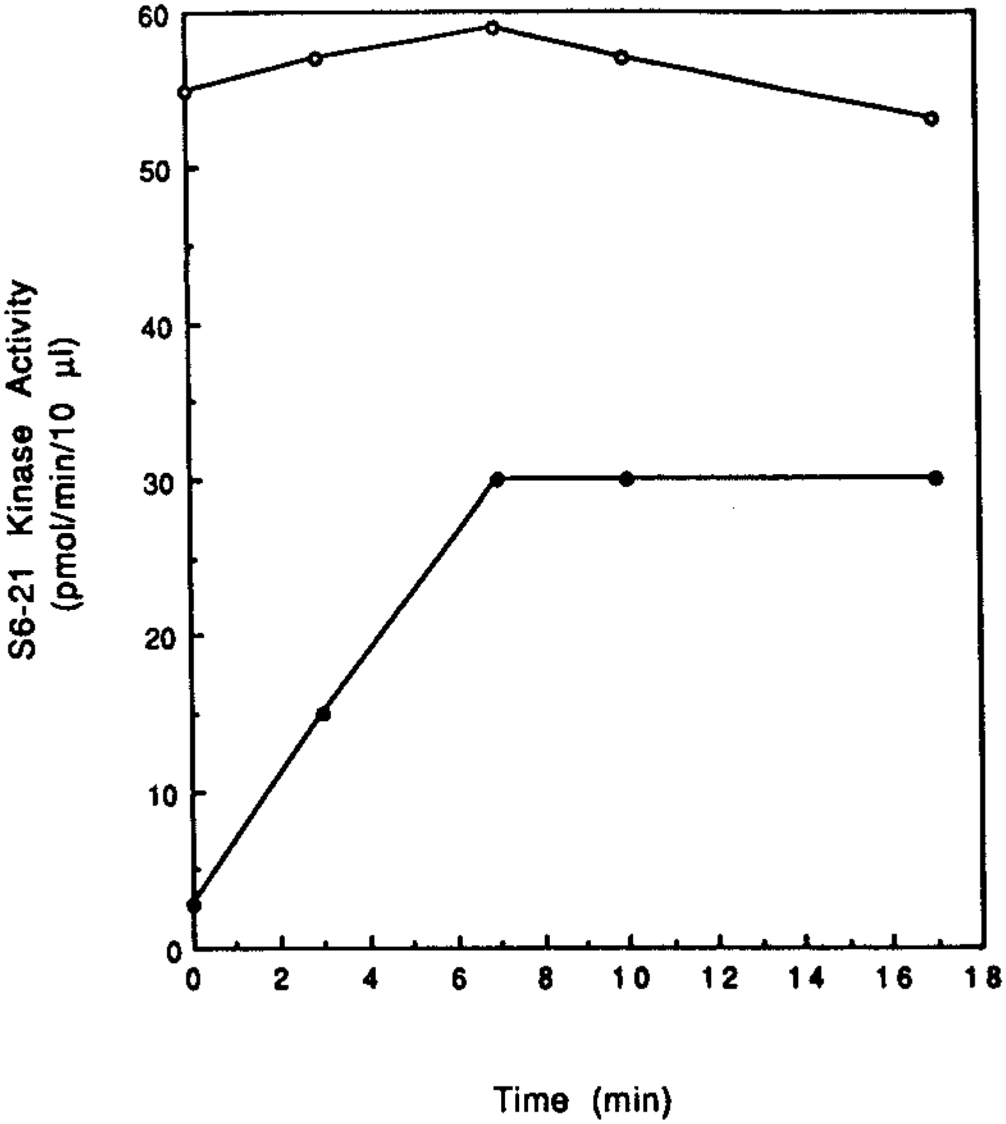
S6-21 Kinase Activity
(pmol/min/10 µl)
60
50
40
30
20
10
0
0
2
4
6
8
10
12
14
16
18
Time (min)

Figure 15. Correlation of trypsin-treated S6/H4 kinase activation and autophosphorylation of p40. Aliquots of trypsin-treated S6/H4 kinase eluted from Mono Q chromatography (shown in Fig.11) were incubated with Mg[γ-^{32}P]ATP for designated time intervals. Reaction mixtures were monitored for S6-21 kinase activity (*lower panel; closed circles*) or stopped with SDS sample buffer for SDS PAGE on a 10% polyacrylamide gel and autoradiographic analysis (*upper panel*). The phosphorylated bands at Mr 40,000 were excised and radioactivity was quantitated by liquid scintillation counting of the dried gels (*lower panel; open circles*). The *arrow* indicates the position of the autophosphorylated pp40 S6/H4 kinase.

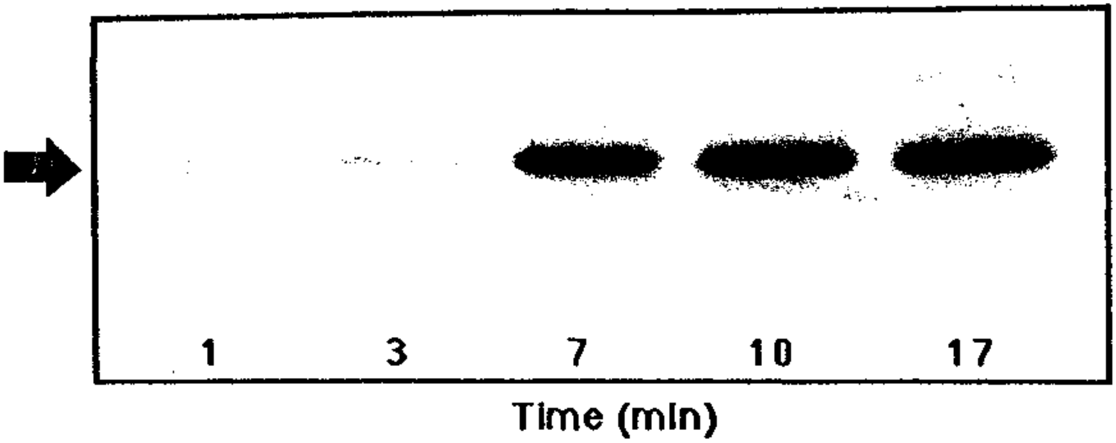
1
3
7
10
17
Time (min)

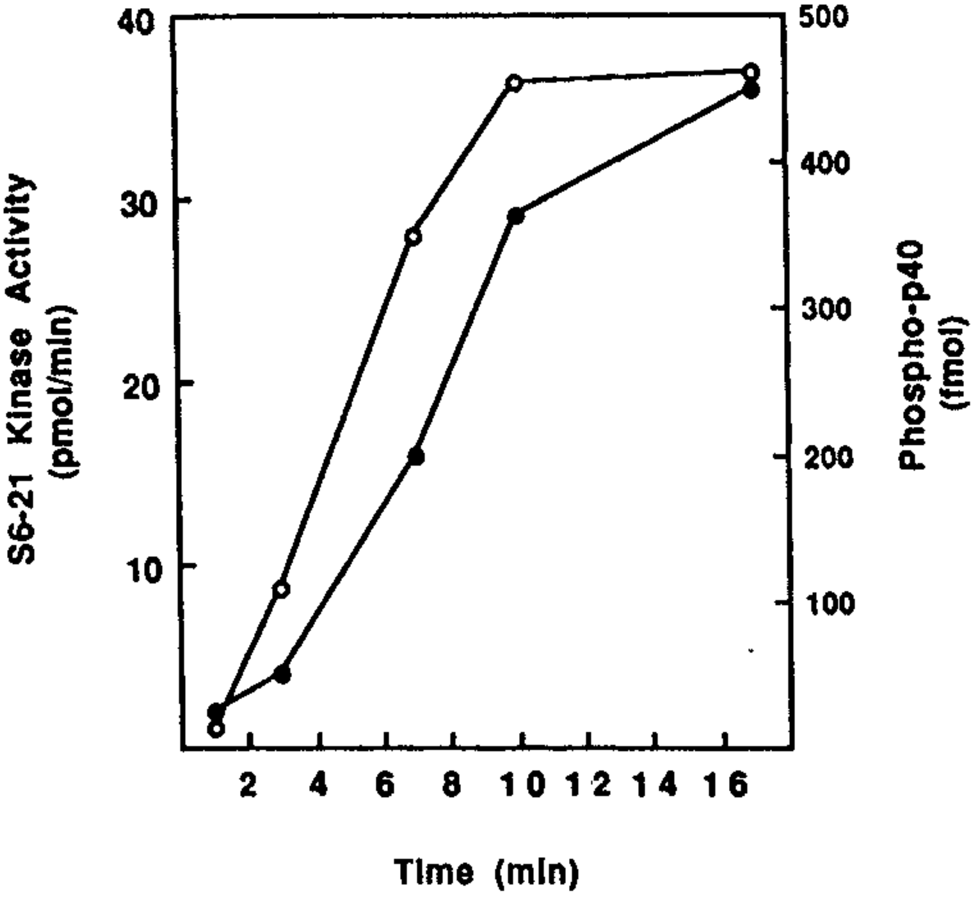
S6-21 Kinase Activity (pmol/min)
40
30
20
10
Phospho-p40 (fmol)
500
400
300
200
100
2
4
6
8
10
12
14
16
Time (min)

Figure 16. Inhibition of p40 autophosphorylation and activation with the H4 substrate. Aliquots of the trypsin-treated S6/H4 kinase eluted from Mono Q (shown in Fig.11) were incubated for 10 min at 30°C with Mg[γ-^{32}P]ATP in the absence (*lane 1*) or presence of histone H4 (1 mg/ml) (*lane 2*). The reactions were stopped with SDS sample buffer and analyzed by SDS PAGE on a 10% polyacrylamide gel and autoradiography (*left panel*). Phosphorylated H4 is not shown in the figure. Phosphorylated bands at Mr 40,000 were excised and radioactivity was quantitated as in Fig.15 (*right panel*). Kinase activity in the presence of H4 (*center panel*) was also monitored. The *arrow* indicates the position of the autophosphorylated pp40 S6/H4 kinase.

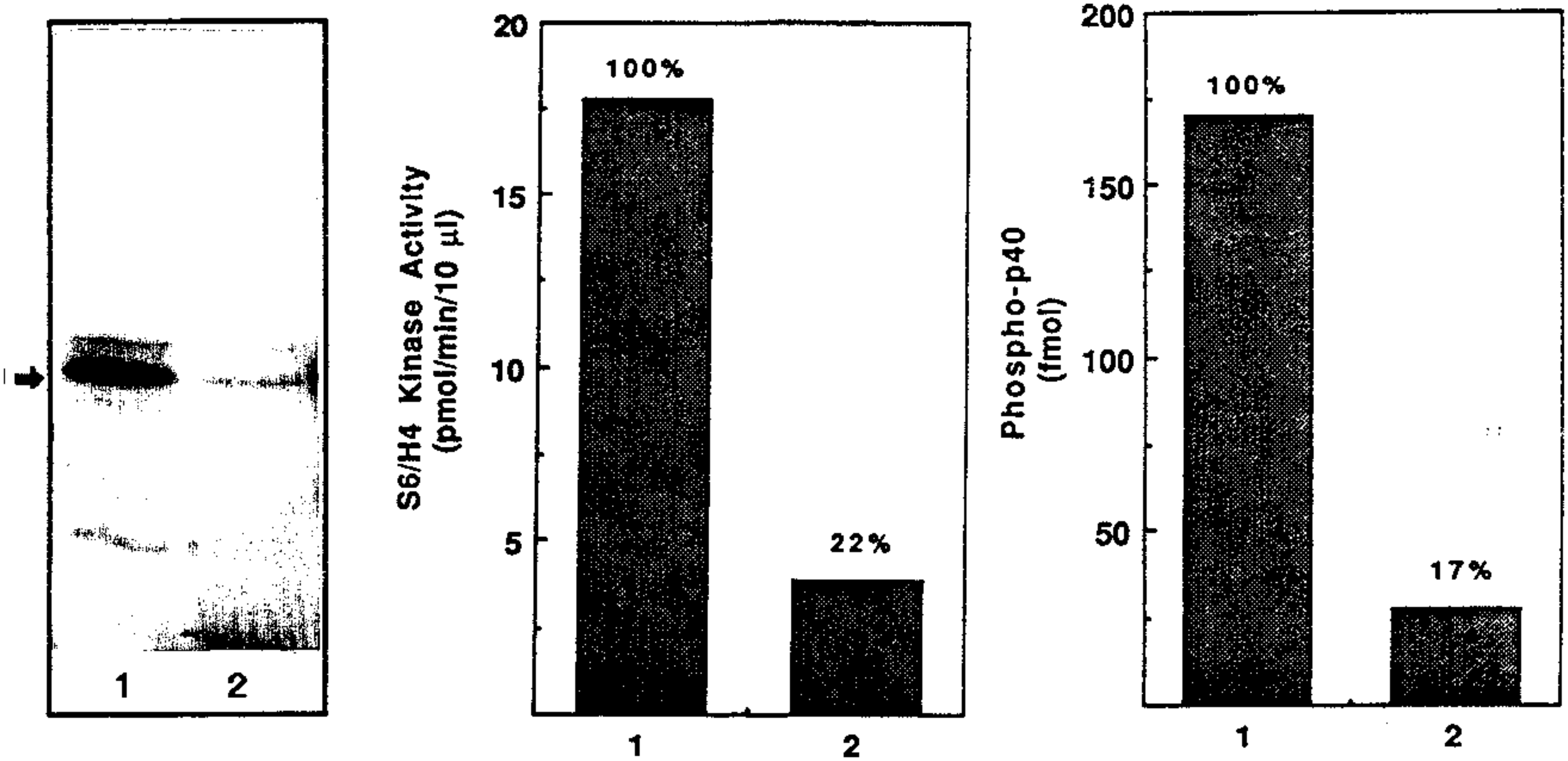
1
2
S6/H4 Kinase Activity
(pmol/min/10 µl)
20
15
10
5
100%
22%
1
2
Phospho-p40
(fmol)
200
150
100
50
100%
17%
1
2

Figure 17. Phosphorylation of the native p60 S6/H4 kinase by the autoactivated p40 form of the enzyme. Mono Q purified p60 S6/H4 kinase from Fig. 3 was incubated with Mg[γ-^{32}P]ATP for 5, 10, and 20 min at 30 °C (*lanes 1, 2 and 3*, respectively) with the reactions being stopped by the addition of SDS-PAGE sample buffer and boiling. Samples were analyzed by SDS-PAGE on a 10% polyacrylamide gel and radiolabelled bands visualized by autoradiography as described under "Experimental Procedures." Purified p40 S6/H4 kinase from Fig. 11 was incubated with Mg[γ-^{32}P]ATP under identical conditions (*lanes 4, 5 and 6*), and the p60 and p40 S6/H4 kinases were incubated together as described above (*lanes 7, 8 and 9*). Molecular weights were determined by comparison to molecular weight standards obtained from BioRad.

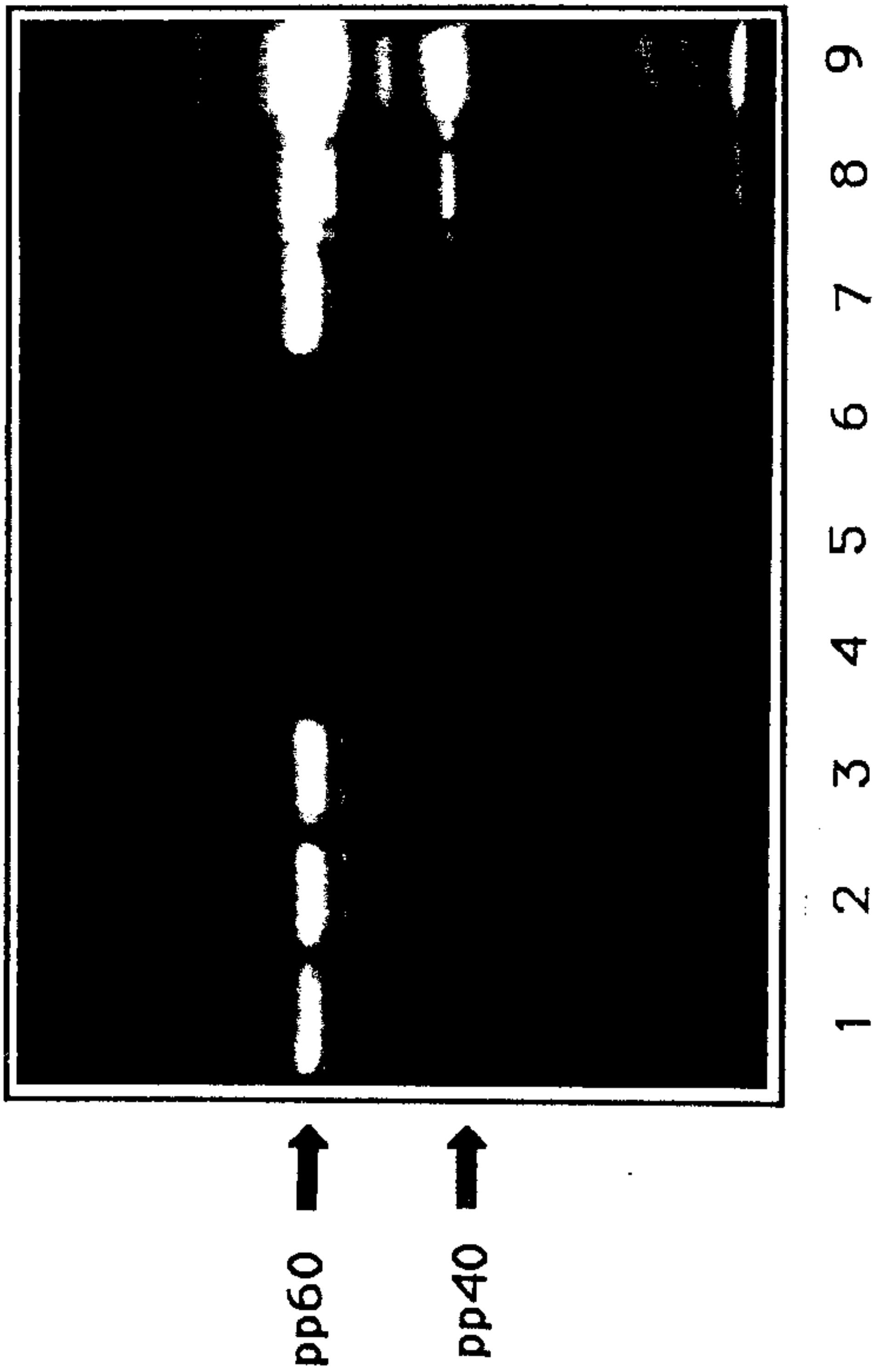
pp60
pp40
1
2
3
4
5
6
7
8
9

Figure 18. Kinetics of p40 S6/H4 kinase autoactivation. Varying concentrations of purified p40 S6/H4 kinase were incubated with Mg[γ-^{32}P]ATP for the time intervals indicated before the addition of S6-21 (190 µM) (*left panel*). The p40 S6/H4 kinase concentrations used were 96 ng/µl (*closed circles*), 72 ng/µl (*open circles*), and 48 ng/µl (*closed squares*). Reactions were incubated for an additional 5 minutes at 30°C and then stopped by acid precipitation of reaction mixture aliquots on P81 filter paper as described under "Experimental Procedures." Autoactivation time points from 2-4 min (*open circles*) were analyzed by plotting the change in kinase specific activity against kinase concentration (*right panel*).

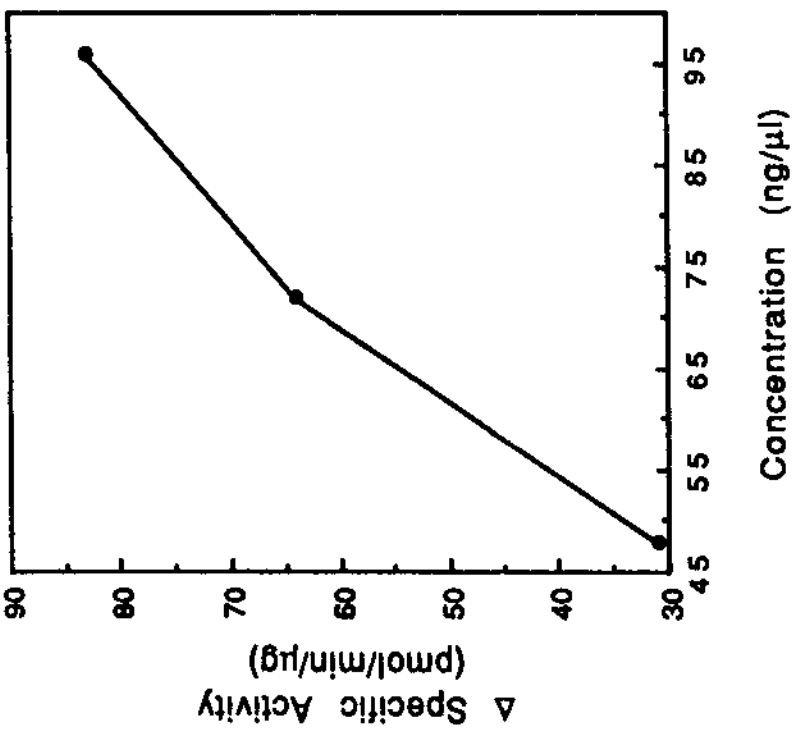
Δ Specific Activity
(pmol/min/µg)
90
80
70
60
50
40
30
Concentration (ng/µl)
45
55
65
75
85
95

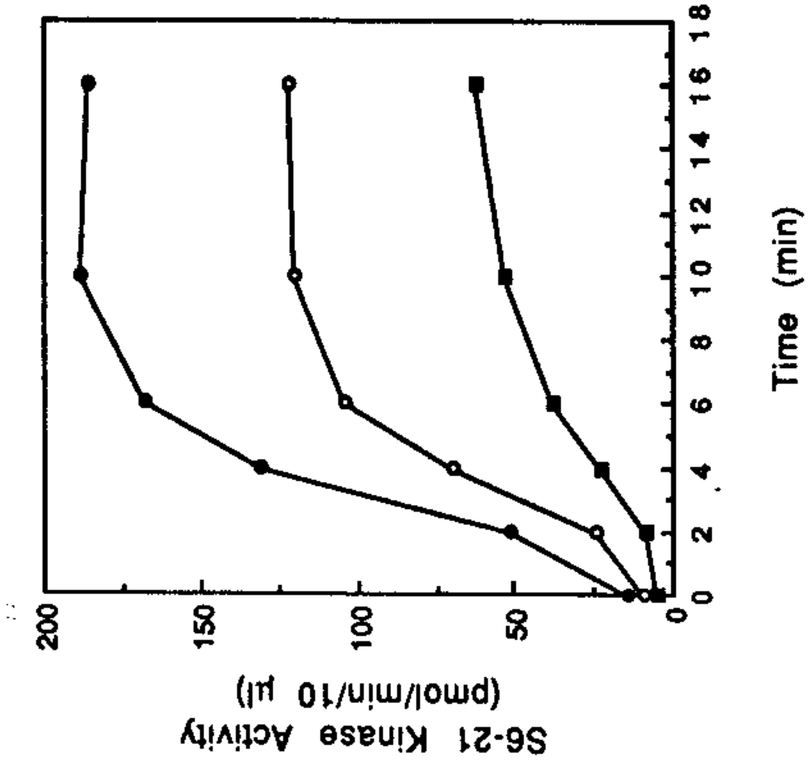
S6-21 Kinase Activity
(pmol/min/10 µl)
200
150
100
50
0
Time (min)
0
2
4
6
8
10
12
14
16
18

Figure 19. Resolution of pp40 S6/H4 kinase phosphoprotein isoforms by two-dimensional SDS-PAGE. Aliquots containing approximately 0.3 µg of purified p40 S6/H4 kinase were incubated with Mg[γ-^{32}P]ATP for designated time intervals before being stopped by the addition of sample buffer containing 9M urea. Samples were electrophoretically focused to their isoelectric points in a pH gradient ranging from 5 to 7 in the first dimension. Focused proteins were then resolved by molecular weight in the second dimension by SDS-PAGE on a 10% polyacrylamide gel. *Closed arrows* indicate the positions of radiolabelled proteins and correspond to pI's of 5.8, 5.9 and 6.2 from left to right. The *open arrow* indicates the position of the unlabelled p40 S6/H4 kinase (pI=6.3) as was determined by silver staining (data not shown).

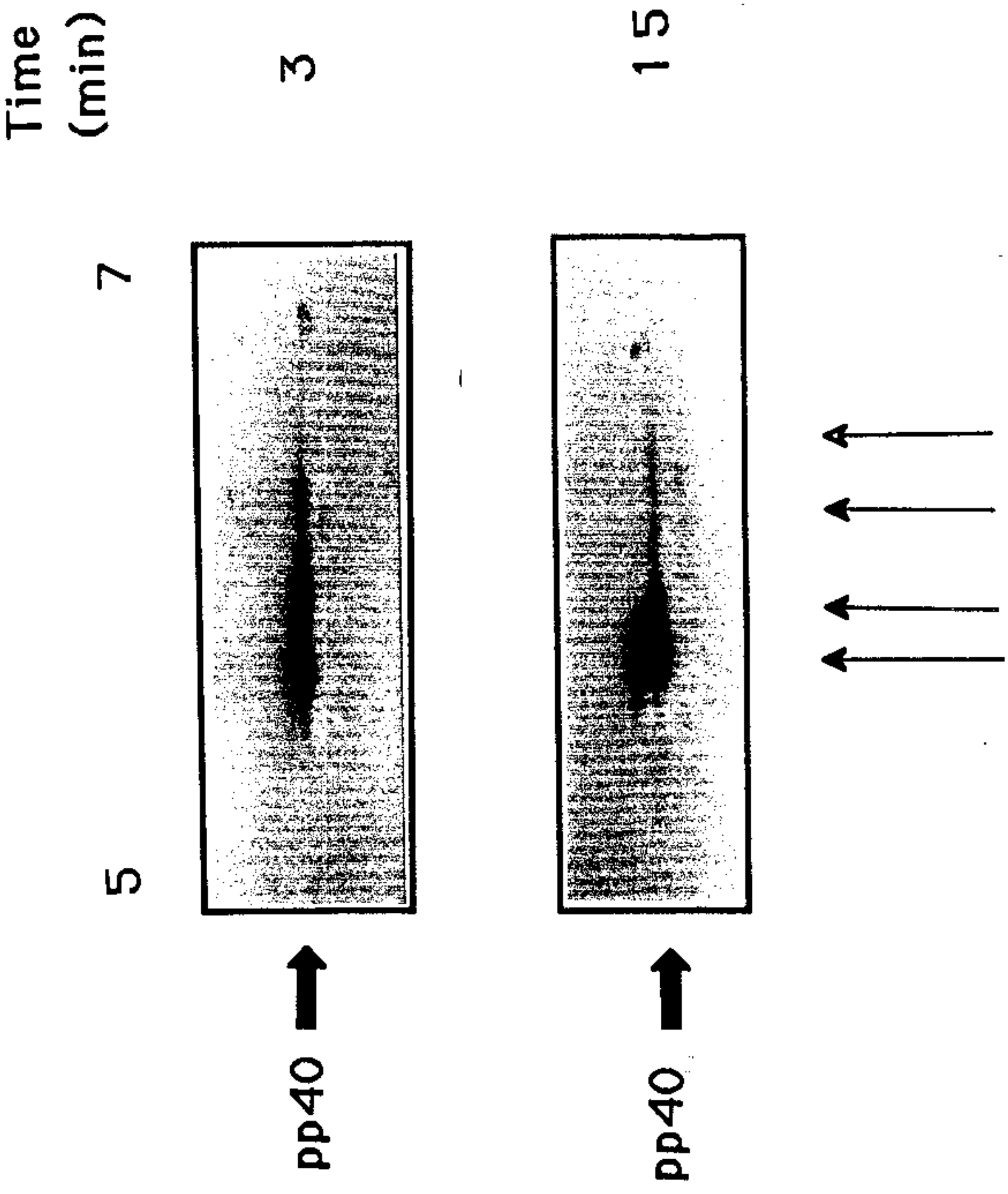
Time (min)
5
7
pp40
3
pp40
15

Figure 20. Mono P chromatofocusing chromatography of the S6/H4 kinase. S6/H4 kinase purified through Mono Q chromatography as described in "Experimental Procedures" was chromatographed over BioRad 10DG desalting column equilibrated with Buffer D to exchange buffers. The S6/H4 fraction was then applied to a Mono P HR 5/5 column equilibrated with Buffer D. The kinase was eluted with a linear pH gradient created with the isocratic application of Buffer E to the column with a flow rate of 1ml/min. Fractions of 1ml each were collected and each was assayed with trypsin and MgATP activation for H4 kinase activity as described under "Experimental Procedures." The pH of each fraction was determined using a pH meter.

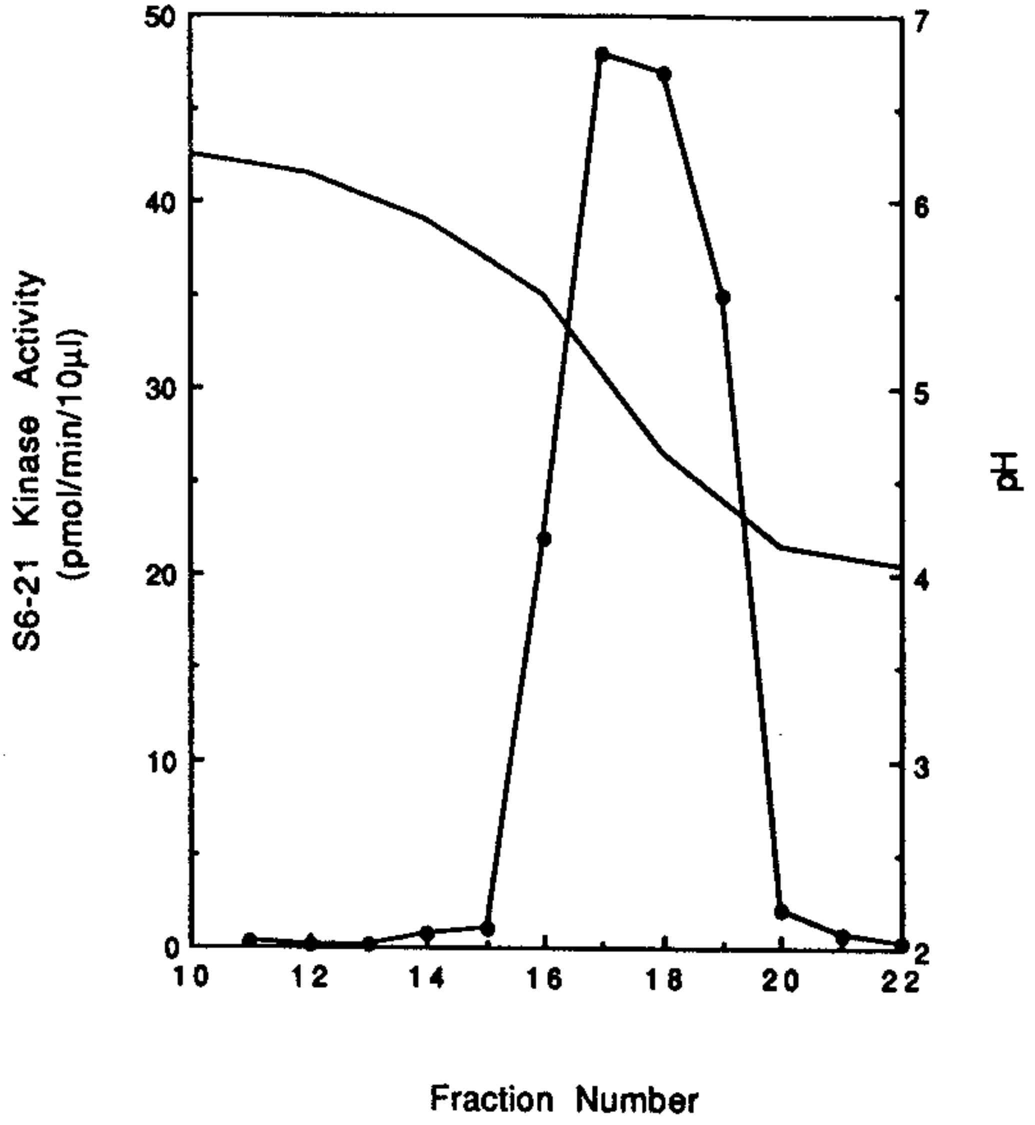
S6-21 Kinase Activity
(pmol/min/10µl)
pH
Fraction Number
50
40
30
20
10
0
7
6
5
4
3
2
10
12
14
16
18
20
22

Figure 21. Purification of pp40 S6/H4 kinase to homogeneity by preparative SDS-PAGE. Approximately 100 μg of p40 S6/H4 kinase from Fig.11 was autophosphorylated in the presence of Mg[γ-^{32}P]ATP (1000-5000 dpm/pmol) for 1 h at 30°C as described under "Experimental Procedures." The reaction was stopped by the addition of SDS-PAGE sample buffer and the samples were boiled for 10 min before being applied to a 3.7 x 12 cm 8% polyacrylamide column with a 3 cm 4% stacking gel. The sample was electrophoresed on the column for 10 h at 10 W constant power, and 4 ml fractions were collected at a flow rate of 60 ml/h as described under "Experimental Procedures." Ten microliter aliquots of the eluted fractions were analyzed by SDS-PAGE on a 10% polyacryalmide gel followed by autoradiography (*left panel*) and peak pp40 fractions were pooled and concentrated for analysis by SDS-PAGE and silver staining (*right panel*).

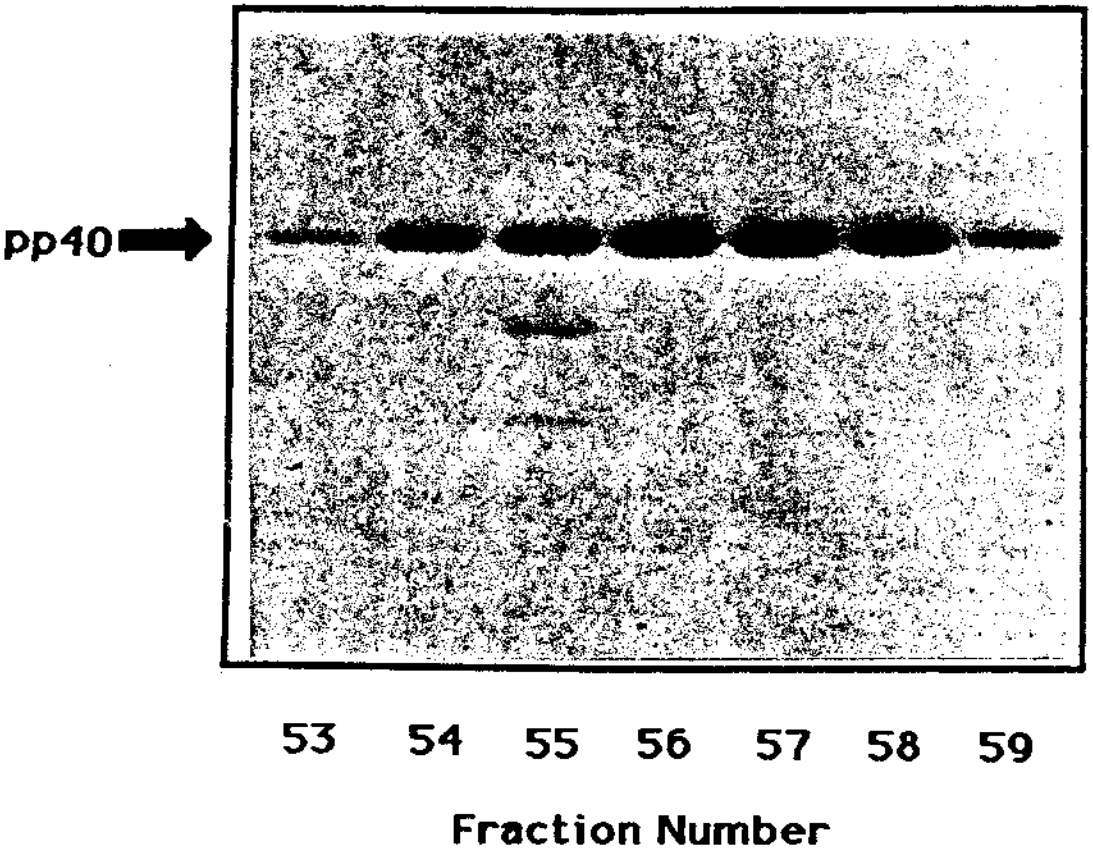
pp40
53
54
55
56
57
58
59
Fraction Number

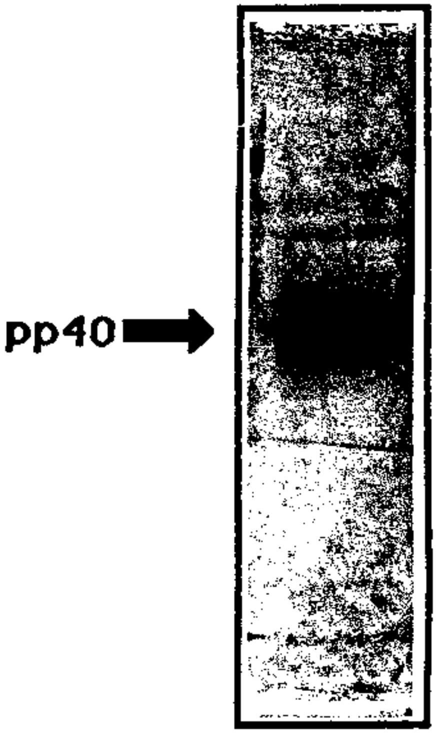
pp40

Figure 22. Release of trypsin-generated pp40 S6/H4 kinase phosphopeptides from nitrocellulose. Approximately 100 μg of purified p40 S6/H4 kinase from Mono Q chromatography was autophosphorylated in the presence of Mg[γ-^{32}P]ATP for 1 h at 30°C. The autophosphorylation reaction was stopped by the addition of SDS-PAGE sample buffer and boiled. [^{32}P]pp40 S6/H4 kinase was then further purified on a BioRad Model 491 Prep Cell. [^{32}P]pp40 S6/H4 kinase was located by SDS-PAGE analysis in a 10% polyacrylamide gel followed by autoradiography. The eluted [^{32}P]pp40 S6/H4 kinase was dialyzed for 24 h against water and concentrated for loading onto a Sephadex G-25 superfine column for removal of SDS. Homogeneous [^{32}P]pp40 S6/H4 kinase was then digested with 5% (w/w) DPCC-treated trypsin for 24 h at 30°C. The resulting digest was applied to a cellulose plate and electrophoresed at pH 1.9. Phosphopeptides were visualized by autoradiography and quantitated by liquid scintillation counting (*shaded bars*). A fraction of the the homogeneous [^{32}P]pp40 prepared above was analyzed by SDS-PAGE in a 10% polyacrylamide gel and electrophoretically transferred to nitrocellulose. [^{32}P]pp40 S6/H4 kinase bands were visualized by autoradiography and excised. Nitrocellulose strips were treated with 0.5% PVP-360 dissolved 100 mM acetic acid for 30 min at 37°C. After washing and neutralization of the nitrocellulose strips with 50 mM ammonium bicarbonate, pH 7.8, the strips were treated with 60 μg of DPCC-treated trypsin (0.2 mg/ml) for 4 h at 37°C. The digestion mixture was then spotted onto a cellulose plate and electrophoresed at pH 1.9 as described above. Phosphopeptides were then visualized by autoradiography and quantitated by liquid scintillation counting (*filled bars*). Phosphopeptides were numbered according to their ability to migrate towards the cathode. All procedures used here are detailed in "Experimental Procedures."

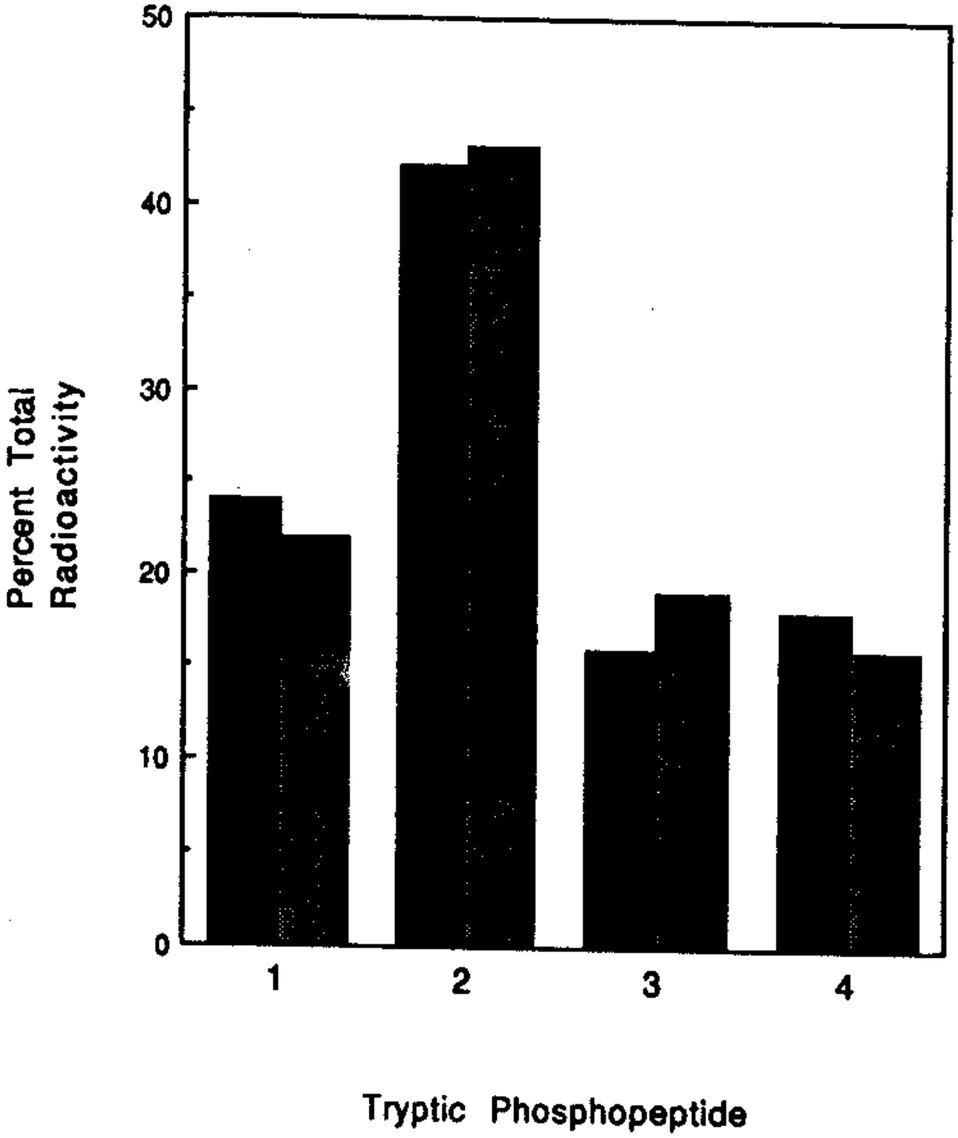
50
40
30
20
10
0
Percent Total Radioactivity
1
2
3
4
Tryptic Phosphopeptide

Figure 23. Tryptic Phosphopeptide Mapping of Autophosphorylated pp40 S6/H4 kinase. Autophosphorylated pp40 S6/H4 was labelled with Mg[γ-^{32}P]ATP and purified as described under "Experimental Procedures." Approximately 100 μg of pure pp40 was incubated with 5 μg of DPCC-treated trypsin for 24 hours at 30 °C at a pp40 concentration of 1 mg/ml. One microliter of the reaction mixture was spotted onto a microcrystalline cellulose plate and electrophoresed in the first dimension at pH 1.9 (formic acid/acetic acid/water, 25:78:897). Second dimension resolution of the sample was accomplished by ascending chromatography (n-butanol/ pyridine/acetic acid/water, 15:10:3:12). Radiolabelled phosphopeptides were visualized by autoradiography and numbered according to their ability to migrate toward the cathode with phosphopeptide 1 being the slowest migrating peptide.

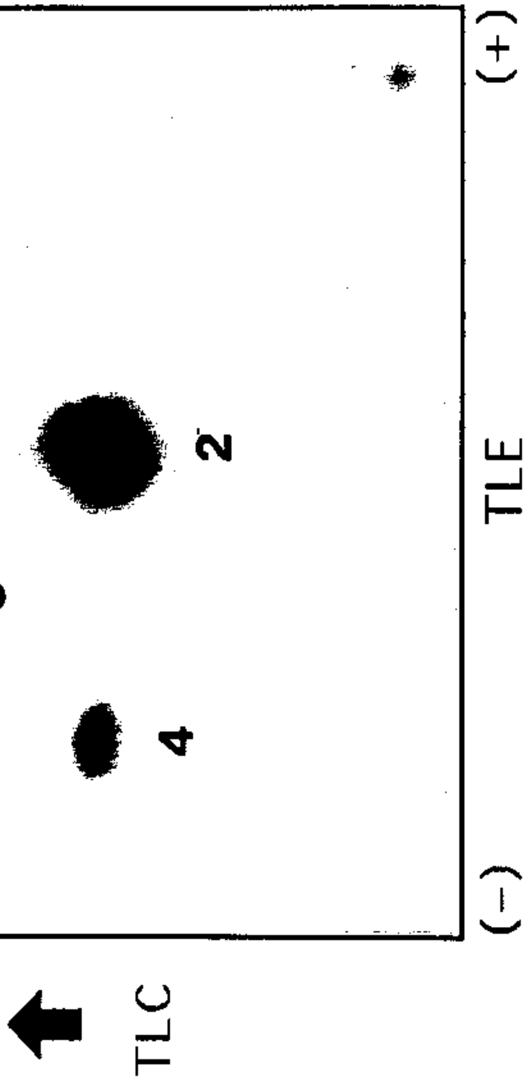
1
2
3
4
(+)
TLE
(−)
TLC

Figure 24. HPLC Analysis of Tryptic Phosphopeptides Generated from Autophosphorylated pp40 S6/H4 Kinase. The tryptic digest described in Fig 23 was chromatographed on a reversed-phase C_{18} column (0.46 x 25 cm) equilibrated with 2.5% acetonitrile/0.1% trifluoroacetic acid. Peptides were eluted with a gradient of 2.5-40% acetonitrile in 100 min. One milliliter fractions were collected at a flow rate of 1 ml/min. Radiolabelled peaks were located by spotting aliquots of each fraction onto ET-31 filter paper and counted as described under "Experimental Procedures." *Solid line*, radioactivity counted from each fraction; *dashed line*, percentage of buffer B. *Arrows* indicate the location of each peak which are numbered according to R_f values determined from TLE at pH 1.9 as shown in Table III.

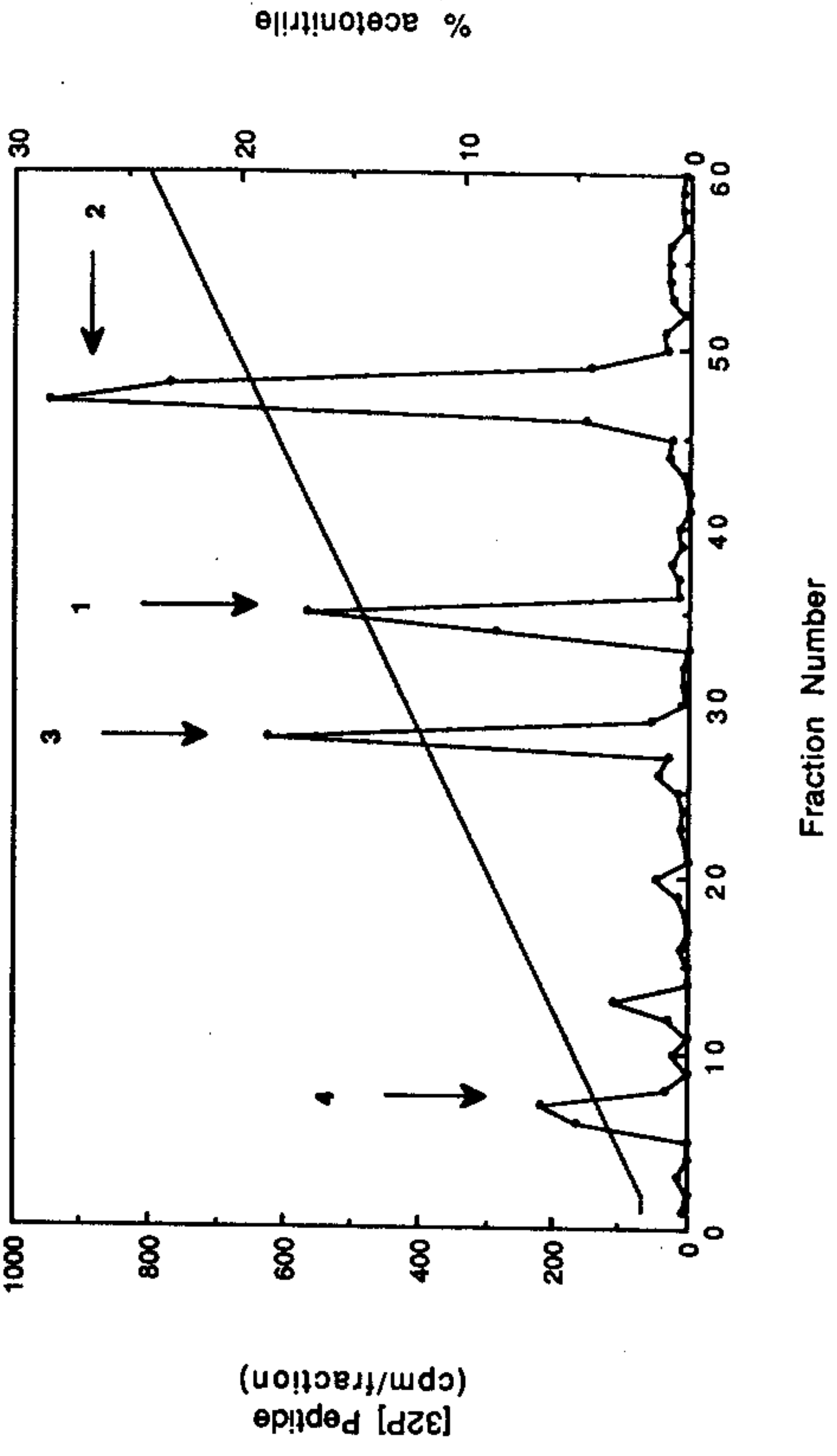
[32P] Peptide
(cpm/fraction)
1000
800
600
400
200
0
Fraction Number
0
10
20
30
40
50
60
% acetonitrile
30
20
10
0
4
3
1
2

Figure 25. Mono S chromatography of tryptic phosphopeptides generated from pp40 S6/H4 kinase. Approximately 100 µg of pp40 S6/H4 kinase from Fig. 21 was digested with trypsin for 24 h at 30°C as described under "Experimental Procedures." The digest was then loaded onto a Mono S HR 5/5 column equilibrated with 10 mM H_3PO_4, pH 2. Peptides were eluted with a 0-0.65 M NaCl linear gradient (50 ml). Fraction volumes of 0.5 ml were collected with a flow rate of 0.5 ml/min. Phosphopeptide peaks were detected by spotting 10 µl aliquots of each fraction onto ET-31 filter paper and quantitating by liquid scintillation counting. Positions of phosphopeptides are numbered for reference.

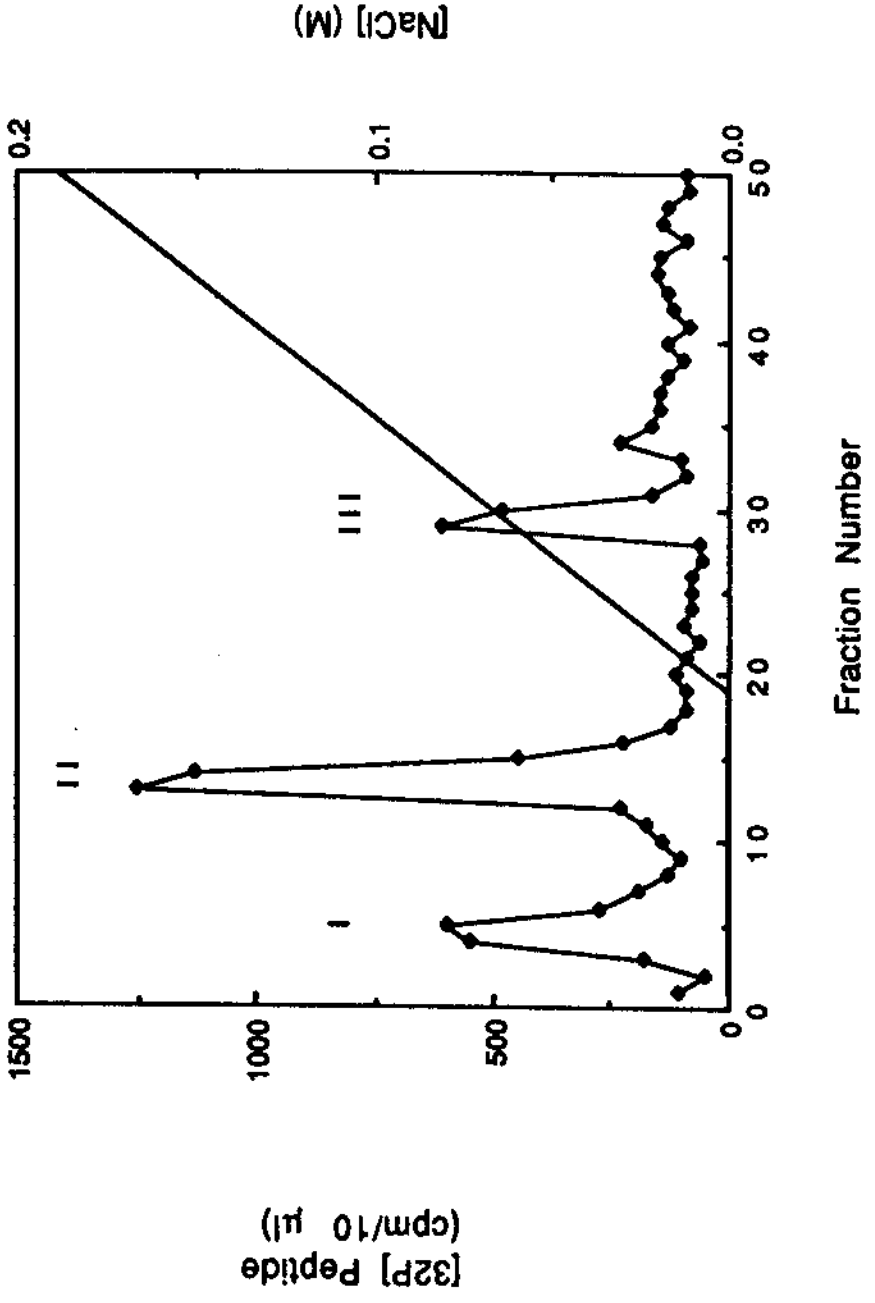
[NaCl] (M)
0.2
0.1
0.0
I
II
III
1500
1000
500
0
[32P] Peptide
(cpm/10 µl)
0
10
20
30
40
50
Fraction Number

Figure 26. Electrophoretic mobilities of trypsin-generated pp40 S6/H4 kinase phosphopeptides as a function of pH. Tryptic phosphopeptides were purified from reversed-phase HPLC as described under "Experimental Procedures." A mixture of phosphopeptides from each of the eluting peaks was spotted onto TLE plates and electrophoresed in two dimensions as described under "Experimental Procedures." Electrophoresis in the first dimension was performed at pH 1.9 (*upper and lower panels*). Electrophoresis in the second dimension was performed at either pH 3.5 (acetic acid/pyridine/water, 10:1:189; *upper panel*) or pH 6.5 (acetic acid/pyridine/water, 4:100:896; *lower panel*). Phosphopeptides were visualized by autoradiography as described under "Experimental Procedures."

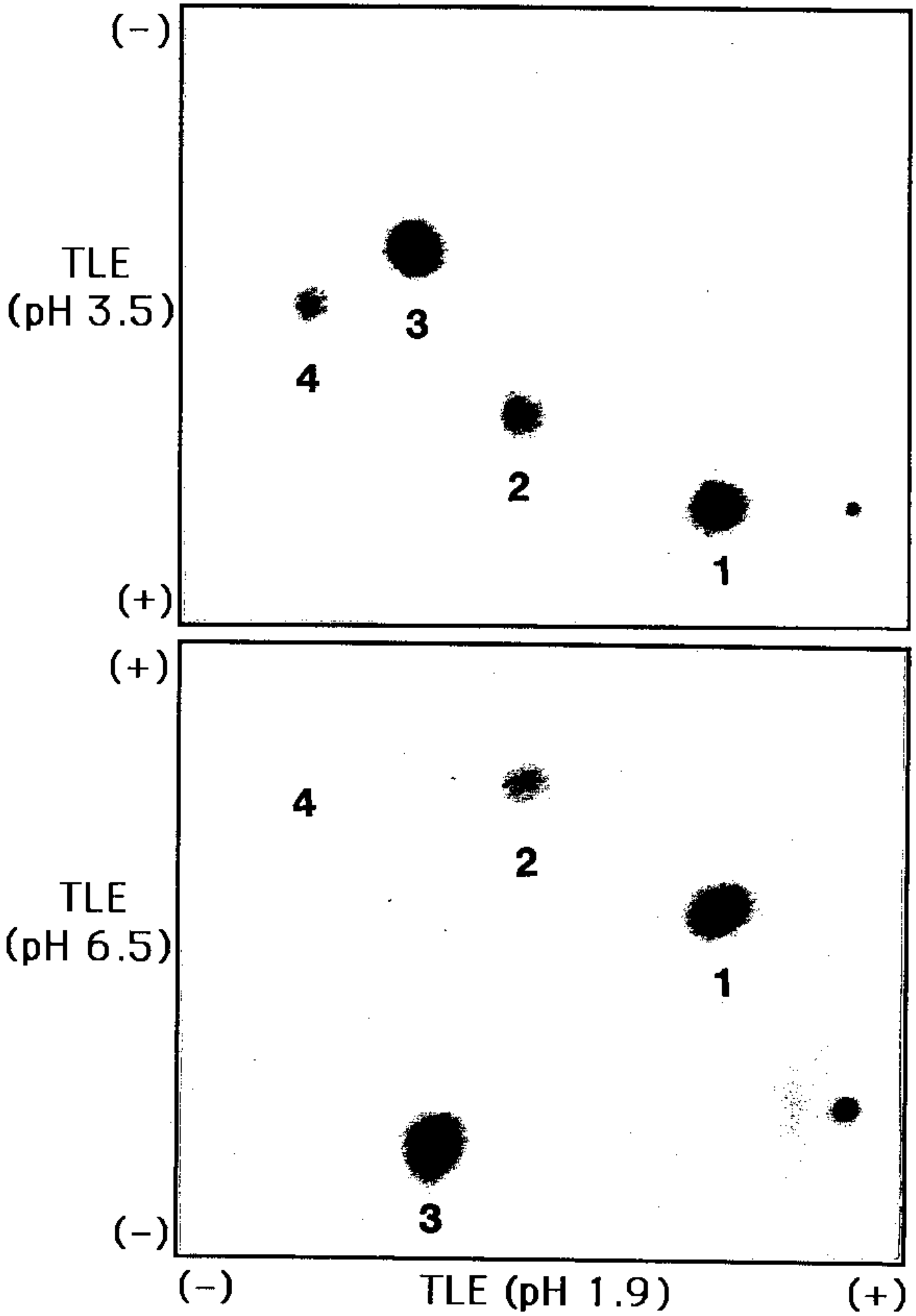
(−)
TLE
(pH 3.5)
(+)
3
4
2
1
(+)
4
2
TLE
(pH 6.5)
1
3
(−)
(−)
TLE (pH 1.9)
(+)

Figure 27. Tryptic phosphopeptide mapping of pp40 S6/H4 kinase autophosphorylated over a time course. Approximately 1 µg of p40 S6/H4 kinase was autophosphorylated in the presence of Mg[γ-^{32}P]ATP for 3, 5, and 10 min (*lanes A, B, and C*, respectively). Reaction mixtures were stopped by the addition of SDS-PAGE sample buffer and boiling. [^{32}P]pp40 S6/H4 kinase was then resolved by SDS-PAGE analysis in a 10% polyacrylamide gel and electrophoretically transferred to nitrocellulose. [^{32}P]pp40 S6/H4 kinase was located by autoradiography and excised. Nitrocellulose strips were treated for 30 min with 0.5% PVP-360 dissolved in 100 mM acetic acid and then washed thoroughly with water followed by 50 mM ammonium bicarbonate, pH 7.8. Nitrocellulose strips were then treated with 60 µg of DPCC-treated trypsin (0.2 mg/ml) for 4 h at 37°C. Phosphopeptides were spotted onto cellulose TLE plates and electrophoresed in one dimension at pH 1.9. Phosphopeptides were visualized by autoradiography. Techniques used here are detailed in "Experimental Procedures." Phosphopeptides are numbered according to their ability to migrate toward the cathode.

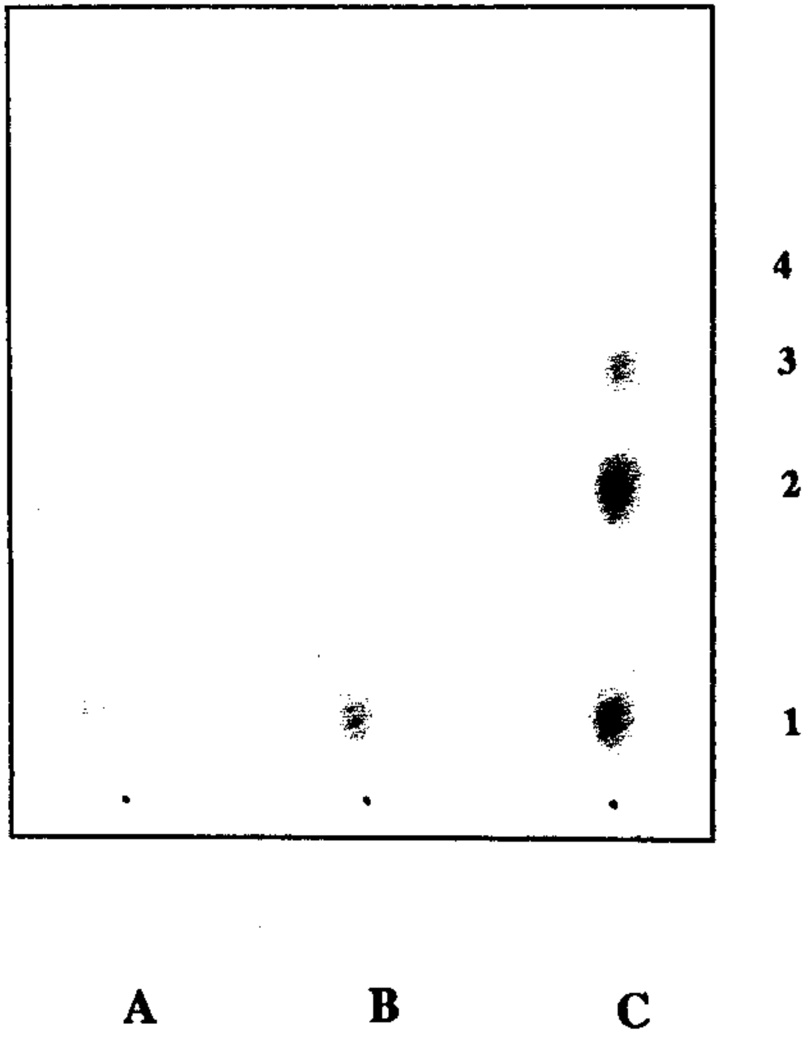
4
3
2
1
A
B
C

Figure 28. Tryptic phosphopeptide mapping of pp40 S6/H4 kinase autophosphorylated at varying dilutions over a time course. Varying concentrations of p40 S6/H4 kinase purified from Mono Q chromatography in Fig. 11 were autophosphorylated in the presence of Mg[γ-^{32}P]ATP for times indicated. The concentrations used were 96 ng/µl (*left panels*), 72 ng/µl (*middle panels*), and 48 ng/µl (*right panels*) with [γ-^{32}P]ATP specific activities of 9,400, 13,000, and 19,000 dpm/pmol respectively. Reactions were stopped by the addition of SDS-PAGE sample buffer and boiling. The generation of [^{32}P]pp40 S6/H4 kinase tryptic phosphopeptides and the resolution of the phosphopeptides by electrophoresis on cellulose plates at pH 1.9 as described in Fig. 27. Phosphopeptides were quantitated directly from the cellulose plate with a Bioscan System 200 Image Scanner.

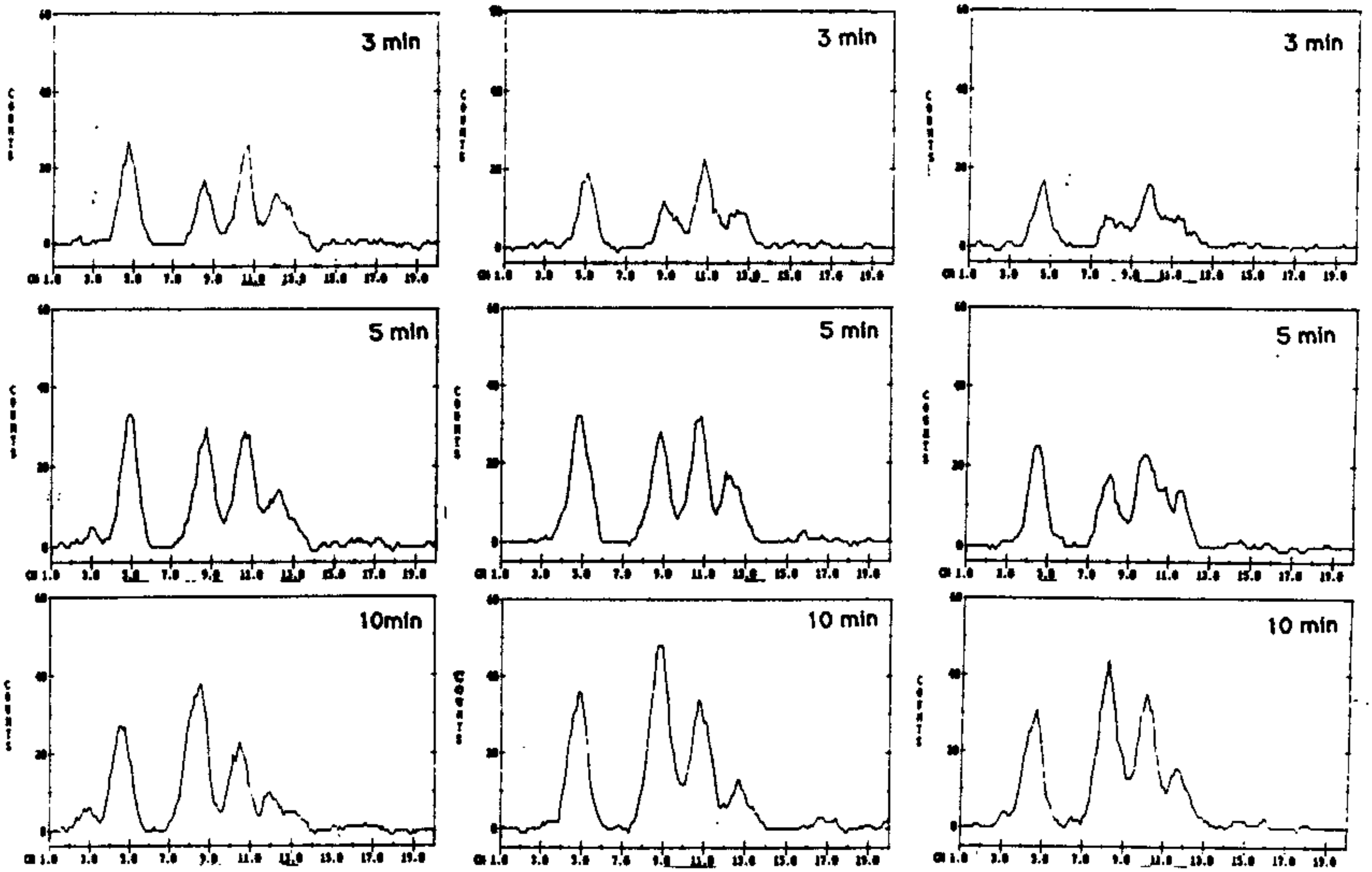
3 min
3 min
3 min
5 min
5 min
5 min
10min
10 min
10 min
COUNTS
0
20
40
60
CH 1.0
3.0
5.0
7.0
9.0
11.0
13.0
15.0
17.0
19.0

Figure 29. Quantitation of total p40 S6/H4 kinase autophosphorylation at varying concentrations over a time course. The areas under the peaks in Fig. 28 were integrated and summed to get the total $^{32}PO_4^{-3}$ incorporated into all four phosphopeptides. Total areas of tryptic phosphopeptides were generated from [^{32}P]pp40 S6/H4 kinase autophosphorylated at concentrations of 96 ng/μl (*closed circles*), 72 ng/μl (*open circles*), and 48 ng/μl (*open squares*) and were plotted against the period of autophosphorylation.

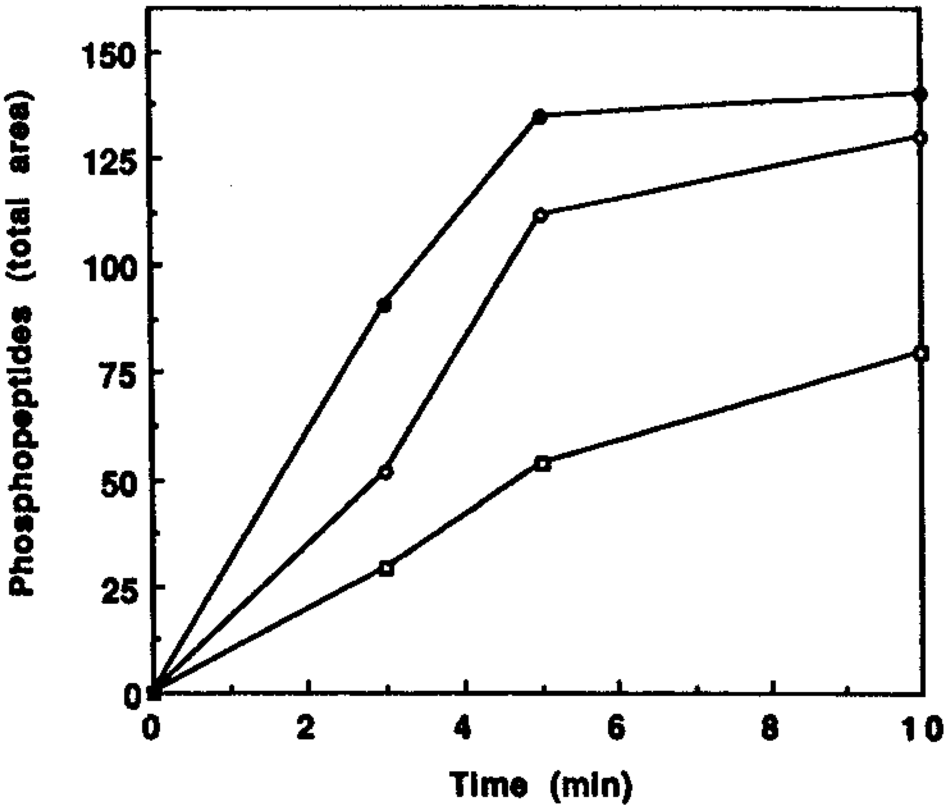
Phosphopeptides (total area)
150
125
100
75
50
25
0
0
2
4
6
8
10
Time (min)

Figure 30. Occurrence of tryptic phosphopeptides generated from autophosphorylated pp40 S6/H4 kinase over the autophosphorylation time course. The areas under the peaks in Fig. 28 were integrated and plotted against the period of autophosphorylation. Areas were integrated for tryptic phosphopeptides 1 (*closed circles*), 2 (*open circles*), 3 (*closed squares*), and 4 (*open squares*) which had been generated from [^{32}P]pp40 S6/H4 kinase autophosphorylated at concentrations of 96 ng/µl (*upper panel*), 72 ng/µl (*middle panel*), and 48 ng/µl (*lower panel*).

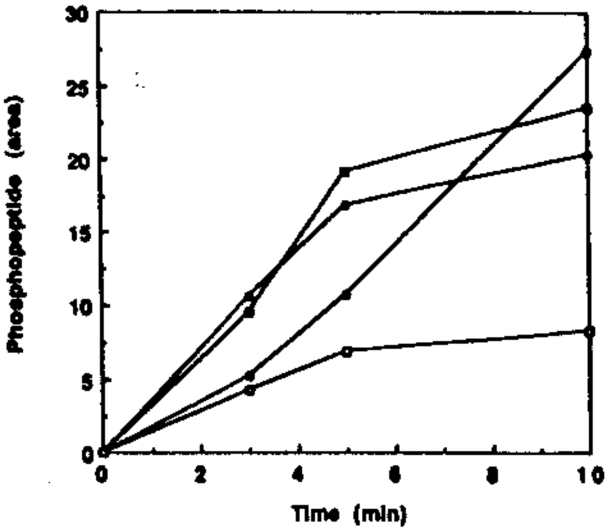
Phosphopeptide (area)
0
5
10
15
20
25
30
0
2
4
6
8
10
Time (min)

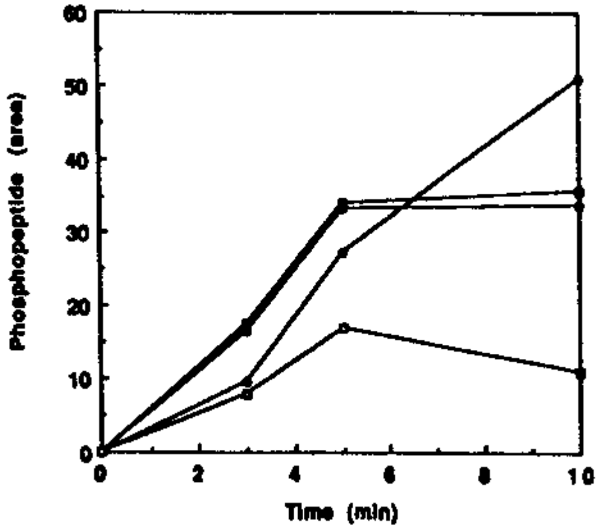
Phosphopeptide (area)
0
10
20
30
40
50
60
0
2
4
6
8
10
Time (min)

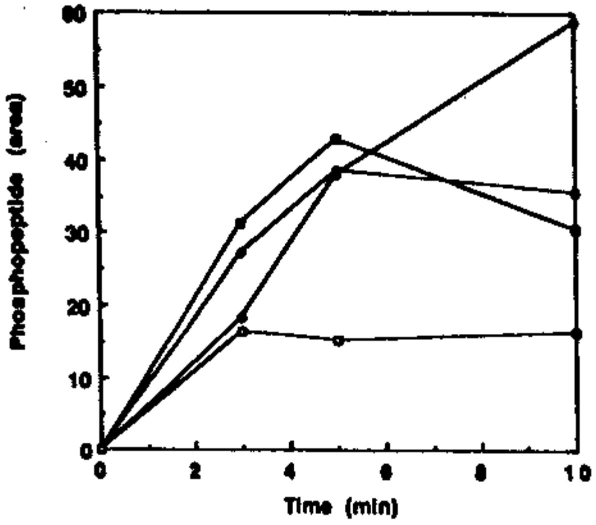
Phosphopeptide (area)
0
10
20
30
40
50
60
0
2
4
6
8
10
Time (min)

Figure 31. Occurence of tryptic phosphopeptides generated from autophosphorylated pp40 S6/H4 kinase as a function of kinase concentration. Areas under the peaks in Fig. 28 were integrated and plotted against the concentrations of the p40 S6/H4 kinase used for the autophosphorylation reactions. Areas were integrated for phosphopeptides 1 (*closed circles*), 2 (*open circles*), 3 (*closed squares*), and 4 (*open squares*) which had been generated from p40 S6/H4 kinase autophosphorylated for 3 min (*upper panel*), 5 min (*middle panel*), and 10 min (*lower panel*).

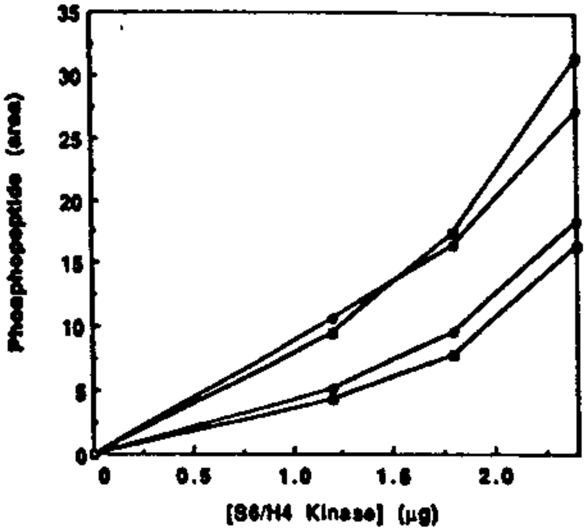
Phosphopeptide (area)
35
30
25
20
15
10
5
0
0
0.5
1.0
1.5
2.0
[S6/H4 Kinase] (μg)

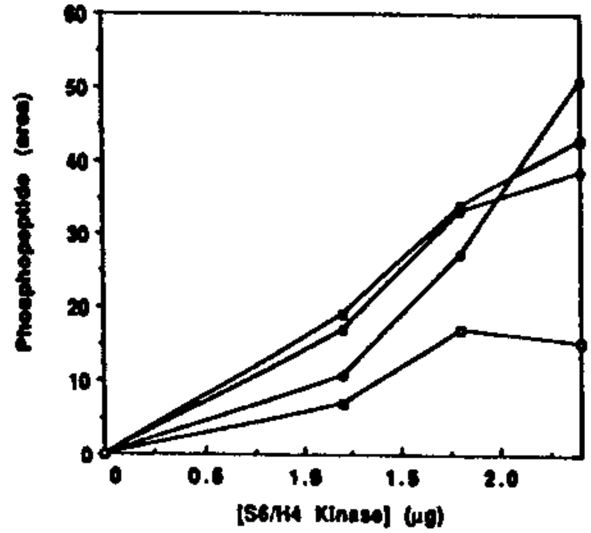
Phosphopeptide (area)
60
50
40
30
20
10
0
0
0.5
1.0
1.5
2.0
[S6/H4 Kinase] (μg)

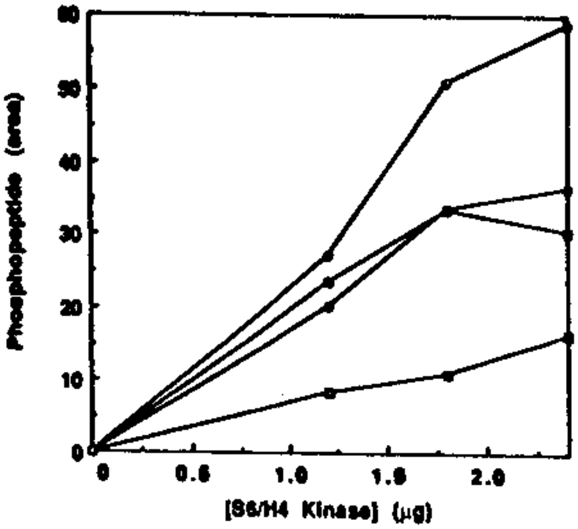
Phosphopeptide (area)
60
50
40
30
20
10
0
0
0.5
1.0
1.5
2.0
[S6/H4 Kinase] (μg)

Figure 32. Mono S chromatography of chymotryptic phosphopeptides generated from pp40 S6/H4 kinase. Approximately 100 μg of p40 S6/H4 kinase from Fig.11 was autophosphorylated in the presence of Mg[γ-^{32}P]ATP for 8 min at 30°C. The [^{32}P]pp40 S6/H4 kinase was then purified as described in Fig. 21 and prepared for digestion with chymotrypsin as described under "Experimental Procedures." Digestion with sequencing grade chymotrypsin (Boehringer Mannheim) was performed for 10 h at 25°C as described under "Experimental Procedures." The digest was then analyzed by Mono S chromatography and phosphopeptides were located as described in Fig.25. Peaks of interest are numbered for reference.

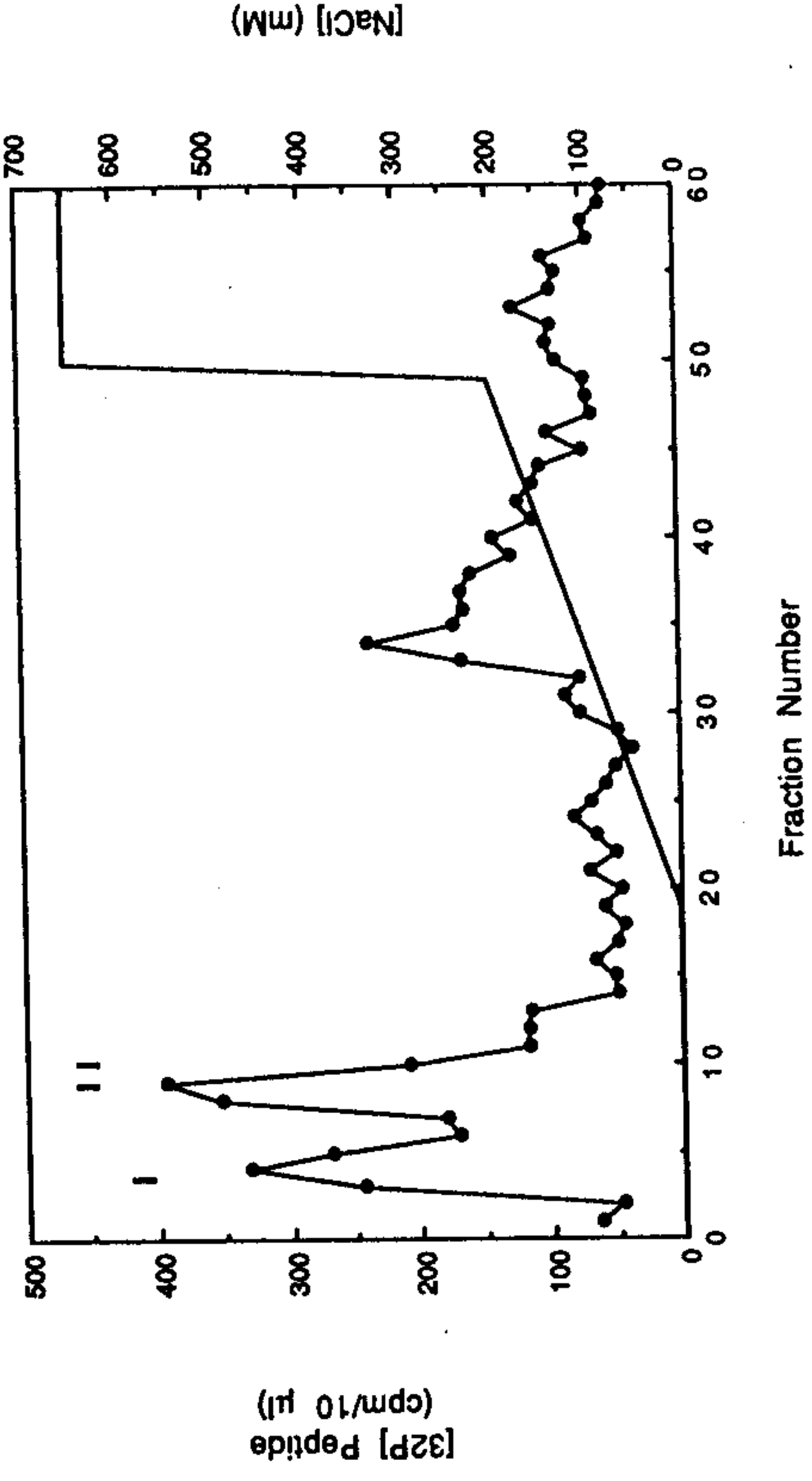

[32P] Peptide
(cpm/10 µl)
[NaCl] (mM)
Fraction Number
I
II
0
100
200
300
400
500
0
100
200
300
400
500
600
700
0
10
20
30
40
50
60

Figure 33. Phosphoamino acid analysis of autophosphorylated pp40 S6/H4 kinase. [^{32}P]pp40 S6/H4 kinase was purified as described in Fig. 21. [^{32}P]pp40 S6/H4 kinase was partially hydrolyzed in the presence of 6N HCl at 110 °C for 1 hour. The acid was removed by drying on a SpeedVac and the sample was reconstituted in water. An aliquot of the hydrolyzed pp40 S6/H4 kinase mixture was applied onto a cellulose plate and electrophoresed in two-dimensions at pH 1.9 and 3.5. Phosphoamino acids were visualized by autoradiography and identified by comparison to phosphoamino acid standards run with the sample as described under "Experimental Procedures." The locations of the standards are indicated on the figure.

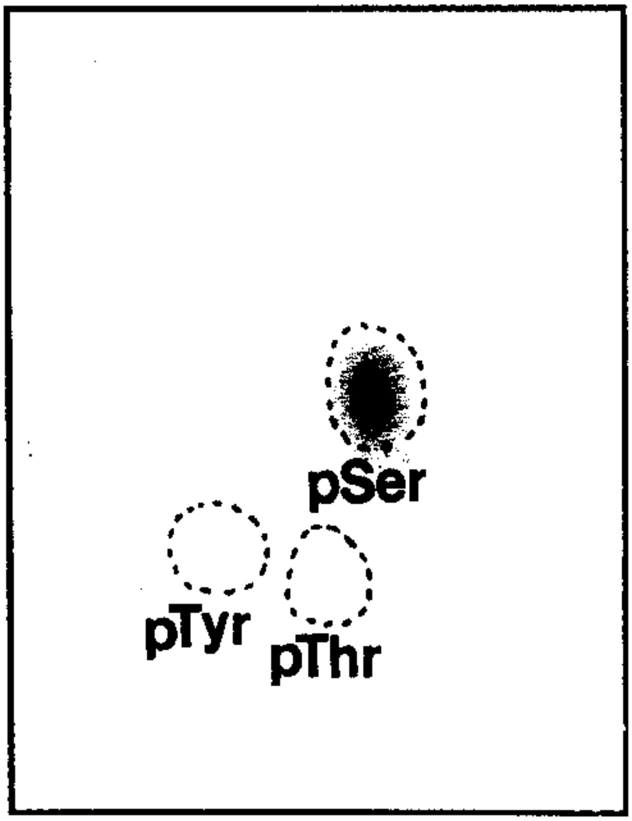
pSer
pTyr
pThr

Figure 34. Proposed model of S6/H4 kinase autophosphorylation and autoactivation.

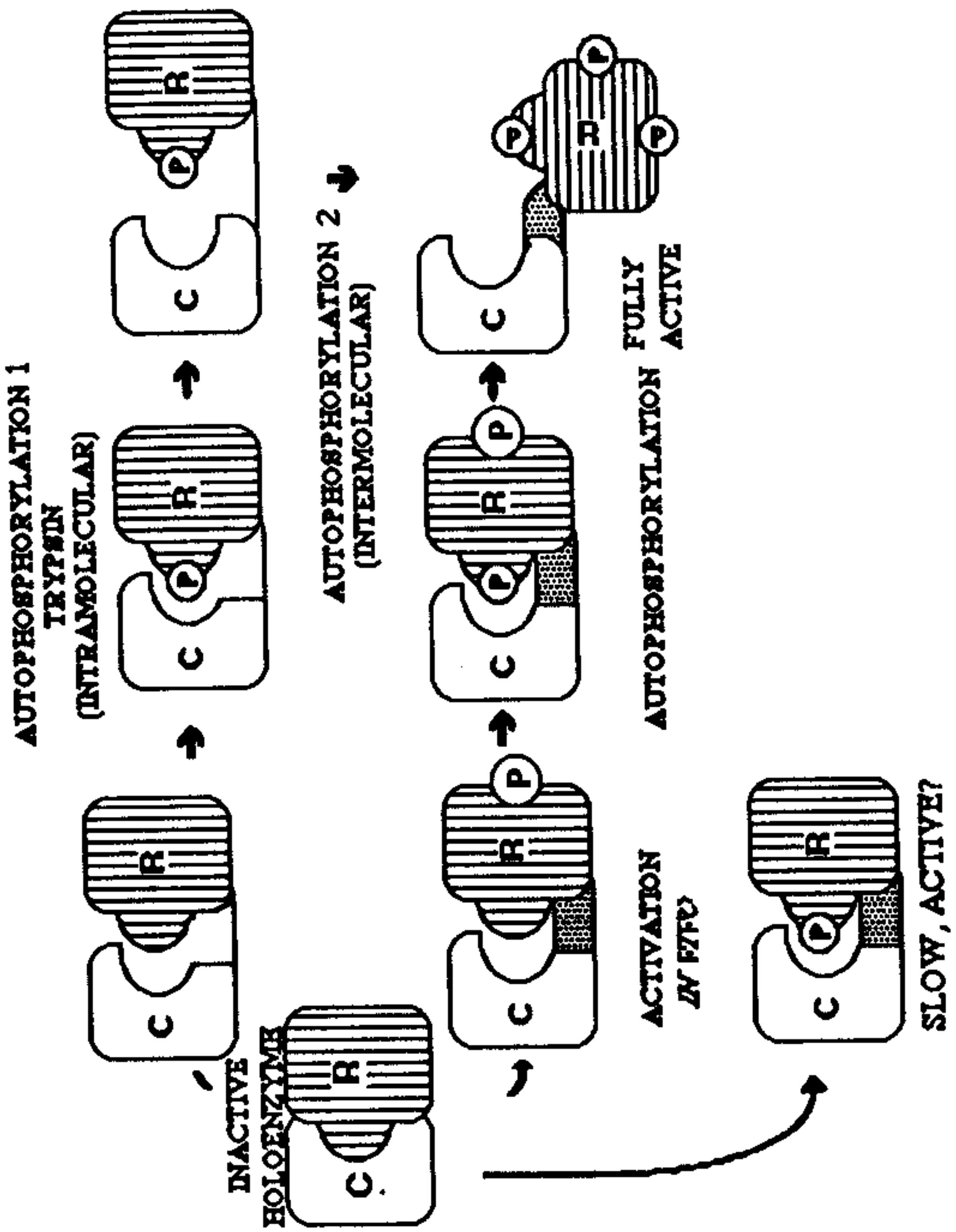
INACTIVE HOLOENZYME
AUTOPHOSPHORYLATION 1
TRYPSIN
(INTRAMOLECULAR)
AUTOPHOSPHORYLATION 2
(INTERMOLECULAR)
ACTIVATION
IN VITRO
AUTOPHOSPHORYLATION
FULLY ACTIVE
SLOW, ACTIVE?
C
R
P

CHAPTER IV

DISCUSSION

The S6/H4 kinase was first purified and characterized from murine lymphosarcoma cells (61,64). The S6/H4 kinase displayed distinct substrate specificity determinants from the cyclic AMP-dependent protein kinase (62) and its activity was unaffected in the presence of protein kinase C effectors (63). The human homologue of this kinase purified from placenta was found to have identical substrate specificities and chromatographic characteristics (74). Chromatography of lymphosarcoma extracts on Mono Q resolved the S6/H4 kinase and the p70 kinase in a manner entirely analogous to that shown in Figure 8 (A. Birdsong and R. A. Masaracchia, unpublished results). Apart from its distinct substrate specificity profile, the S6/H4 kinase is different from other proteolytically-activated kinases in that after proteolysis, autophosphorylation is necessary to generate the active kinase. By all criteria examined, it appears that the S6/H4 kinase is a major S6 kinase activity in both placenta and lymphosarcoma.

Based on purification strategies outlined previously (61,74), the S6/H4 kinase has been further purified 5700-fold. The S6/H4 kinase is resolved from another S6 kinase by gel filtration chromatography. This second S6 kinase can also be activated by mild trypsin digestion but does not utilize H4 as a substrate. The two S6 kinases can be differentiated by their preferred phosphorylation sites on the synthetic peptide S6-21. The S6/H4 kinase catalyzed rapid phosphorylation of sites in both the amino and carboxyl terminal domains of the peptide. In contrast, the second S6 kinase isolated shows a strong preference for phosphorylation sites at the amino terminal domain. Thermolysin peptide mapping indicated that this site contained Ser-236 which has been shown to be phosphorylated by protein kinase C and other proteolytically-activated protein kinases (79,80). Perhaps another proteolytically-activated protein kinase or the proteolytic fragment of protein kinase C is resolved from the S6/H4 kinase at this step in the purification procedure.

SDS-PAGE analysis of the S6/H4 kinase indicates a molecular weight of 60,000 although elution from a Sephacryl S200 gel filtration column indicates a higher molecular weight of approximately 120,000. The possibility that the S6/H4 kinase forms a dimeric complex with itself or another protein has been considered since elution characteristics from gel filtration do not agree with SDS PAGE analysis. SDS-PAGE analysis and Coomassie Blue staining of highly purified S6/H4 kinase show a major protein migrating with a Mr of 60,000. As shown in Figure 6, this appears to be the S6/H4 kinase; however a second protein with an apparent molecular weight of 60,000 seems to be present in the S6/H4 kinase fractions throughout most of the purification procedure. It is not known if this protein specifically interacts with the S6/H4 kinase.

Further supporting the idea that the S6/H4 kinase has a subunit Mr of 60,000 were antibody and 8-azido-ATP labeling studies. The antibody used in these studies was raised against a peptide derived from the catalytic subunit of the cyclic AMP-dependent protein kinase which contains a sequence conserved in all protein kinases (75). This antibody, which has been shown to react with several, but not all, protein kinases, reacted with the Mr 60,000 protein, indicating the presence of a protein kinase catalytic domain. A radiolabeled ATP analogue, 8-azido-[α-^{32}P]ATP, was observed to label a protein of Mr 60,000 indicating an ATP binding site in this protein. Since the phosphate in the probe was labelled in the α position, the binding of ATP could easily be distinguished from phosphate transfer or autophosphorylation. Collectively, these results are consistent with the interpretation that the S6/H4 kinase has an apparent subunit molecular weight of 60,000.

Two peaks of S6/H4 kinase activity were resolved by Mono S chromatography. These two peaks did not comigrate when analyzed by SDS-PAGE and Coomassie Blue staining or visualized by autophosphorylation and autoradiography. Peak I migrated with an apparent Mr of 60,000 and peak II with an apparent Mr of 55,000. This apparent molecular weight difference had no detectable effect on substrate specificity or activity subsequent to purification. Both peaks could be significantly activated by trypsin and MgATP incubation. Phosphorylation has been documented to cause mobility shifts of certain proteins on SDS-PAGE, though this is not true for all proteins. The fact that autophosphorylation of the S6/H4 kinase does not result in any discernable increase or decrease in electrophoretic mobility minimizes the possibility that the difference between these two peaks is simply that of phosphorylation state. Differential splicing of the mRNA coding for the kinase or two translational start sites on the mRNA could also be involved in the formation of the two isoforms. The p70 S6 kinase has an isoform termed p85 S6 kinase which contains a 23 amino acid tail thought to localize it to the nucleus. This isoform is created by differential splicing of mRNA derived from the same gene (81). Another possibility is that the two S6/H4 kinase isoforms are generated by proteolytic digestion during the course of purification or perhaps in the cell prior to purification.

Consistent with its role as an S6 kinase, the S6/H4 kinase has been shown to phosphorylate a 21 amino acid peptide derived from the carboxyl terminus of the S6 protein (64,65). In addition, histone H4 and myelin basic protein were also shown to be actively phosphorylated by the S6/H4 kinase. In earlier reports, S6/H4 kinase isolated from murine lymphosarcoma was shown to have substrate specificity determinants distinct from that of the cyclic AMP-dependent protein kinase and was also shown to be a cyclic nucleotide-independent protein kinase (56). The tumor enzyme is also clearly distinguished from protein kinase C and its proteolytic fragments (62). MLC (3-13), an excellent substrate for protein kinase C, and protamine are not phosphorylated by the placenta S6/H4 kinase, nor are the casein kinase substrates casein and phosvitin. This distinguishes S6/H4 kinase from protein kinase C, casein kinases, and protamine kinases, including the insulin-activated protamine kinase described by Damuni and coworkers (76). S6/H4 kinase can also be distinguished from the MAP kinases which phosphorylate myelin basic protein, but not H4 (77).

Two rabbit reticulocyte protein kinases which are activated by mild trypsin or chymotrypsin proteolysis have been termed protease-activated kinase I and II (PAK I and II) (7,46). S6 is a common substrate for PAK II and S6/H4 kinase, but PAK II does not catalyze phosphorylation of histones. PAK I, like PAK II, can be activated by mild proteolysis and catalyzes H4 phosphorylation. However, PAK I is distinct from both PAK II and S6/H4 kinase in its selective phosphorylation of the ribosomal protein S10 over that of S6 (7).

A possible relationship between the S6/H4 kinase and the S6 kinases of the *rsk* and p70 families was considered. It is unlikely that the S6/H4 kinase is related to the *rsk* family since *rsk* kinases show little kinase activity towards H4. However, a relationship between S6/H4 kinase and the p70 S6 kinase could not be discounted. To test this, placenta was rapidly processed with few purification steps in order to minimize the possibility of proteolytic degradation that may occur throughout a typical purification scheme. Western blot analysis revealed that there was no reactivity between the antibody directed against p70 S6 kinase and proteins which coeluted with trypsin-dependent S6/H4 kinase activity. Also, no reactivity was observed between the antibody and purified S6/H4 kinase (data not shown). These results are consistent with the conclusion that S6/H4 kinase is distinct from the p70 S6 kinase.

The antibody raised against a conserved sequence in the cyclic AMP-dependent protein kinase (anti-APE antibody) reacted with both purified S6/H4 kinase and a p60 protein which coeluted with the S6/H4 kinase activity in Figure 8 (data not shown). Although the p60 protein was a minor component of these partially purified fractions, no other protein reacted with the antibody. Other protein kinases which react with the anti-APE peptide antibody include phosphorylase kinase and calmodulin kinase II (71). Sequence homology between phosphorylase kinase and the *rsk* kinases has been noted (21), but the p70 kinase does not possess the same sequence similarities (20). In our studies the p70 kinase does not crossreact with the anti-APE antibody. Other protein kinases which contain the APE sequence but do not not react with this antibody include the cyclic GMP-dependent protein kinase and protein kinase C (71).

A distinguishing feature of the S6/H4 kinase is its ability to autoactivate by autophosphorylation after mild trypsin digestion. Without prior incubation with MgATP, the trypsin-treated kinase demonstrates only 5-20 % of the maximum activity observed when fully autoactivated. Autoradiographic analysis of the nontrypsin-treated S6/H4 kinase shows the existence of a single phosphoprotein at Mr 60,000. The migration of phospho-p60 on SDS-PAGE corresponds to p60 observed with Coomassie Blue staining, labeling with antibody, and azido ATP labeling, suggesting that this phosphoprotein is a product of autophosphorylation. Autophosphorylation of p60 S6/H4 kinase does not result in a measurable increase in protein kinase activity over time. When autoradiography is performed on trypsin-treated S6/H4 kinase, a major phosphoprotein is seen migrating at Mr 40,000. The presence of this pp40 fragment coincides with the activity profile of trypsin-treated S6/H4 kinase chromatographed on Mono Q. Also, the disappearance of the autophosphorylated pp60 S6/H4 kinase correlates inversely with the appearance of phosphorylated p40, suggesting that p40 is a product of p60 S6/H4 kinase proteolysis and rapidly autophosphorylates in the presence of MgATP. Autophosphorylation of p60 S6/H4 kinase is relatively slow compared to that of the p40 S6/H4 kinase. This slow autophosphorylation may reflect the relative inaccessibility of the active site to MgATP. The generation and phosphorylation of p40 corresponds to the activation of the S6/H4 kinase indicating a cause and effect relationship between the two events. Rapid autophosphorylation and activation of the trypsin-treated S6/H4 kinase lends credibility to the hypothesis that this event is physiologically significant.

Since the p40 S6/H4 kinase had the ability to autophosphorylate and autoactivate, the phosphorylation and activation of p60 S6/H4 kinase by p40 S6/H4 kinase was investigated. When the p40 and p60 forms of the S6/H4 kinase were incubated together in the presence of MgATP, autophosphorylation of both forms increased. Subsequent activity studies where constitutively active pp40 S6/H4 kinase was incubated with the p60 S6/H4 kinase showed that the individual S6/H4 kinase activities were additive, and no net increase in protein kinase activity above the combined activities was generated over time. Therefore, the apparent generation of S6/H4 kinase activity demonstrated by the increased phosphorylation of the two kinase forms was not due to the activation of the p60 S6/H4 kinase. The increase in p40 S6/H4 kinase phosphorylation was most likely due to increased autophosphorylation of the kinase. This may have been caused by a protein stabilization effect due the protein mass of the p60 S6/H4 kinase, since it was present in excess compared to the p40 S6/H4 kinase. The addition of bovine serum albumin or myoglobin to p40 S6/H4 kinase autophosphorylation reactions has been shown to increase the activity of the kinase. Without the addition of one of these proteins in the reaction mixtures, the activity of the p40 S6/H4 kinase rapidly diminishes over time. This is most likely due to the instability of the proteolytic p40 S6/H4 kinase fragment at reaction incubation temperatures. Therefore, it can be concluded that bimolecular autophosphorylation of the p60 S6/H4 kinase is not sufficient to activate the kinase. This may be due to inaccessibility of the autophosphorylation site(s) which mediate autoactivation of the p60 S6/H4 kinase or to the presence of a domain on the pp60 S6/H4 kinase which suppresses activation of the kinase when the autophosphorylation sites are phosphorylated.

The observation that p40 S6/H4 kinase requires autophosphorylation subsequent to trypsin treatment indicates the presence of an autoinhibitory domain associated with the active site. Though not proven, it can be deduced that the p40 S6/H4 kinase contains the catalytic site since it is unlikely the remaining fragment would have enough sequence to define a catalytic site. This would suggest that the catalytic and regulatory domains exist on the same polypeptide after trypsin digestion. This model differs from the "hinge" model in which the regulatory domain is removed from the catalytic site after proteolytic digestion.

Data presented here do not rule out the remote possibility that a contaminating kinase exists in the S6/H4 kinase preparations which activates the kinase by phosphorylation. This possibility can be argued against by the fact that the S6/H4 kinase has a unique substrate specificity, and each substrate has the ability to block activation of the kinase subsequent to trypsin treatment. Therefore, the possibility of a minor contaminating kinase copurifying and activating the trypsin-treated S6/H4 kinase would have to include the condition that this kinase has a substrate specificity identical to the S6/H4 kinase. Although many protein kinases have been shown to phosphorylate the protein S6, the substrates H4 and myelin basic protein are more selective. This indicates that only a very few kinases may exist that phosphorylate all three proteins with the S6/H4 kinase being the sole member of this group identified to date.

The addition of $MgCl_2$ in the running buffers of both Mono S and Mono Q causes a shift in the chromatographic behavior of the S6/H4 kinase. This shift in elution from the columns has no effect on the ability of the kinase to autoactivate subsequent to trypsin treatment. If the ATP-dependent activation of the kinase was caused by another kinase, it would have to shift its elution from the columns in the same manner. This seems an unlikely event since many other proteins in the S6/H4 sample do not show any change in chromatographic behavior in the presence of $MgCl_2$.

The autophosphorylation event was studied in more detail by first investigating how many autophosphorylation sites were modified during activation of the S6/H4 kinase. Multiple phosphorylated forms of the pp40 S6/H4 kinase were detected with this technique. Nonphosphorylated p40 S6/H4 kinase, detected by silver staining of the two-dimensional SDS PAGE, was focused at a higher pH than the pp40 S6/H4 kinase isoforms. In addition to the major silver-stained protein, several minor proteins were observed to focus at the lower pH's. These proteins may be autophosphorylated forms of the kinase which were present throughout purification. Since the S6/H4 kinase required MgATP incubation for activation subsequent to treatment with trypsin, the autophosphorylation site(s) responsible for autoactivation had either been dephosphorylated or was not phosphorylated at the time of cell lysis. Other phosphorylation sites which play no role in the activation of the kinase may not turn over as rapidly as the regulatory sites and could still be phosphorylated in the purified, inactive kinase.

Two-dimensional SDS-PAGE resolved autophosphorylated pp40 S6/H4 kinase isoforms by isoelectric point and molecular weight. A total of three isoforms which were generated during the autoactivation step were resolved. Each phosphoprotein isoform demonstrated a lower isoelectric point than the untreated enzyme. As incubation time with MgATP increased, the pp40 S6/H4 kinase became more acidic, indicating progressive autophosphorylation. The spacing of the phosphoproteins was not constant throughout the pH gradient. As the protein became more acidic, the spacing interval between the proteins decreased. The most likely explanation for this is based on the the fact that the second pK_a for phosphoserine in the presence of 9M urea is approximately 6.5 (81). The pH gradient used in this experiment was from 5 to 7. Therefore, as the protein becomes more acidic and focuses into a more acidic environment, the added phosphates contribute less of a negative charge. This will cause proteins to focus closer together at a lower pH than at a higher pH. Taken together, multiple autophosphorylation sites seem to be modified during autoactivation of the S6/H4 kinase.

Tryptic phosphopeptide mapping with TLE/TLC analysis supported the observations from two-dimensional SDS-PAGE. Four phosphopeptides were resolved in both dimensions and were numbered according to their electrophoretic migration at pH 1.9. Reversed-phase chromatography resolved four phosphopeptide peaks, and each peak could be correlated with the products observed with the phosphopeptide map. Phosphopeptides 1, 2, and 3, the major phosphopeptides, eluted well into the acetonitrile gradient whereas phosphopeptide 4 eluted much earlier. This suggests that phosphopeptide 4 may be small. This is consistent with the observation that phosphopeptide 4 has the highest charge to mass ratio of the four phosphopeptides when TLE analysis is performed at pH 1.9 or pH 6.5.

Generation of [^{32}P]pp40 S6/H4 kinase for the phosphopeptide mapping experiments involved prolonged incubation with Mg[γ-^{32}P]ATP. This was done to achieve the highest degree of autophosphorylation possible so that all of the autophosphorylation sites could be mapped. To determine which autophosphorylation sites correlated to the autoactivation of the p40 S6/H4 kinase, autophosphorylation of the p40 S6/H4 kinase was carried out at time points occurring before full activation of the kinase. It is predicted that autophosphorylation of sites responsible for the autoactivation of the S6/H4 kinase would be phosphorylated first, since no kinase activity would be present prior to their modification. Additionally, sites which mediate activation would be autophosphorylated at levels consistent with the amount of activation observed. Tryptic phosphopeptide maps of the kinase autophosphorylated at time points preceding full activation indicated that phosphopeptides 1 and 3 were the predominant phosphopeptides generated at the early points in autoactivation. The levels of phosphopeptides 2 and 4 at the early time points were approximately half the levels of 1 and 3, and phosphopeptide 4 levels never increased beyond 50% of phosphopeptide 1 and 3 levels. The data suggest that autophosphorylation sites contained in phosphopeptides 1 and 3 are the first to be modified, and support the hypothesis that autophosphorylation of sites contained in phosphopeptides 1 and 3 is responsible for the activation of S6/H4 kinase. At longer autophosphorylation times, the level of phosphopeptide 2 became greater than that of the other three phosphopeptides. The longer autophosphorylation time points demonstrated a decrease in the rate of autoactivation due to the fact that the kinase was approaching full activation. Levels of phosphopeptides 1 and 3 reached a relative maximum at the longer autophosphorylation times coordinate with the decrease in autoactivation rate. Phosphopeptide 2 levels continued to increase through the point where full activation was reached. Therefore, the phosphorylation of sites contained in phosphopeptides 1 and 3 parallels the autoactivation of the S6/H4 kinase providing further evidence that the sites play an important role in the regulation of S6/H4 kinase activity. However, it cannot be established whether autophosphorylation of sites contained in phosphopeptides 1 and 3 occurs through an intramolecular or intermolecular mechanism. Autophosphorylation of sites contained in phosphopeptides 2 and 4 does not fit the criteria predicted for important regulatory phosphorylation sites and suggests that phosphorylation of these sites plays a limited role in the autoactivation mechanism.

Phosphorylation of peptide 2 increased in a linear manner throughout the autoactivation time course. In the region of the autoactivation profile which demonstrated the most rapid autoactivation kinetics the amount of phosphate transferred to phosphopeptide 2 increased from 28% to 41% of the total. However, the levels of phosphopeptide 2 continued to increase at a nearly linear rate after the enzyme was fully activated. In addition, phosphopeptide 2 concentrations were lower than phosphopeptides 1 and 3 at the time points where autoactivation was initiated. In phosphopeptide maps of p40 S6/H4 kinase which had been phosphorylated for long time intervals, phosphopeptide 2 consistently contained twice as much phosphate as either phosphopeptide 1 or 3. These data suggest that there may be two autophosphorylation sites associated with phosphopeptide 2.

Phosphopeptides 2 and 3 were purified and sequenced. The partial sequence of phosphopeptide 3 was SSMVGTPY. Two serines at the amino terminus of the peptide and a threonine and tyrosine located at positions 6 and 8, respectively, are potential phosphorylation sites. Since trypsin cleaves at the carboxyl terminus of the basic amino acids lysine and arginine, the entire sequence of the peptide was probably not determined. The tyrosine residue was detected in the last sequencing cycle would not be a predicted trypsin cleavage site. The data do not exclude the possibility that a second phosphorylation site exists in a portion of the peptide which was not sequenced.

A chymotryptic phosphopeptide containing the phosphorylation site in phosphopeptide 3 was fully sequenced. The chymotryptic sequence confirmed the existence of a phosphorylation site in the sequence generated from tryptic phosphopeptide 3. Since dehydroalanine, the degradation product of phosphoserine (82), was detected in the first two rounds of sequencing, either one or both of the N-terminal serines may be phosphorylated. The trypsin cleavage site on phosphopeptide 3 established that basic residues occur N-terminal to these serines. This is consistent with the predicted specificity determinants for the S6/H4 kinase (62). The S6-21 peptide contains the sequence KRRRLSSL near the amino terminus of the peptide. At least one of the serines in this sequence was phosphorylated by the S6/H4 kinase, although this was shown to be a slower phosphorylation site which required high S6/H4 kinase concentrations and long incubation periods to effect significant phosphorylation (66). However, the affinity for the sequence in the intact S6/H4 kinase may be increased since higher order structural features may promote enhanced binding kinetics in the catalytic cleft.

To establish the identity of the residue phosphorylated during autoactivation, phosphoamino acid analysis was performed. Phosphoamino acid analysis clearly demonstrated that autophosphorylation occurred exclusively on serine with no phosphothreonine or phosphotyrosine being detected. Since the MAP kinases have been shown to autophosphorylate on threonine and tyrosine (54), the phosphoamino acid analysis confirms that the S6/H4 kinase is not a member of the MAP kinase family.

The sequence of tryptic phosphopeptide 2, the major phosphopeptide identified after long autophosphorylation periods, contained the sequence SVIDPVPAPVGDS-HVDGAAK. Two serines, one at the amino terminal end of the peptide and the second found 12 residues further into the sequence, occur in this peptide. The second serine in phosphopeptide 2 is not likely to be an autophosphorylation site since it lacks the dibasic substrate determinants. Although the sequencing of phosphopeptide 2 terminated with lysine, the low signal strength at this point in the sequencing precluded concluding that the end of the peptide was reached. Therefore, the possibility exists that another autophosphorylation site with substrate determinants specific for the S6/H4 kinase occurs in phosphopeptide 2. Since the stoichiometry of phosphate incorporation into phosphopeptide 2 was twice that of the other phosphopeptides, a second autophosphorylation site in phosphopeptide 2 might be predicted.

When the sequences of the two tryptic phosphopeptides were analyzed through the Swiss Gene Bank to search for sequence homologies no significant homology was found with any known kinase or phosphatase sequences. This is further evidence that the S6/H4 kinase is unique from protein kinases previously characterized. Only a small section of amino acids in phosphopeptide 2 was found to be homologous to primary structure in other proteins. The sequence PVPAPVG or portions of it were found in six other proteins including mouse alpha adoptin, phosphoenol pyruvate phosphotransferase, steroid receptor proteins is unknown.

A model can be proposed for the *in vitro* activation mechanism of the S6/H4 kinase. (Figure 34). The data indicate that the native p60 S6/H4 kinase contains an autoinhibitory domain which functions to down-regulate kinase activity by sterically blocking entry of substrates such as MgATP, proteins and peptides into the active site. The low level of S6/H4 kinase activity and the slow rate of autophosphorylation associated with this kinase support this conclusion. Mild digestion of the S6/H4 kinase with trypsin increases the rate of autophosphorylation 6-fold and is observed to occur with a protein exhibiting an apparent molecular weight of 40,000. The activity of the p40 S6/H4 kinase increases coordinately with autophosphorylation indicating that the activation of the kinase occurs through an autophosphorylation mechanism. Subsequent to trypsin proteolysis, but prior to incubation with MgATP, the p40 S6/H4 kinase exhibits low activity which indicates that even though MgATP can bind to the active site more freely, the larger peptide and protein substrates are still excluded from the active site by the autoinhibitory domain. The conclusion that trypsin digestion causes a conformational change which opens the active site to small substrates is supported by the data. Therefore, the proposed model of S6/H4 kinase activation *in vitro* starts with a change in the association of the autoinhibitory domain with the active site so that binding of MgATP to the active site occurs more readily but binding of peptides and proteins is still prohibited. Once MgATP binds to the active site, rapid autophosphorylation of the S6/H4 kinase occurs. Autophosphorylation causes another conformational change which completely dissociates the autoinhibitory domain from the active site and generates a fully active kinase.

Kinetic studies demonstrate that autoactivation of the p40 S6/H4 kinase occurs through an intermolecular mechanism. Time course analysis of the autoactivation event shows initial rates of autoactivation to be slow. The period of slow activation is immediately followed by a period of rapid autoactivation which exhibits bimolecular kinetics. To explain these observations and how intermolecular autoactivation kinetics are observed with an initial population of inactive p40 S6/H4 kinase, a possible mechanism is proposed which is consistent with these observations and can be incorporated into the overall p40 S6/H4 kinase activation model. The proposed mechanism would involve an initial autophosphorylation of the p40 S6/H4 kinase occurring through an intramolecular mechanism. Autophosphorylation by this mechanism would occur on the autoinhibitory domain associated with the active site of the kinase and would generate kinase activity sufficient to start the rapid intermolecular autophosphorylation observed at later autoactivation time points. The intramolecular autophosphorylation may fully activate the kinase but proceed more slowly than the intermolecular mechanism so intramolecular kinetics would not be observed at high kinase concentrations. Two sites of autophosphorylation which mediate S6/H4 kinase autoactivation are invoked with this model. Consistent with the proposed model, multiple sites have been shown to be autophosphorylated during the autoactivation of the S6/H4 kinase. Tryptic phosphopeptide 2 contains sites which demonstrate clear intermolecular kinetics. The kinetics of autophosphorylation at the sites implicated in the mediation of S6/H4 kinase activity were consistent with their proposed role as sites which would mediate the initial autoactivation event. Data described here agree with this model, but further studies into the autophosphorylation of sites during the autoactivation of the S6/H4 kinase will be needed to confirm it.

The activation of S6 kinases has been implicated to function in signalling pathways that govern cell growth (1-6). The mechanics of protein kinase autoactivation are important in understanding how a receptor signal is propagated throughout a mitogen-stimulated cell. S6/H4 kinase has been shown to autoactivate through an autophosphorylation mechanism. One caveat to this is that the kinase must be mildly digested with trypsin before autoactivation can occur. This implies the existence of a prerequisite event in the S6/H4 kinase activation scheme as it would occur in the cell. The activation of other S6 kinases takes place through both small molecule second messenger binding and phosphorylation mechanisms (35-37). The step in the *in vivo* S6/H4 kinase activation scheme analogous to trypsin digestion could occur by one of the previously mentioned mechanisms although the existence of a specific protease that initiates activation of the kinase cannot be ruled out at this point. Regardless of the "upstream" event, knowledge that the S6/H4 kinase is capable of rapidly autophosphorylating and autoactivating will be important in determining the specific course of events that lead to activation of this kinase *in vivo* and the function of the multiple phosphorylation sites observed in the activated enzyme.

REFERENCES

1. Thomas, G., Martin-Peréz, J., Siegmann, M., and Otto, A.M. (1982) *Cell* **30**, 235-242
2. Smith, C.J., Rubin, C.S., and Rosen, O.M. (1980) *Proc. Natl. Acad. Sci. USA* **77**, 2641-2645
3. Hasebacher, G.K., Humbel, R.E., and Thomas, G.F. (1979) *FEBS Lett.* **100**, 185-190
4. Nishimura, J., and Devel, T.F. (1983) *FEBS Lett.* **156**, 130-134
5. Pelech, S.L., Olvin, B.B., and Krebs, E.G. (1986) *Proc. Natl. Acad. Sci. USA* **83**, 5968-5972
6. Novak-Hofer, I. and Thomas, G. (1984) *J. Biol. Chem.* **259**, 5995-6000
7. Smith, C.J., Wejknora, P.J., Warner, J.R., Rubin, C.S., and Rosen, O.M. (1979) *Proc. Natl. Acad. Sci. U.S.A.* **76**, 2725-2729
8. Matsuda, Y. and Guroff,G. (1987) *J. Biol. Chem.* **262,** 2832-2844
9. Blenis, J. and Erikson, R. L. (1985) *Proc. Natl. Acad. Sci. USA* **82**, 7621-7625
10. Erikson, E. and Maller, J. L. (1985) *Proc. Natl. Acad. Sci. USA* **82**, 742-746
11. Chan, Y.-L., and Wool, I.G. (1988) *J. Biol. Chem.* **263**, 2891-2896
12. Kreig, J., Hofsteenge, J.and Thomas, G. (1988) *J. Biol. Chem.* **263**, 11473-11477
13. Erikson, E., and Maller, J.L. (1986) *J. Biol. Chem.* **261**, 350-355
14. Lavoinne, A., Erikson, E., Maller, J. L., Price, D. J., Avruch, J. and Cohen, P. (1991) *Eur. J. Biochem.* **199**, 723-728
15. Tabarini, D., Garcia de Herreros, A., Heinrich, J. and Rosen O.M. (1987) *Biochem.*

Biophys. Res. Commun. **144**, 891-899

16. Gregory, J.S., Boulton T.G., Sang, B.-C. and Cobb, M.H. (1989) *J. Biol. Chem.* **264**, 18397-18401
17. Price, D.J., Nemenoff, R.A. and Avruch, J. (1989) *J. Biol. Chem.* **164**, 13825-13833
18. Jenö, P., Jäggi, N., Luther, H., Siegmann, M. and Thomas, G. (1989) *J. Biol. Chem.* **264**, 1293-1297
19. Erikson, R. L. (1991) *J. Biol. Chem.* **266**, 6007-6010
20. Kozma, S.C, Ferrari, S., Bassand, P., Siegmann, M., Totty, N. and Thomas, G. (1990) *Proc. Natl. Acad. Sci. USA.* **87**, 7365-7369
21. Jones, S.W., Erikson, E., Blenis, J., Maller, J., and Erikson, R.L. (1988) *Proc. Natl. Acad. Sci. USA* **85**, 3377-3381
22. Banerjee, P., Ahmad, M.F., Grove, J.R., Kozlosky, C., Price, D.J., and Avruch, J. (1990) *Proc. Natl. Acad. Sci. U.S.A.* **87**, 8550-8554
23. Ballou, L.M., Siegman, M.P., Thomas, G. (1988) *Proc. Natl. Acad. Sci.* **85**, 7154-7158
24. Sturgill, T.W., Ray, L.B., Erikson, E., Maller, J.L. (1988) *Nature* **334**, 715-718
25. Pelech, S.L., Sanghera, J.S.(1992) *Trends in Biol Sci.* **17**, 233-238
26. Sturgill, T.W., and Wu, T. (1991) *Biochem. Biophys. Acta.* **1092**, 350-357
27. Davis, R.J. (1993) *J. Biol. Chem.* **268**, 14553-14556
28. Wood, K.W., Sarnecki, C., Roberts, T.M., and Blenis, J. (1992) *Cell* **68**, 1041-1050
29. Lange-Carter, C.A., Pleiman,C.M., Gardner, A.M., Blumer, K.J., Johnson, G.L.

(1993) *Science* **260**, 315-319

30. Ballou, L.M., Luther, H., and Thomas, G.(1991) *Nature* **349**, 348-350
31. Jeno, P., Ballou, L.M., Novak-Hofer, I., and Thomas, G. (1988) *Proc. Natl. Acad. Sci. U.S.A.* **85**, 406-410
32. Lane, H.A., Fernandez, A., Lamb, N.J.R., and Thomas, G. (1993) *Nature* **363**, 170-172
33. Chung, J., Kuo, C.J., Crabtree, G.R., and Blenis, J. (1992) *Cell* **69**, 1227-1236
34. Ferrari, S., Bannworth, W., Morley, S.J., Totty, N.F., and Thomas, G. (1992) *Proc. Natl. Acad. Sci. U.S.A.* **89**, 7282-7286
35. Soderling, T.R. (1990) *J. Biol. Chem.* **265**, 1823-1826
36. Hanks, S.K., Quinn, A.M. and Hunter, T. (1988) *Science* **241**, 42-52
37. House, C. and Kemp, B.E. (1987) *Science* **238**, 1726-1728
38. Knighton, D. R., Zheng, J., Ten Eyck, L. J., Ashford, V. A., Xuong, N., Taylor, S. and Sowadski, J. M. (1991) *Science* **253**, 407-414
39. Corbin, J.D., Sugden, P.H., West, L., Flockhart, D.A., Lincoln, T.M., and McCarthy, D. (1978) *J. Biol. Chem.* **253**, 3997-4003
40. Brostrom, C.O., Corbin, J.D., King, C.A. and Krebs, E.G. (1971) *Proc. Natl. Acad. Sci. USA* **68**, 2444-2447
41. Gill, G.N., Walton, G.M. and Sperry, P.J. (1977) *J. Biol. Chem.* **252**, 6443-6449
42. Walsh, D.A., Perkins, J.P., Brostrom, C.O., Ho, E.S. and Krebs, E.G. (1971) *J. Biol. Chem.* **246**, 1968-1976
43. Friedman, D. L. and Larner, J. (1963) *Biochemistry* **2**, 669-675
44. Ray, L. B. and Sturgill, T. W. (1987) *Biochemistry* **84**, 12502-1506
45. Potter, R. L. and Taylor, S. S. (1979) *J. Biol. Chem.* **254**, 2413-2418

46. Huang, K-P. and Huang, F.L. (1986) *Biochem. Biophys. Res. Commun.* **139**, 320-326

47. Lubben, T. H. and Traugh, J. A. (1983) *J. Biol. Chem.* **258**, 13992-13997

48. Edelman, A.M., Takio, K., Blumenthal, D.K., Hansen, R.S., Walsh, K.A., Titani, K.and Krebs, E.G. (1985) *J. Biol. Chem.* **260**, 11275-11285

49. Rangel-Aldao, R. and Rosen, O.M. (1976) *J. Biol. Chem.* **251**, 3375-3380

50. Levin, L.R., Zoller, M.J. (1990) *Mol. Cell. Biol.* **10**, 1066-1075

51. Sutherland, C., Campbell, D.G., and Cohen, P. (1993) *Eur. J. Biochem.* **212**, 581-588

52. Anderson, N.G., Maller, J.L., Tonks, N.K., and Sturgill, T.W. (1990) *Nature* **343**, 651-653

53. Boulton, T.G., Gregory, J.S., and Cobb, M.H. (1991) *Biochemistry* **30**, 278-286

54. Seger, R., Ahn, N.G., Boulton, T.G., Yancopoulos, G.D., Panayotatos, N., Radziejewska, E., Ericsson, L., Bratlien, R.L., Cobb, M.H., and Krebs, E.G. (1991) *Proc. Natl. Acad. Sci.* **88**, 6142-6146

55. Reddy, S.A.G., Guo, H., Tarun, S.Z., and Damuni, Z. (1993) *J.Biol. Chem.* **268**, 15298-15304

56. Price, D.J., Gunsalus, J.R. and Avruch, J. (1990) *Proc. Natl. Acad. Sci. USA* **87**, 7944-7948

57. Roth, R.A., and Cassel, D.J. (1983) *Science* **219**, 299-301

58. Ushiro, H. and Cohen, S. (1980) *J. Biol. Chem.* **255**, 8363-8365

59. Guo, H., Reddy, S.A.G., and Damuni, Z. (1993) *J. Biol. Chem.* **268**, 11193-11198

60. Guo, H., and Damuni, Z. (1992) *Proc. Natl. Acad. Sci.* **90**, 2500-2504
61. Masaracchia, R.A., Kemp, B.F., and Walsh, D.A. (1977) *J. Biol. Chem.* **252**, 7109-7177
62. Eckols, T.K., Thompson, R. E. and Masaracchia, R.A. (1983) *Eur. J. Biochem.* **134**, 249-254
63. Magnino, P.E., de la Houssaye, B.A., and Masaracchia, R.A. (1983) *Biochem. Biophys. Res. Commun.* **116**, 675-681
64. Donahue, M.J. and Masaracchia, R.A. (1984) *J. Biol. Chem.* **259**, 435-440
65. de la Houssaye, B.A., Echols, T.K., and Masaracchia, R.A. (1983) *J. Biol. Chem.* **258**, 4272-4278
66. Brandon, S. D. and Masaracchia, R. A. (1991) *J. Biol. Chem.* **266**, 380-385
67. Hassell, T.C., Magnino, P.E. and Masaracchia, R.A. (1988) *Biochem. Biophys. Acta* **957**, 1-10
68. Glass, D.B., Masaracchia, R.A., Feramisco, J.R. and Kemp, B.E. (1978) *Anal. Biochem.* **87**, 566-575
69. Reimann, E.M., Walsh, D.A. and Krebs, E.G. (1971) *J. Biol. Chem.* **246**, 1986-1995
70. Laemmli, U.K. (1970) *Nature (Lond.)* **227**, 680-685
71. Amons,R., and Schrier, P.I. (1981) *Anal. Biochem.* **116**, 439-443
72. Boyle, W.J., van der Geer, P., and Hunter, T. (1991) *Meth in Enzymol.* **201**, 110-149
73. Juhl, H., and Soderling, T.R. (1983) *Meth. in Enzymol.* **99**, 37-48
74. Masaracchia, R.A., Mallick, S., and Murdock, F.E. (1988) in *Insulin Action and Diabetes* (Goren, H.J., Hollenberg, M.D., and Roncari, D.A.K., eds) pp. 169-172,

Raven Press, New York

75. Hagedorn, C.H., Tettelbach, W.H. and Panella, H.L. (1990) *FEBS Lett.* **264**, 59-62
76. Grove, J.R., Banerjee, P., Balasubramanyam, A., Coffer, P.J., Price, D.J., Avruch, J. and Woodgett, J.R. (1991) *Mol. Cell. Biol.* **11**, 5541-5550
77. Luo, K., Hurley, T.R., and Sefton, B.M. (1991) *Meth in Enzymol.* **201**, 149-152
78. Bradford, M.M. (1976) *Anal. Biochem.* **72**, 248-254
79. Reddy, S. A. G., Amick, G. D., Cooper, R. H. and Damuni, Z. (1990) *J. Biol. Chem.* **265**, 7748-7752
80. Kyriakis, J. M. and Avruch, J. (1990) *J. Biol. Chem.* **265**, 17355-17363
81. Wettenhall, R.E.H., Gabrielli, B., Morrice, N., Bozinova, L., Kemp, B.E., Stapleton, D. (1991) *Peptide Res.* **4**, 158-170
82. House, C., Wettenhall, R.E.H., and Kemp, B.E. (1987) *J. Biol. Chem.* **262**, 772-777
83. Reinhard, C., Thomas, G., and Kozma, S.C. (1992) *Proc. Natl. Acad. Sci.* **89**, 4052-4056
84. Cooper, J.A. (1991) *Meth. in Enzymol.* **201**, 251-261
85. Meyer, H.E., Hoffman-Posorske, E., and Heilmeyer, Jr., L.M.G. (1991) *Meth. in Enzymol.* **201**, 169-185.